Advanced Seismic Interpretation
For the Harvey Area
In the SW Hub

A Report by ODIN Reservoir Consultants

DMIRS/2018/1

December 2017

John Lamberto

Government of **Western Australia**
Department of **Mines, Industry Regulation and Safety**

Contents

List of Figures

LIST OF TABLES

Declaration

ODIN Reservoir Consultants was commissioned to undertake to provide a reservoir modelling study for the SW Hub CO_2 Sequestration Project on behalf of the Department of Mines, Industry Regulation and Safety (DMIRS))

The evaluation of Carbon Capture and Storage is subject to uncertainty because it involves judgments on many variables that cannot be precisely assessed, including CO_2 sequestration rates and capture, the costs associated with storing these volumes, sequestration gas distribution and potential impact of fiscal/regulatory changes.

The statements and opinions attributable to us are given in good faith and in the belief that such statements are neither false nor misleading. In carrying out our tasks, we have considered and relied upon information supplied by the DMP and available in the public domain. Whilst every effort has been made to verify data and resolve apparent inconsistencies, neither ODIN Reservoir Consultants nor its servants accept any liability for its accuracy, nor do we warrant that our enquiries have revealed all of the matters, which an extensive examination should disclose.

We believe our review and conclusions are sound but no warranty of accuracy or reliability is given to our conclusions.

Neither ODIN Reservoir Consultants nor its employees has any pecuniary interest or other interest in the assets evaluated other than to the extent of the professional fees receivable for the preparation of this report

Note:

ODIN has conducted the attached independent technical evaluation with the following internationally recognised specialist:

John Lamberto is a Senior Geophysicist with over 25 years' experience in 2D and 3D seismic interpretation (regional and development). John has worked in multi-disciplinary teams undertaking field development studies, reservoir modelling, interpretive processing projects and exploration operations. John has specific experience in 3D interpretation, building synthetic seismograms, depth conversion, uncertainty analysis, Quantitative Interpretation (QI) and Fluid Substitution Modelling.

1. SUMMARY AND CONCLUSIONS

The objectives of the 2017 data reprocessing and interpretation were;

- To improve the data quality and seismic imaging which can enable a more detailed interpretation of the Yalgorup and Wonnerup Members that comprise the Lesueur Formation which is the section of interest.
- Investigate and undertake qualitative and quantitative facies prediction using 3D seismic data.
- Undertake detailed fault interpretation of the Harvey 3D seismic data.

The data reprocessing of the Harvey 3D dataset that was undertaken by Curtin University has enhanced the data quality in comparison to the previous version that was done by Velseis in Brisbane. In particular, fault imaging has been improved as has the general signal to noise ratio in the data. However, in places the data is over-migrated and migration smiles are common throughout. The data processing is not assisted by the fact that the data acquisition had limited access and therefore, significant data gaps exist within the volume.

A detailed interpretation of horizons and faults has been completed. Additional horizons within the Yalgorup Member and the Wonnerup Member have been included compared to the previous study. The fault interpretation comprises greater detail as the reprocessing has allowed.

Time and depth maps for all horizons interpreted have been completed for this study. A structural model has been proposed that appropriately fits the detailed Harvey 3D interpretation into a regional context.

A comprehensive effort has been applied to investigate the validity of qualitative and quantitative facies prediction using a variety of attributes. These included amplitude extraction grids across many surfaces and intervals, horizon attributes at all key surfaces and coherency attribute analysis at many levels. Unfortunately, the limitations in the data acquisition and the subsequent impact this has had on the data processing has precluded the derivation of meaningful attributes that can be reliably used for facies prediction.

Finally, the two high-resolution surveys that were acquired across the DMP Harvey 3 and the DMP Harvey-4 well locations have not been able to provide any additional information to assist with the interpretation of potentially sub-resolution faults in the existing and more extensive Harvey 3D. Rather than a failure of method, it is considered that the reason for this result is more likely a function of the limited area of the high-resolution surveys. The high-resolution surveys were designed to be effective above -1000mSS but the objectives of this study (Yalgorup & Wonnerup Members) are deeper than this within the survey areas.

2. INTRODUCTION

Horizon and Fault interpretation are necessary to define the limits of the grid and the structural elements within the grid which are the foundation for the 3D Geological Model (Figure 2.1). Seismic attributes may assist with defining the distribution of properties such as facies and porosity.

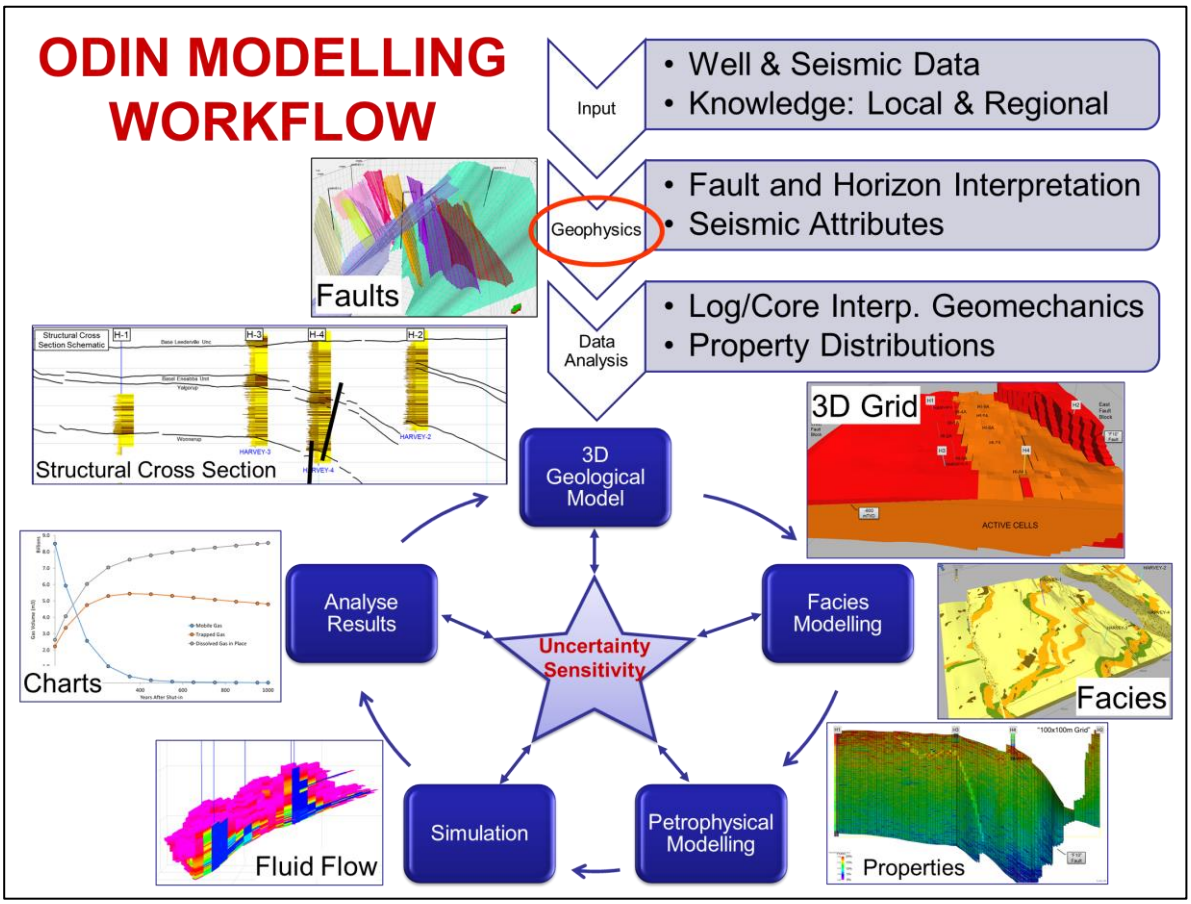

Figure 2.1: ODIN Modelling Workflow

2.1 Study Objectives

The objectives of the 2017 data reprocessing and interpretation were;

- To improve the data quality and seismic imaging which can enable a more detailed interpretation of the Yalgorup and Wonnerup Members that comprise the Lesueur Formation which is the section of interest.
- Investigate and undertake qualitative and quantitative facies prediction using 3D seismic data.

- Undertake detailed fault interpretation of the Harvey 3D seismic data.

As a more regional interpretation had been previously undertaken, the scope of the study was limited to the Harvey 3D survey area. The location of the study area is highlighted in (Figure 2.2).

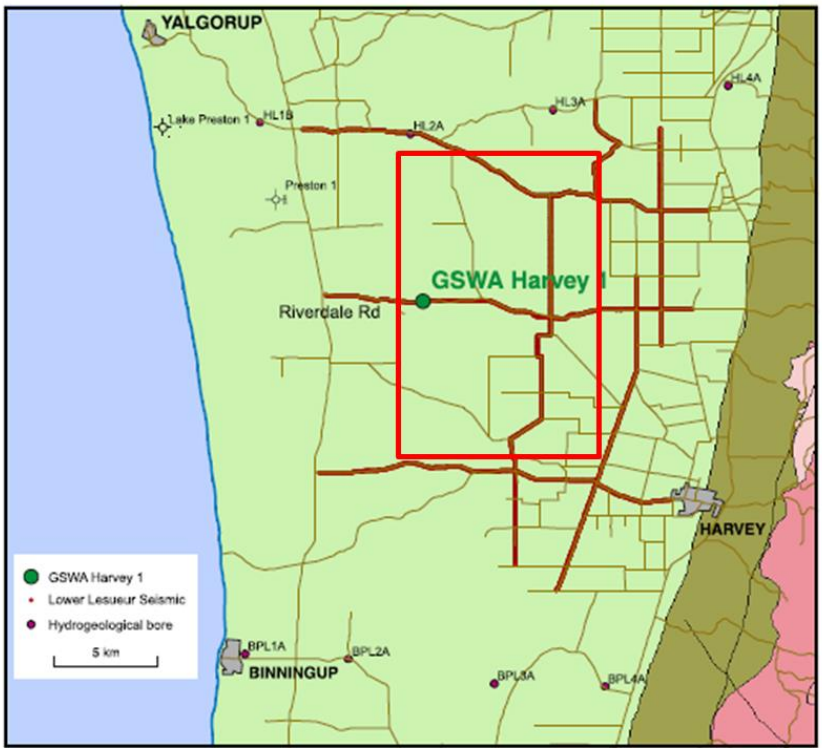

Figure 2.2 Location of the Harvey 3D seismic survey

3. REGIONAL SETTING

The Perth Basin formed during the separation of Australia and India from the Permian to the Early Cretaceous. Rifting in the Late Triassic and Early Jurassic was associated with widespread fluvial and deltaic deposits. Breakup occurred during the Early Cretaceous and was associated with widespread inversion, erosion, strike-slip tectonics and volcanism. There was significant erosion of the Harvey Ridge which removed the late and middle Jurassic sections, including the Yarragadee Formation.

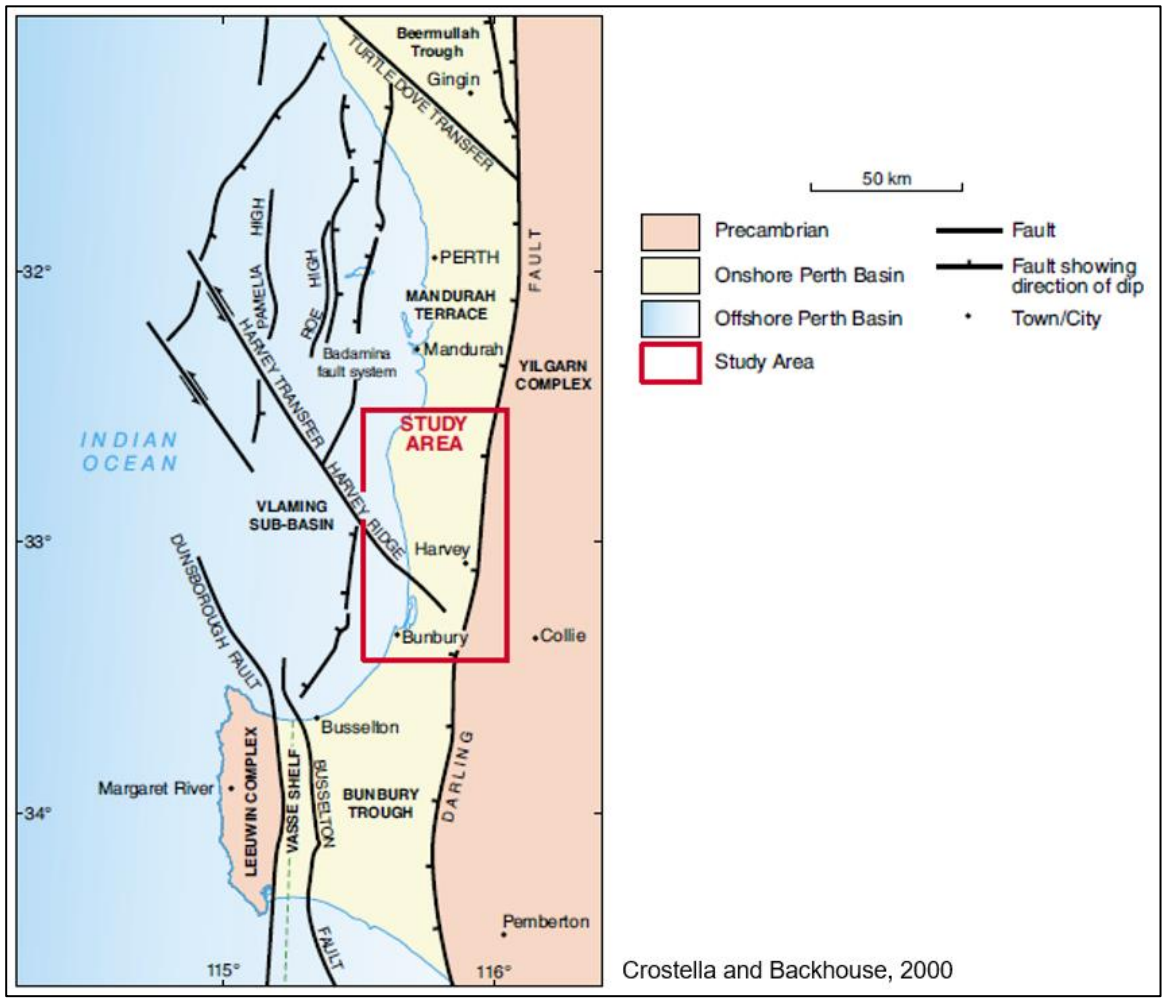

Figure 3.1 Tectonic elements map surrounding study

Previous studies (Iasky, 1993; Crostella and Backhouse,2000; Iasky and Lockwood, 2004) have suggested that the Harvey Ridge in the onshore part of the southern Perth Basin was a result of northwest–southeast trending transfer movement. However, the nature and timing of this movement remains unresolved.

The stratigraphic succession in the southern Perth Basin ranges from Permian to Quaternary in age (Figure 3.2). The Triassic–Jurassic stratigraphic nomenclature in the southern Perth Basin is not satisfactorily established. Nevertheless, the section intersected at GSWA Harvey 1 and Lake Preston 1 (Young and Johanson, 1973), informally refers to the two members of the 'Lesueur Sandstone' as the 'Wonnerup' (lower) and 'Yalgorup (upper) based on lithological correlations. The former member consists of over 1km of homogeneous sandstone showing low-amplitude chaotic reflectors, whereas the latter consists of about 700m of sandstone interbedded with shale, expressed on seismic data as a series of strong parallel reflectors. The 'Eneabba Formation', overlying the 'Lesueur Sandstone', has a basal unit of over 100m of pedogenic shale, informally referred to herein as the 'basal Eneabba unit'. Overall, this formation is probably greater than 1km thick, but is partially eroded on the Harvey Ridge. Within the study area the 'Cattamarra Coal Measures' have been intersected in Pinjarra 1 in the northern part of the study area. The Lower Cretaceous Warnbro Group is relatively extensive, but generally no greater than 250m thick, and is overlain by a thin Cenozoic section.

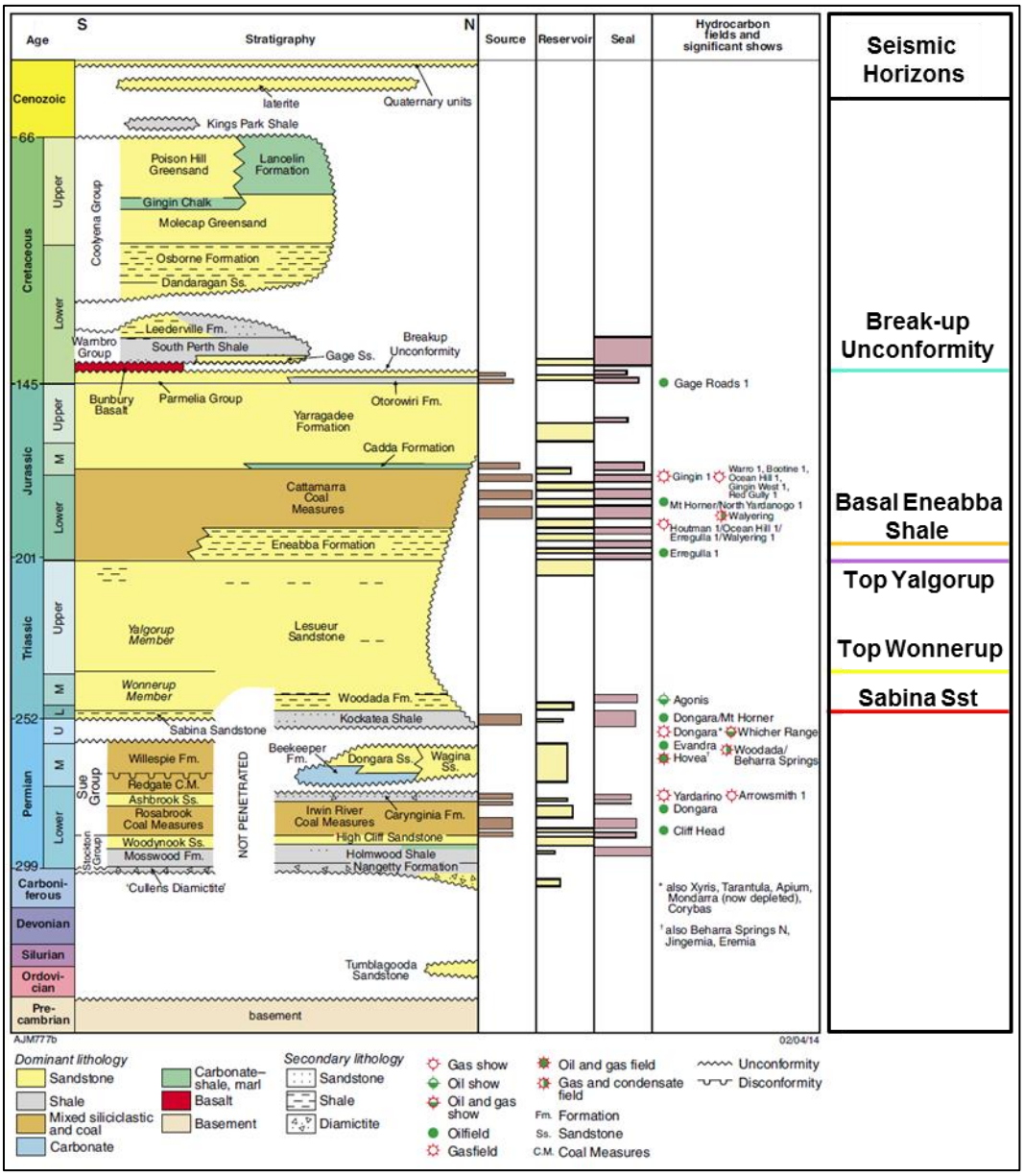

Figure 3.2 Perth Basin stratigraphy (from Y Zhan)

3.1 Seismic data sets

The seismic data set used for the interpretation was the 2017 reprocessed Harvey 3D survey. This survey was acquired by Geokinetics (Australiasia) Pty Ltd in 2014 as part of the DMP WA South West Hub Carbon Capture Storage Flagship Project. The 3D survey was acquired using vibroseis seismic sources and totals 114.81 square kilometres.

Much of the surveyed area was inaccessible due to restricted access on private properties, sensitive environmental zones, and infrastructure corridors. As such, there remain significant

data gaps within the final processed 3D volume. The impact of the data gaps extends vertically through the zone of interest for this study. The affected zones are manifested as cones of noise emanating from the surface where the restriction occurred.

As a consequence, the fold coverage is inconsistent and highly variable across the 3D area. Therefore, any horizon-based amplitude extractions will be very limited in their ability to highlight patterns that may be interpreted as geological facies variations or depositional geometries.

The original seismic data processing of the Harvey 3D was conducted by Velseis in Brisbane in 2014. This data was subsequently reprocessed by Curtin University in 2017 in an effort to improve the data quality. The specific objectives of the reprocessing were;

- To provide a more reliable data set for facies interpretation, and
- To provide a better imaged data set to enable more detailed fault interpretation.

In addition to the Harvey 3D survey, two further, high-resolution 3D surveys were acquired. These are limited in area and are located within the Harvey 3D survey area. The outline of these surveys is highlighted in (Figure 3.3) below.

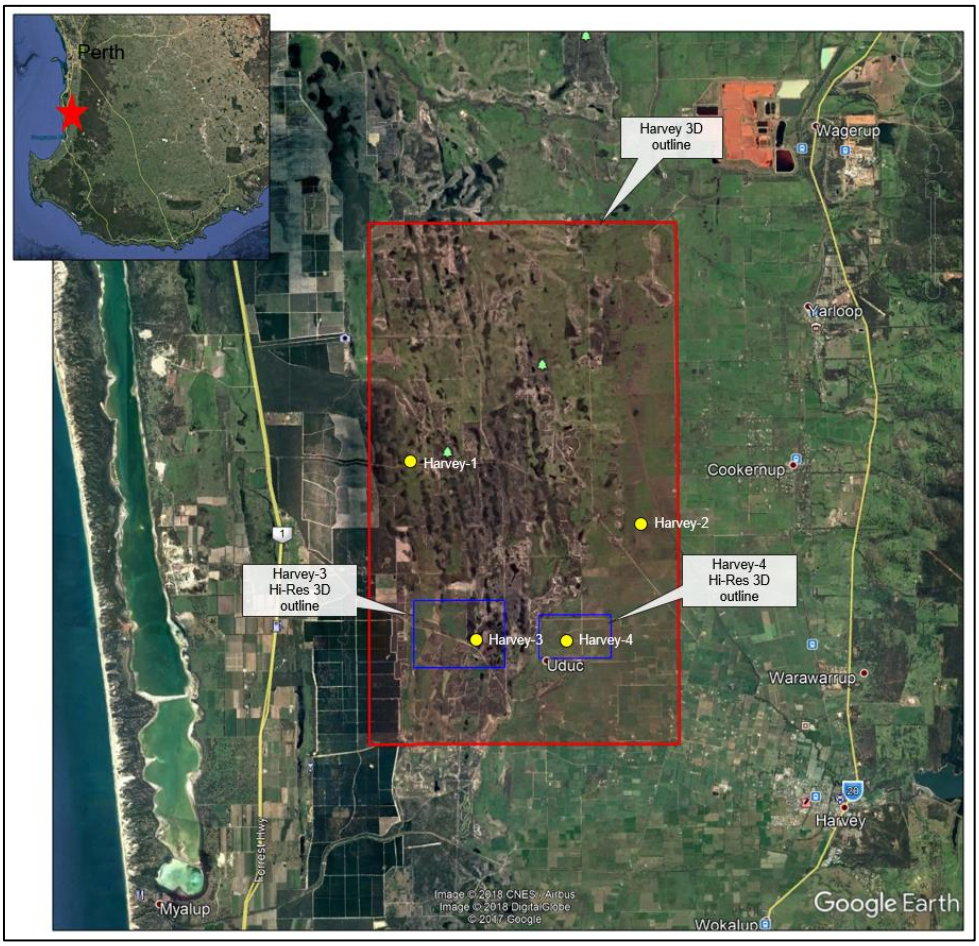

Figure 3.3 Survey Outline

These surveys are approximately centred around the DMP Harvey 3 and DMP Harvey 4 well locations.

The following SEGY products were utilised for the interpretation;

- Harvey_3D_PSTM_Gen2_agc_filt_stk_4_09_2017_Top40m.sgy
- (pre-stack Time Migrated, scaled and filtered)
- Harvey_3D_PSTM_Gen2_agc_UNfilt_stk_4_09_2017_Top40m.sgy
- (Pre-stack Time Migrated, scaled and un-filtered)
- Harvey_3D_PSTM_Gen2_PRA_stk_4_09_2017_Top40m.sgy
- (Pre-stack Time Migrated, amplitude preserved)
- Harvey_3D_Generation3_cube_PSTM_merged_Gne2_H3_H4_stk_26_10_2017.sgy
- (merged Pre-stack Time Migrated Harvey 3D, H3 Hi-Res 3D and H4 Hi-Res 3D)

In addition, the following coherency products were also utilised;

- Gen_2_Coherency_cube.sgy
- H3_Coherency_cube.sgy
- H4_Coherency_cube.sgy

3.2 Data Quality Comparison

In general, the 2017 Reprocessed Harvey 3D data set that was processed by Curtin University (Curtin) provided an improved data product in comparison to the original 2014 data processing by Velseis. A number of direct comparisons are provided in (Figure 3.4 to Figure 3.9).

A problem that affects both versions of the processing are the gaps in the data. The data gaps are the result of restricted access at the time the Harvey 3D survey was acquired. As a consequence the fold of coverage is spatially and vertically in the vicinity of the acquisition gaps. Processing is further hampered by the “data edges” the gaps have introduced – these edges typically result in migration “smiles” at these boundaries. These are unfortunately prevalent across the 3D area and thus make interpretation difficult and less reliable where they exist.

Also, as a result of the data gaps, variable fold and dispersed amplitudes where migration has been compromised, any amplitude extraction interpretation will have very limited usefulness. This is discussed later in Section 7.1.

Figure 3.4 is a direct comparison taken from an east-west line from the northern end of the Harvey 3D survey area. The inset map at the upper right corner of each figure outlines the position of the line as posted on a gridded structure surface of the Top Wonnerup Formation. The left-hand panel is the Pre-Stack Time Migrated (PSTM) from the 2014 Velseis Processing, the right-hand panel is the PSTM version of the same line taken from the 2017 Curtin reprocessed data. Please note that the labelling of In-lines (IL) and Crosslines (XL) is reversed relative to each between the two versions of processing.

The comparison in (Figure 3.4) shows improved imaging the shallow section of the Curtin version. Curtin have relaxed the mutes across the data gaps evident in the Velseis section

thereby providing the impression of better coverage. However, there is little useful signal across these zones.

The interpretation of faults is clearer on the Curtin section as the imaging is a little sharper. The Velseis version appears to have better continuity in the reflectors in the deeper section.

Similar comments apply to XL 420 and XL 317 which are provided as further examples at (Figure 3.5 and Figure 3.6) respectively. The overall signal to noise is better in the Curtin processed data albeit the appearance of lower frequency content

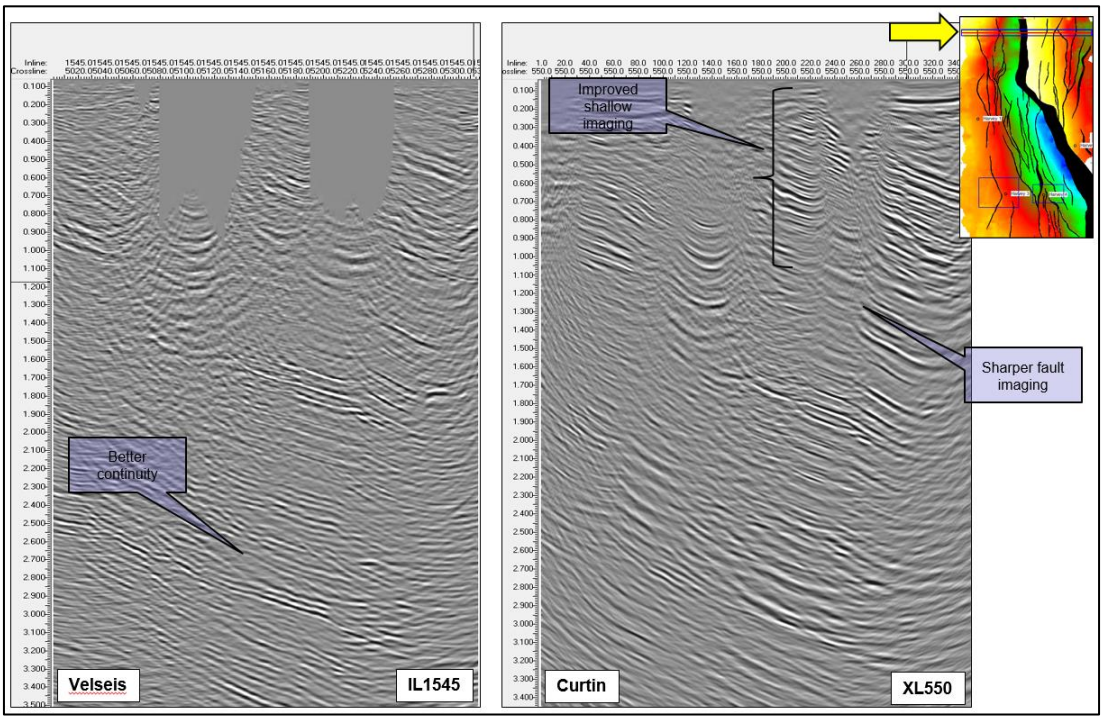

Figure 3.4 Data Processing Comparison – Curtin XL 550

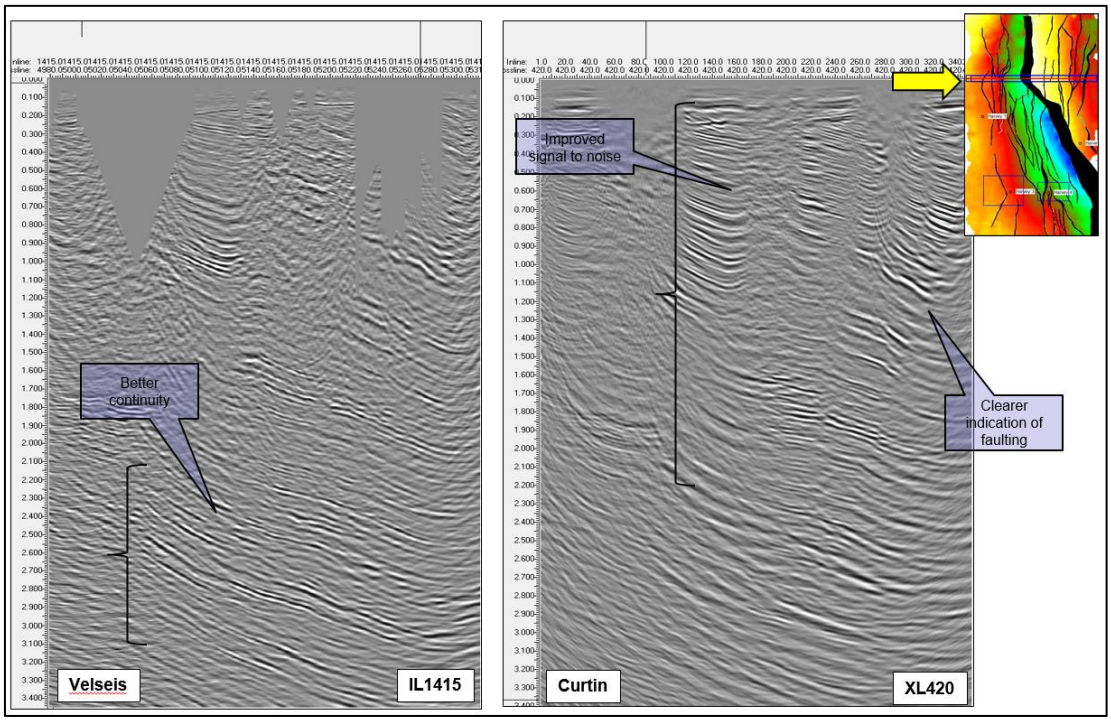

Figure 3.5 Data Processing Comparison – Curtin XL 420

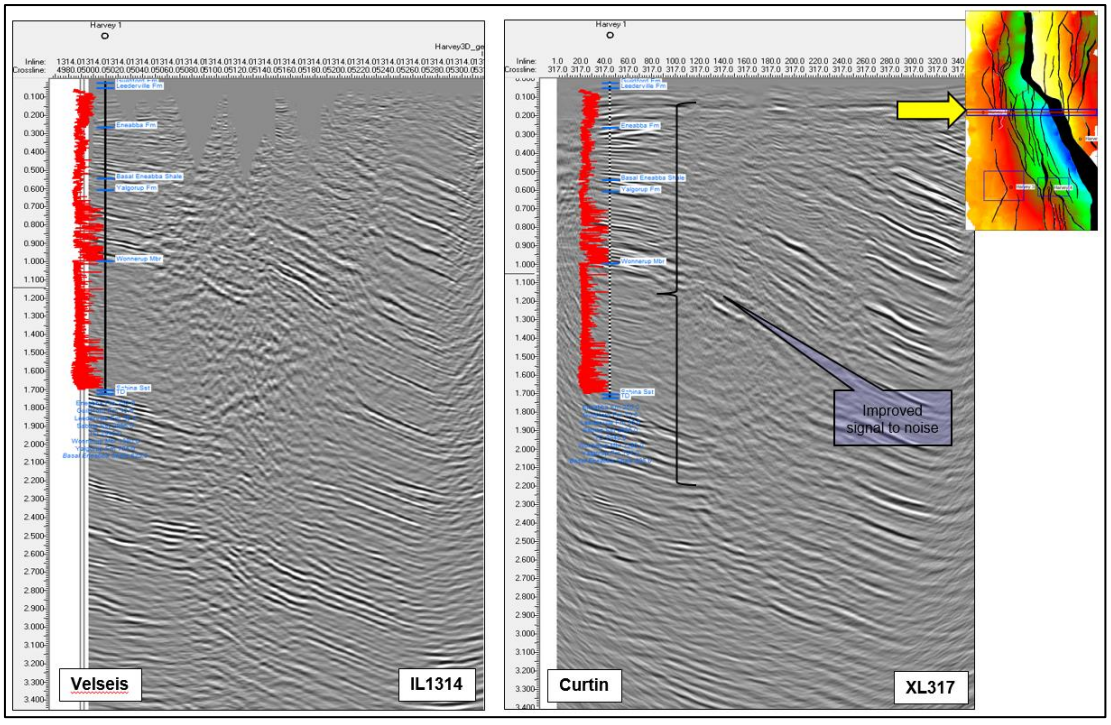

Figure 3.6 Data Processing Comparison – Curtin XL 317

Curtin XL 114 (Figure 3.7) provides a clear example of the improved fault imaging in the Curtin reprocessed data. The faults indicated on the Curtin panel are barely discernible on the Velseis section. A further point of difference is highlighted by the red, dashed ellipses on Figure 3.7 within which the dips of the reflectors is different between the two reprocessed versions. This difference is most likely the result of differing processing velocity fields that have been applied to the data. Whilst it is difficult to assess which of these is most reliable, it would be a reasonable assumption that the version with the better imaging i.e the Curtin version, would have a more appropriate velocity field and therefore better address the dips highlighted within the ellipse.

Figure 3.8 and Figure 3.9 are two further processing comparisons of sections in Curtin IL orientation (north-south). Similar comments apply.

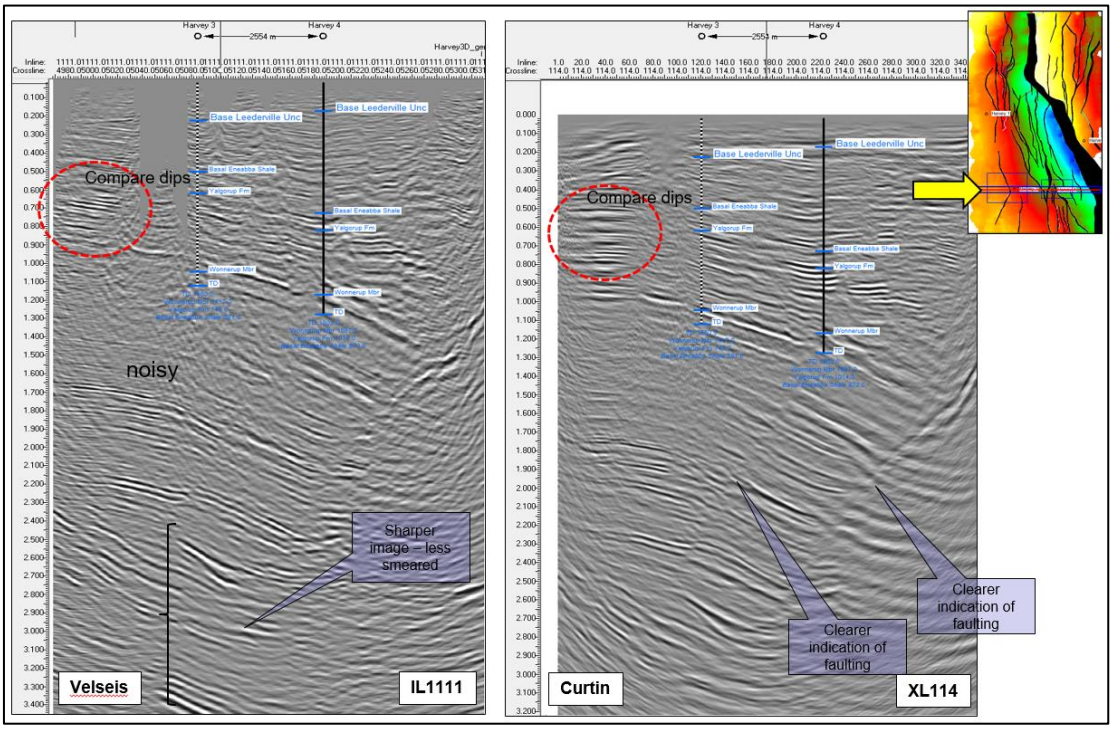

Figure 3.7 Data Processing Comparison – Curtin XL 114

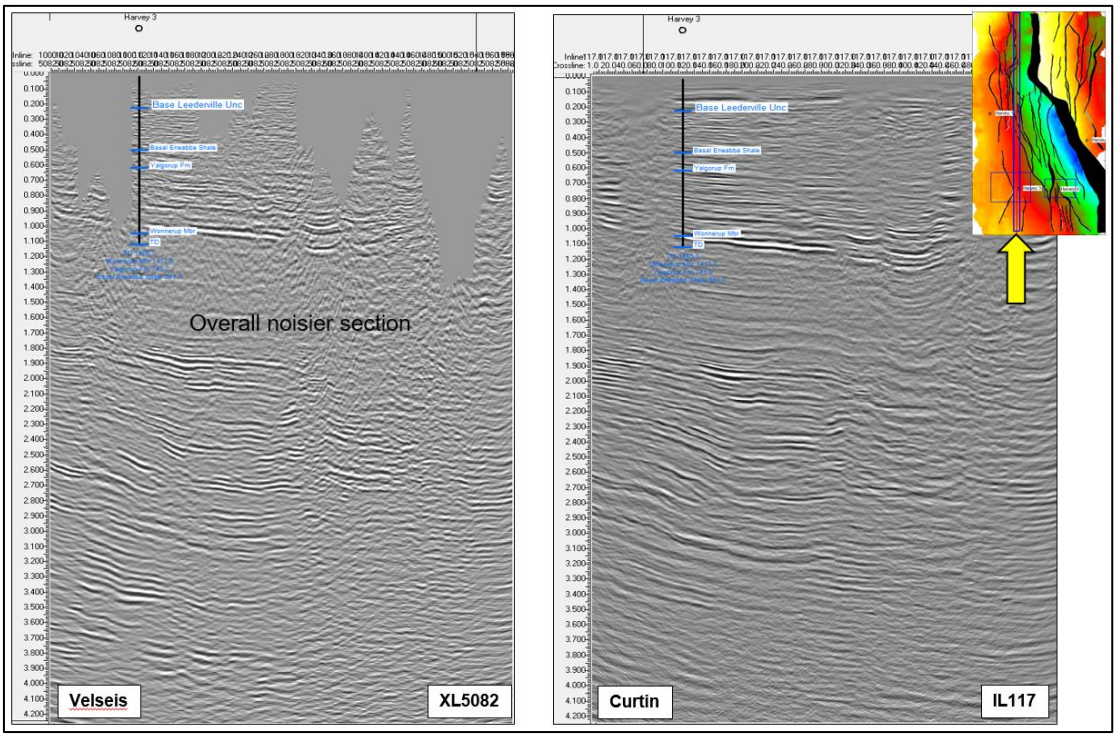

Figure 3.8 Data Processing Comparison – Curtin IL 117

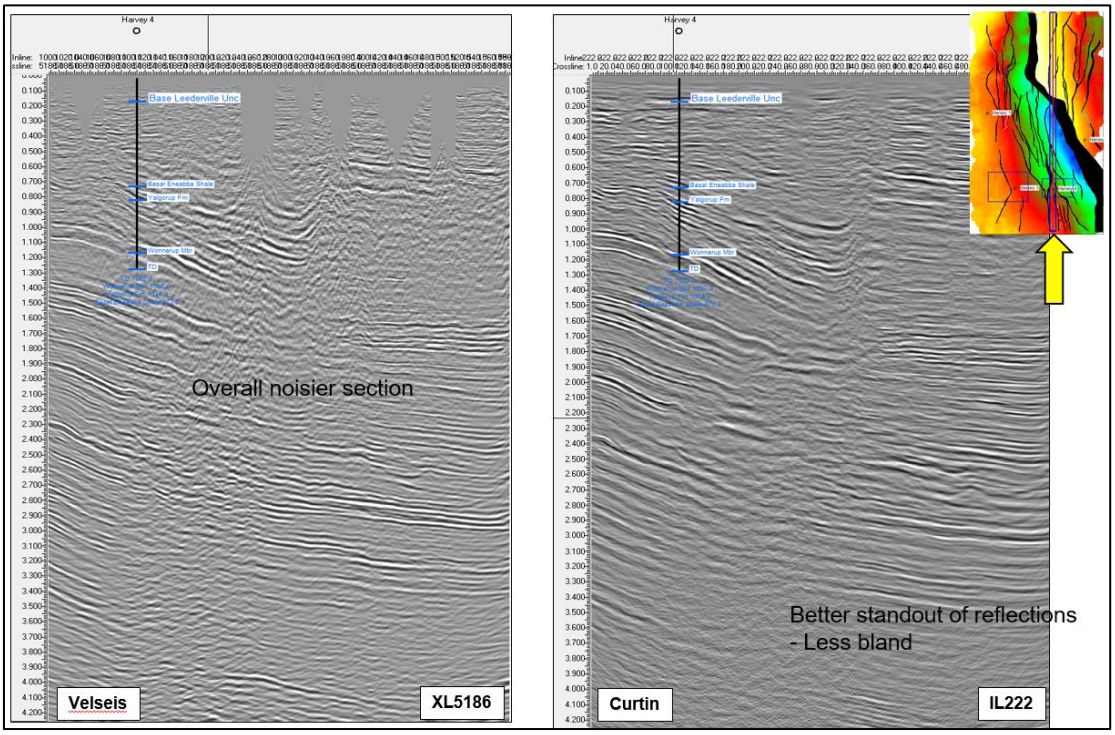

Figure 3.9 Data Processing Comparison – Curtin IL 222

4. SEISMIC INTERPRETATION

The seismic interpretation of the Harvey 3D data was undertaken in the IHS Kingdom software interpretation system.

4.1 Well Ties

There are four wells that are located within the area of the Harvey 3D survey. These are listed in Table 1 below and their locations are shown in Figure 3.3.

Table 1: Wells located within the Harvey 3D study area

Well Name	Latitude	Longitude	X(m)	Y(m)	Elevation(m)	Total Depth(m)
Harvey 1	-32.9918695	115.7744703	385502.04	6348947.56	24.48	2945
Harvey 2	-33.0088239	115.8443597	392052.65	6347141.74	16	1351
Harvey 3	-33.0376236	115.7940781	387392.24	6343895.95	20.8	1550
Harvey 4	-33.0383669	115.8214158	389946.08	6343842.51	19.89	1802

The formation tops that were used to tie the seismic interpretation to the wells are tabulated in Table 2. Time-depth data was available for each of the wells within the Harvey 3D. Sonic, density and gamma ray logs (as well as other logs), were also available for the seismic well calibration.

The GSWA Harvey 1 well is the deepest of the wells and the only well that has drilled thorough the full Wonnerup section within the Harvey 3D area. A VSP was acquired at the GSWA Harvey 1 well however, it was acquired only down to 1189m MD due to a cable failure and no points below this were acquired. Beyond that depth the integrated sonic log was used to attain time depth information. Subsequent wells DMP Harvey 2, DMP Harvey 3 and DMP Harvey 4 drilled into the Wonnerup Formation but did not drill through the complete Wonnerup section. A checkshot survey was acquired in these wells.

Table 2: Formation Tops

Surface	Harvey 1		Harvey 2		Harvey 3		Harvey 4	
	TVDSS (m)	MD (m)	TVDSS (m)	MD (m)	TVDSS (m)	MD (m)	TVDSS (m)	MD (m)
Basal Eneabba Fm	-600.5	625	-392	408	-560.2	581	-853.1	873
Yalgorup Mbr	-679.5	704	-533	549	-722.2	743	-994.1	1014
Wonnerup Mbr	-1355.5	1380	-1226	1242	-1396.2	1417	-1577.1	1597
Sabina Sst	2895.0	-2870						

The GSWA Harvey 1 well to seismic (dip section) tie is shown at (Figure 4.1). An east-west seismic line that passes through the GSWA Harvey 1 location is illustrated. The gamma log is also included for reference. For the purpose of this study, the synthetic seismograms were not created. Rather, the tops as posted on the seismic section provided a reliable and logical tie points for the Top Yalgorup member pick and the Top Wonnerup member pick. At the Top Wonnerup, this point coincides with a relatively strong reflector that marks the lithological contrast at the interface of the Yalgorup and the Wonnerup members. The gamma ray clearly reflects this contrast (see zoomed-in panel on the right-hand side of Figure 4.2). The strength and continuity of the Top Wonnerup pick (red horizon) is readily recognised across the full extent of the seismic section on the left-hand panel of (Figure 4.2).

The Top Yalgorup pick also coincides with a prominent reflector. The strength and continuity of this reflector (green horizon) is also evident on the left-hand panel of (Figure 4.2).

The corresponding well to seismic (dip section) well tie for DMP Harvey 2 is shown at (Figure 4.3) and the seismic well tie (dip section) that passes through DMP Harvey 3 and DMP Harvey 4 is shown at (Figure 4.4).

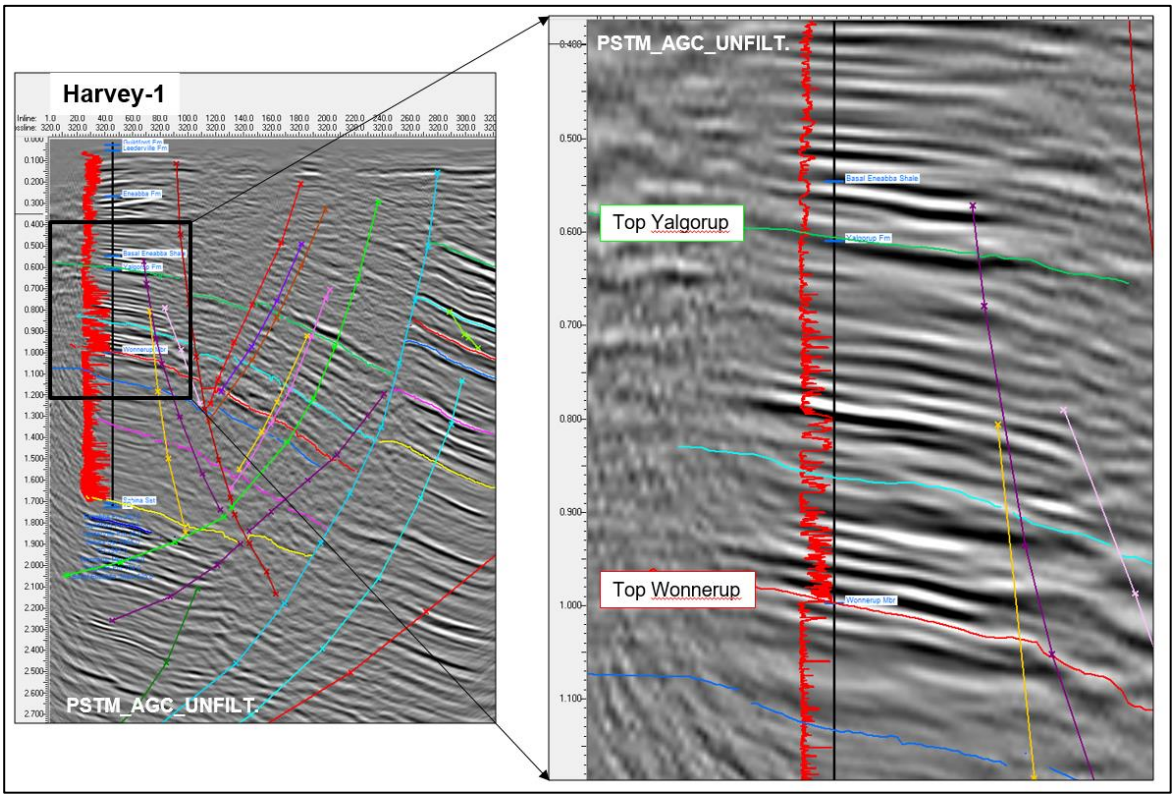

Figure 4.1 GSWA Harvey 1 Well Tie

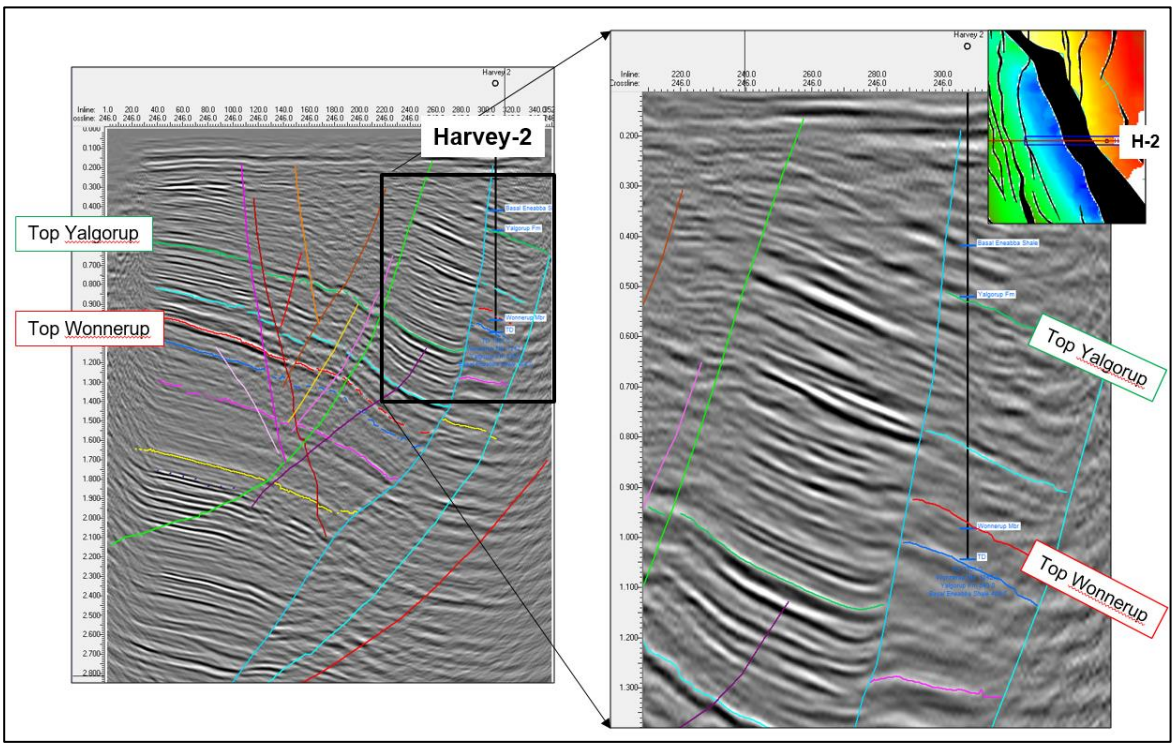

Figure 4.2 DMP Harvey 2 Well Tie

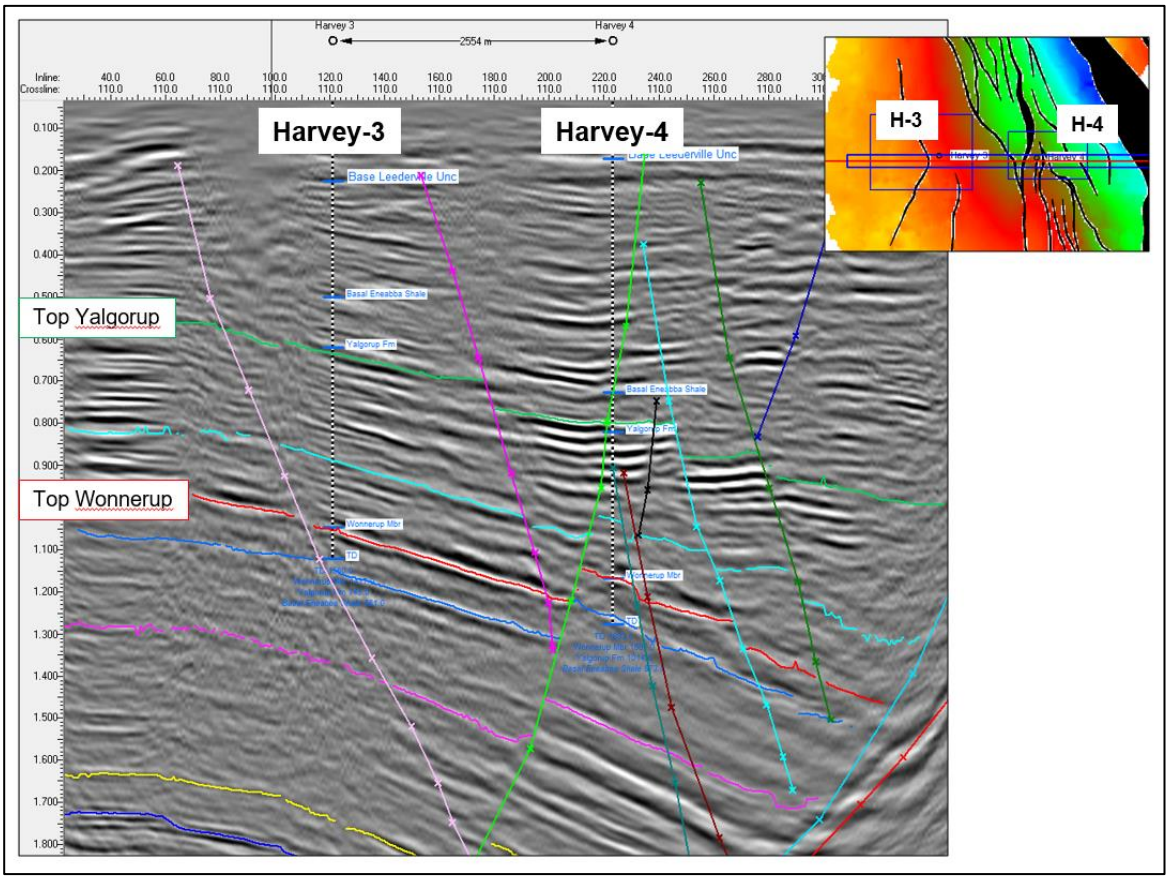

Figure 4.3 DMP Harvey 3 and DMP Harvey 4 Well Tie

A composite seismic line that passes through each of the wells (GSWA Harvey 1, DMP Harvey 2, DMP Harvey 3 and DMP Harvey 4) is provided at (Figure 4.4). This section illustrates the clear and confident pick at the Top Wonnerup (red horizon). The Top Yalgorup (green horizon) is also clear albeit to a lesser degree. Other horizons have been correlated across the study area – these are also included on the section at (Figure 4.4) and preceding sections. These are not tied to specific markers in the wells, but rather, these were interpreted as consistent intra-formational seismic events to provide additional structural control within the Yalgorup and Wonnerup sections. The consistency of the seismic markers and the tie points to the wells as seen in (Figure 4.4) provides the basis for a sound and confident interpretation.

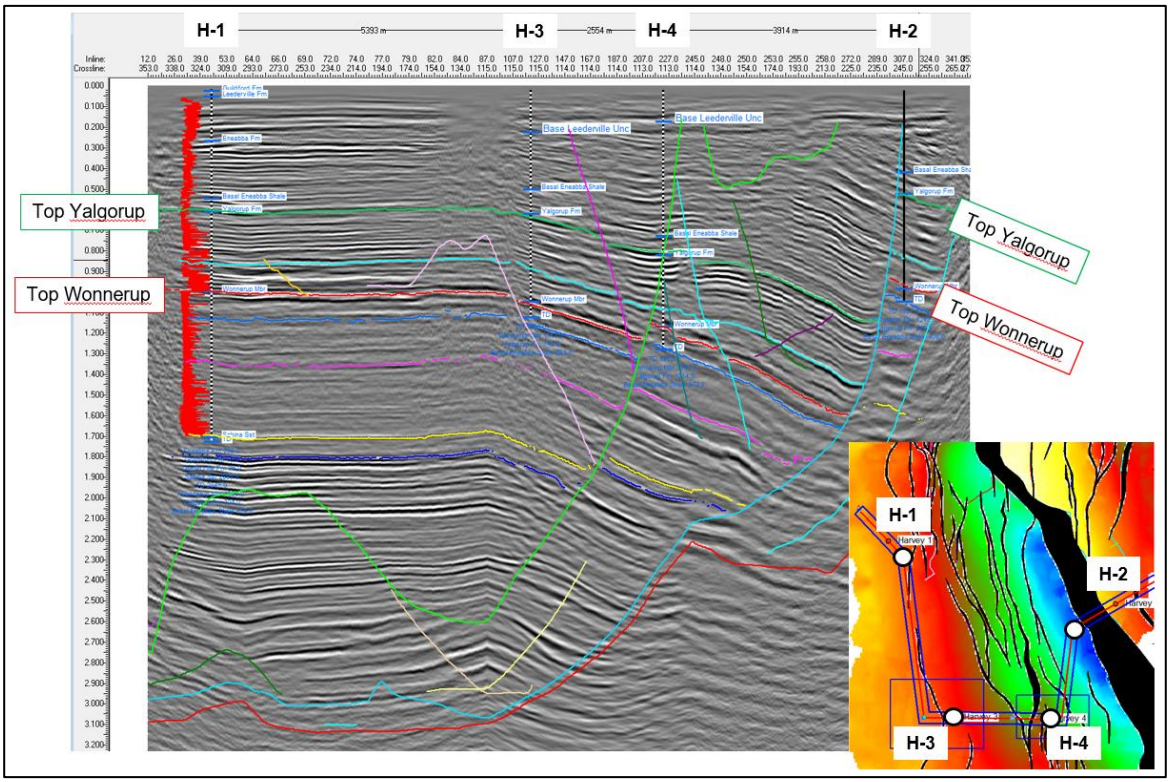

Figure 4.4 Composite Seismic Section though all four Harvey wells

4.2 Seismic Interpretation

The Pre-Stack Time Migration (PSTM) provided by Curtin University was used for the interpretation of the Harvey 3D survey. Specifically, the scaled (AGC -Automatic Gain Control) and filtered volume (Harvey_3D_PSTM_Gen2_agc_filt_stk) was used as the primary data set for the interpretation. Other volumes that were provided by Curtin, as well the previously processed version by Velseis, were utilised to validate and/or provide additional insights where variability between the volumes was observed.

4.2.1 Fault Interpretation

In this interpretation, as a matter of preference, the faults were picked before the horizons. Given the variability in the data quality and coverage, it was considered that an appropriately resolved fault model would provide a more reliable basis for the horizon interpretation. With the fault planes already established there would be better control and “boundaries” in place to limit the horizon interpretation, especially for the automatic picker. This would also prevent

the overrun of horizon picks across the fault planes (if not yet interpreted) where the position of the fault and horizon terminations are indistinct.

Figure 4.5 below is a 3-dimensional view of all the assigned fault planes in this interpretation. In total, 56 fault segments were interpreted. Faults were initially picked on the dip sections – these were the east-west crosslines of the Curtin reprocessed Harvey 3D data. These were typically picked on every 10th crossline. The faults cuts were reviewed on the north-south Inline sections and edited where required. Additional faults were interpreted on the in-lines in cases where imaging may have been clearer in the north-south orientation.

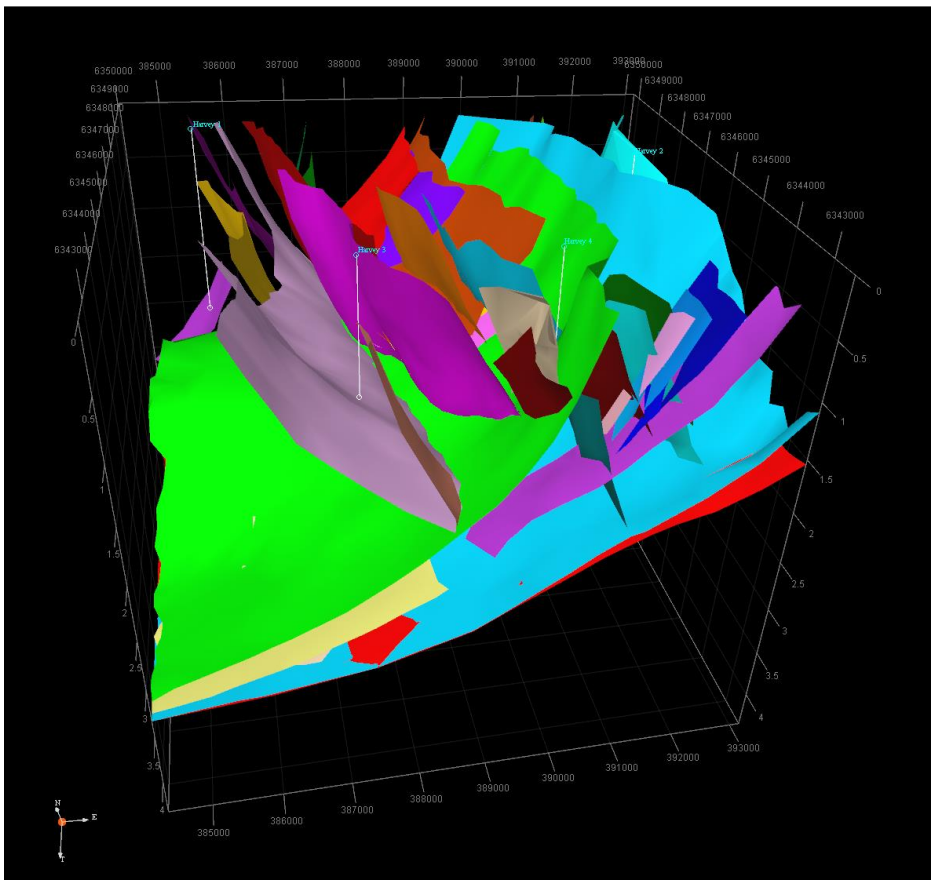

Figure 4.5 Interpreted faults – 3D view

In general, the Harvey 3D area appears to be defined by two sets of fault orientations. The area is dominated by a north-northwest-south-southeast trending fault (referred to as the F10 fault) which swings to a north-south orientation in the northern sector of the survey area. In the downthrown section of the main fault, there are a series of en-echelon sub-parallel faults with two distinct orientations – these are north-south and north-northwest and south-southeast. These fault trends as readily apparent in the representative map at (Figure 4.6).

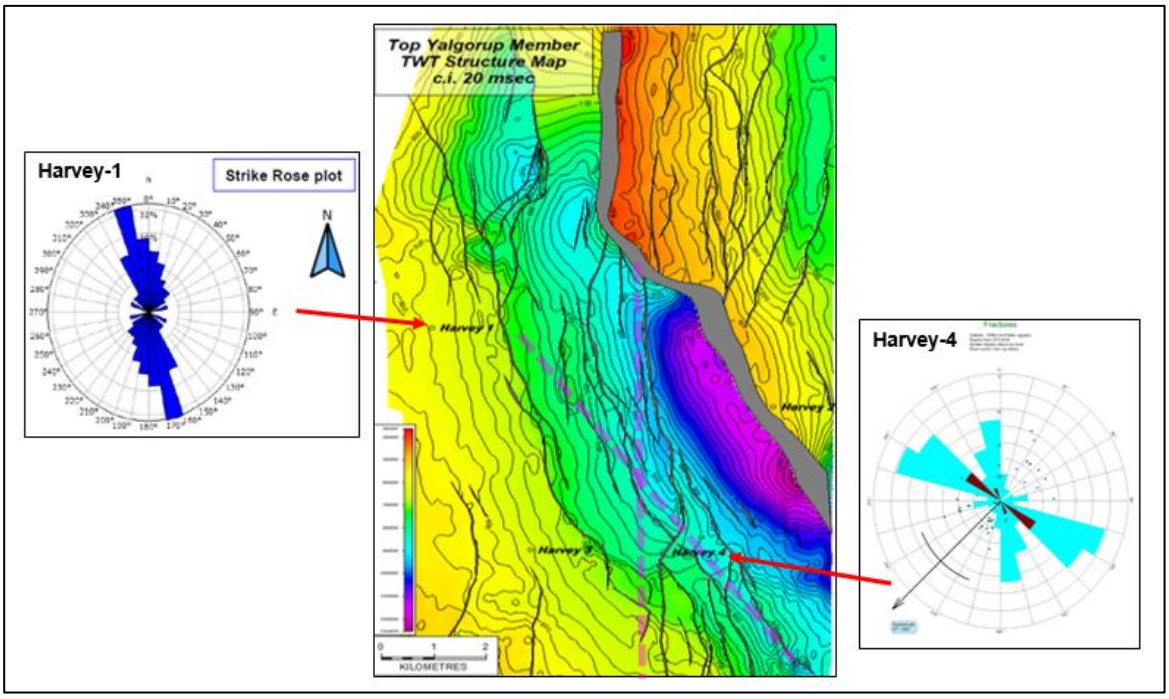

Figure 4.6 Fault orientations

The fault orientations on the map are consistent with those indicated in the Rose Plot displays for GSWA Harvey 1 and DMP Harvey 4. The magenta dashed lines on the map at (Figure 4.6) are representative of the fault trends in the vicinity of DMP Harvey 4 – these very similar to the two trends indicated in the Rose Plot for DMP Harvey 4. The Rose plot for GSWA Harvey 1 shows a single dominant trend of north-northwest – south-southeast – this too is very consistent with the orientations of the fault(s) in the vicinity of GSWA Harvey 1.

4.2.2 Horizon Interpretation

Six horizons were interpreted across the Harvey 3D area. These are listed below;

1. Top Yalgorup Member
2. Intra-Yalgorup Marker
3. Top Wonnerup Member
4. Intra Wonnerup Marker 2
5. Intra Wonnerup Marker 1
6. Top Sabina Sandstone

These are also highlighted on a representative section at (Figure 4.7).

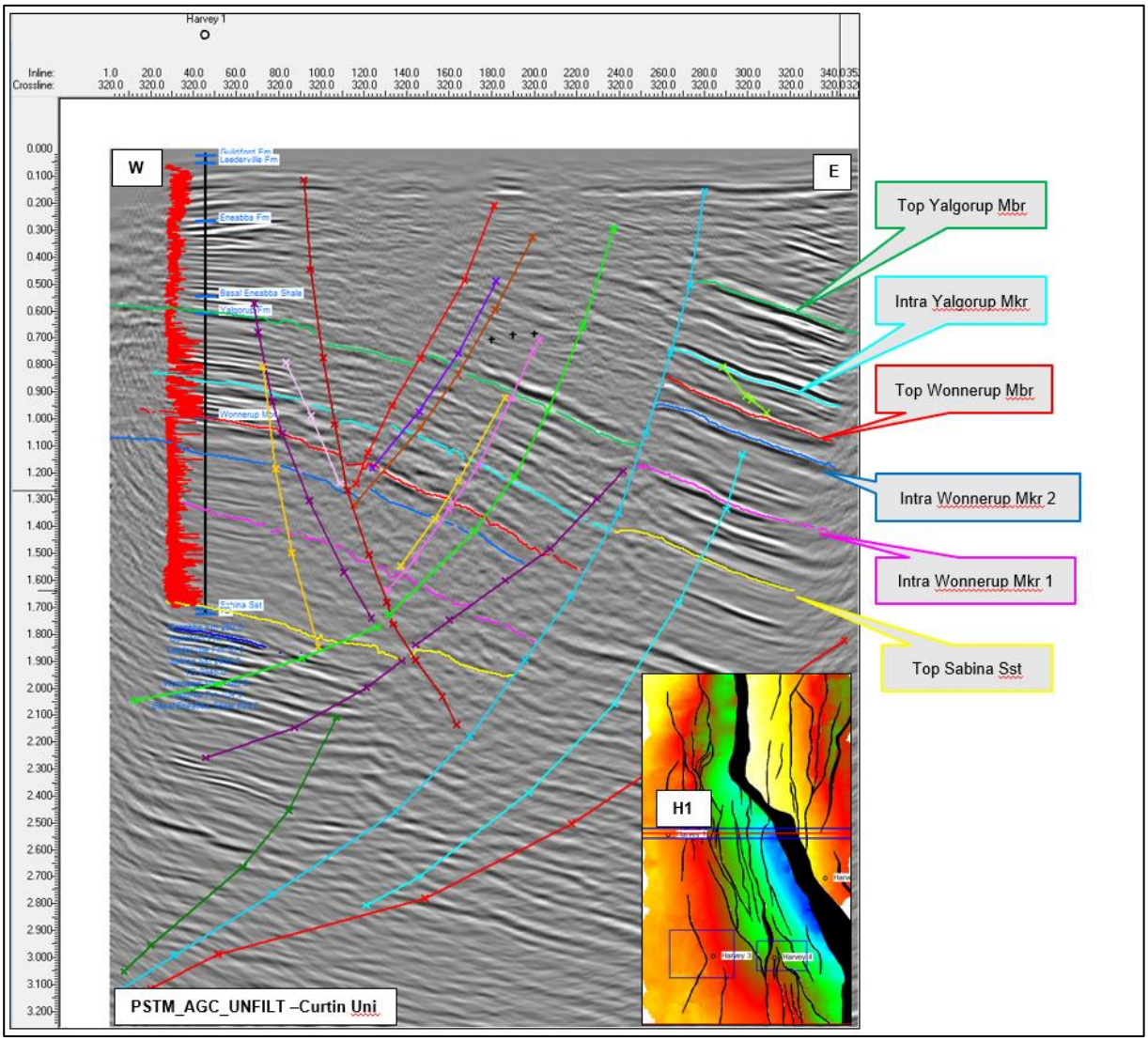

Figure 4.7 Horizons interpreted with GSWA Harvey 1 well tie

Surfaces shallower than the Top Yalgorup were not interpreted for this study as these were not particularly relevant to the scope of the study. In any case, these had been interpreted in a previous study using the Velseis processed Harvey 3D data set. Given the relatively simple structuring at the shallow levels, an interpretation of these shallow horizons on the reprocessed data will provide little additional value.

Wherever possible, the autotracker was employed for the interpretation however, given the generally poor data quality due to acquisition access restrictions, the autotracker had limited range capability. To assist the autotracker across more difficult areas, horizons were often picked manually across an approximate uniformly spaced grid network of lines to then guide

the autotracker. Data quality was certainly better in the southern sector of the 3D area allowing for a more consistent and complete interpretation.

Figure 4.8 to Figure 4.13 are series of dip lines (east-west) across the extent of the 3D area – these have been included below to illustrate how the geology and interpretation vary from north to south. Figure 4.14 to Figure 4.18 illustrate the same by viewing a series of strike lines (north-south) from west to east.

It is readily evident that the Yalgorup section (green horizon to red horizon) is seismically more reflective than the underling Wonnerup section (red horizon to yellow horizon). This is particularly clear on (Figure 4.11) and (Figure 4.12) for example.

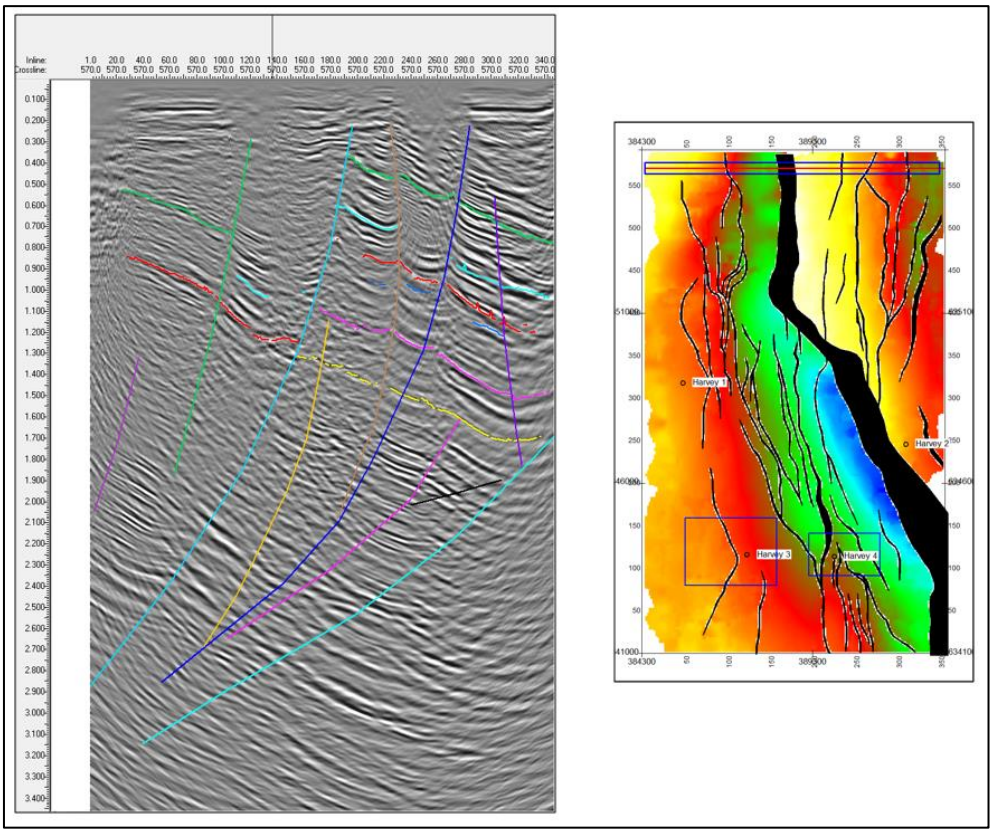

Figure 4.8 Seismic Interpretation Example: XL 570

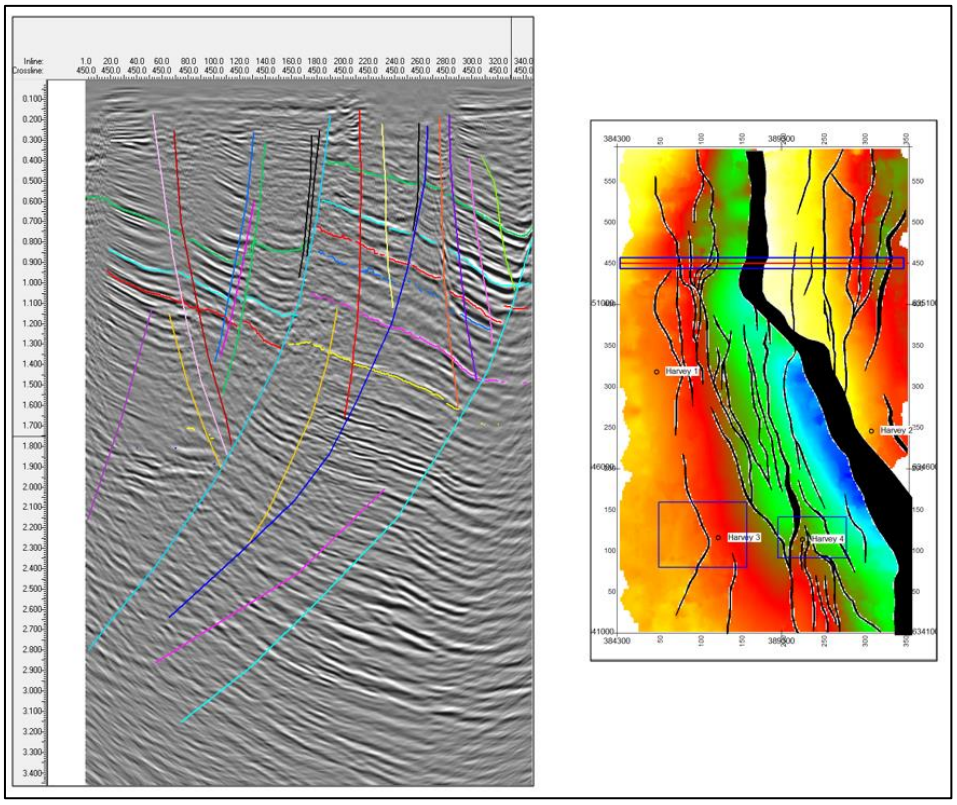

Figure 4.9 Seismic Interpretation Example: XL 450

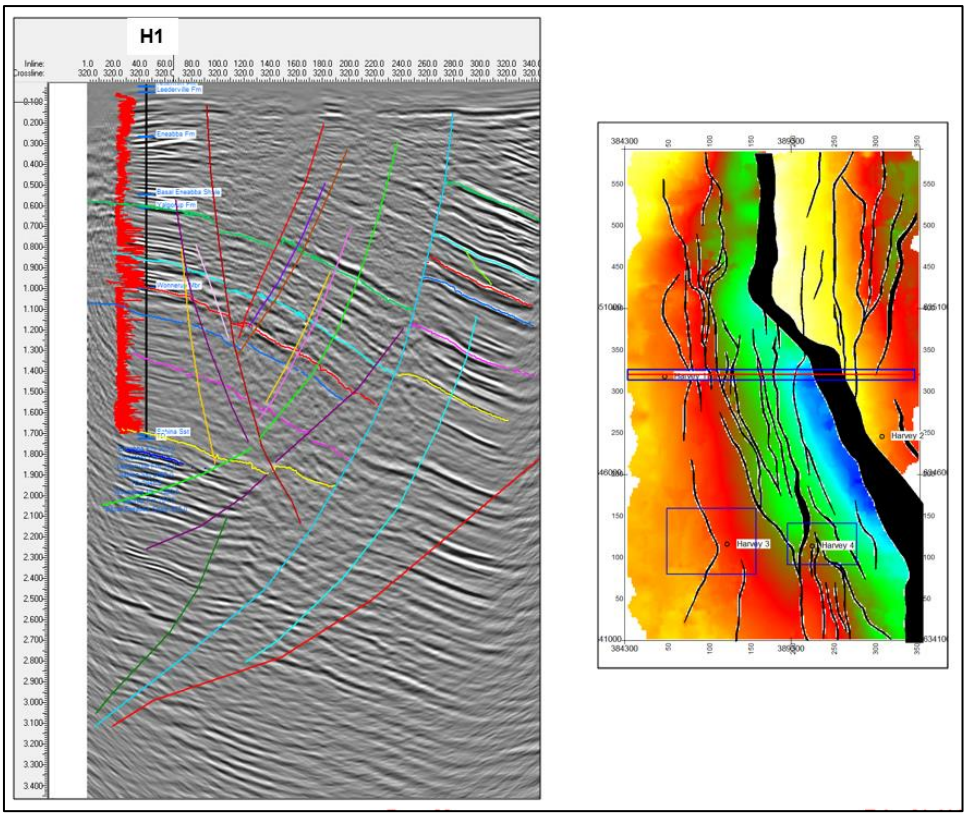

Figure 4.10 Seismic Interpretation Example: XL 320

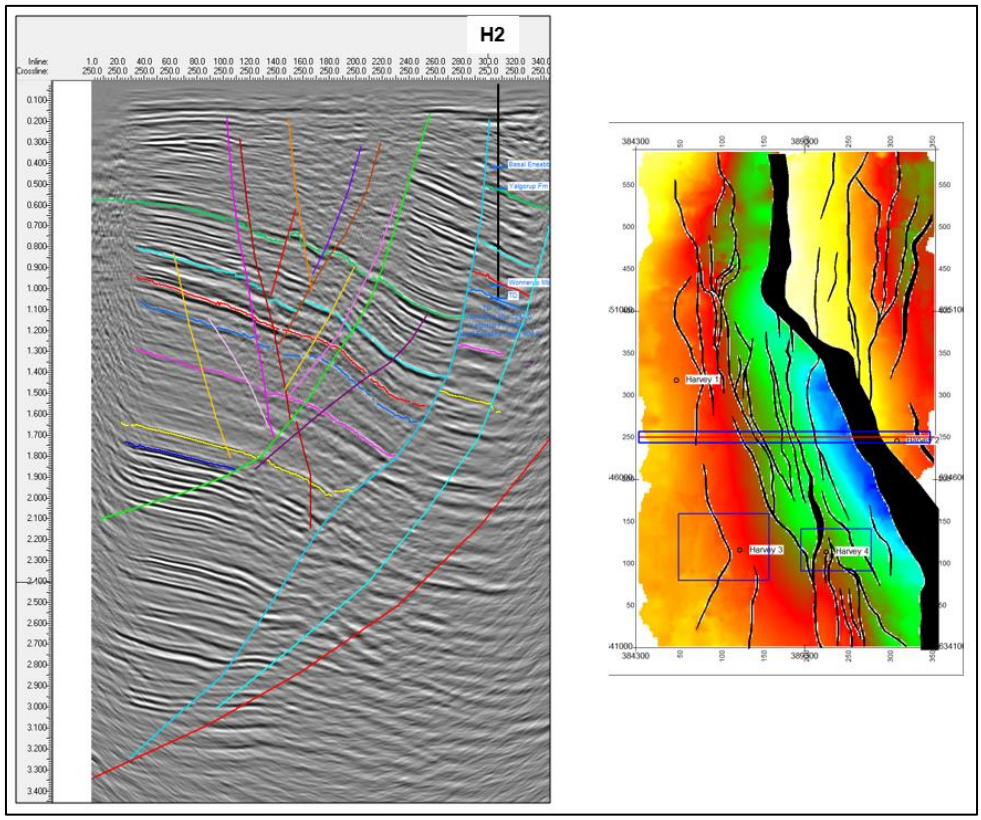

Figure 4.11 Seismic Interpretation Example: XL 250

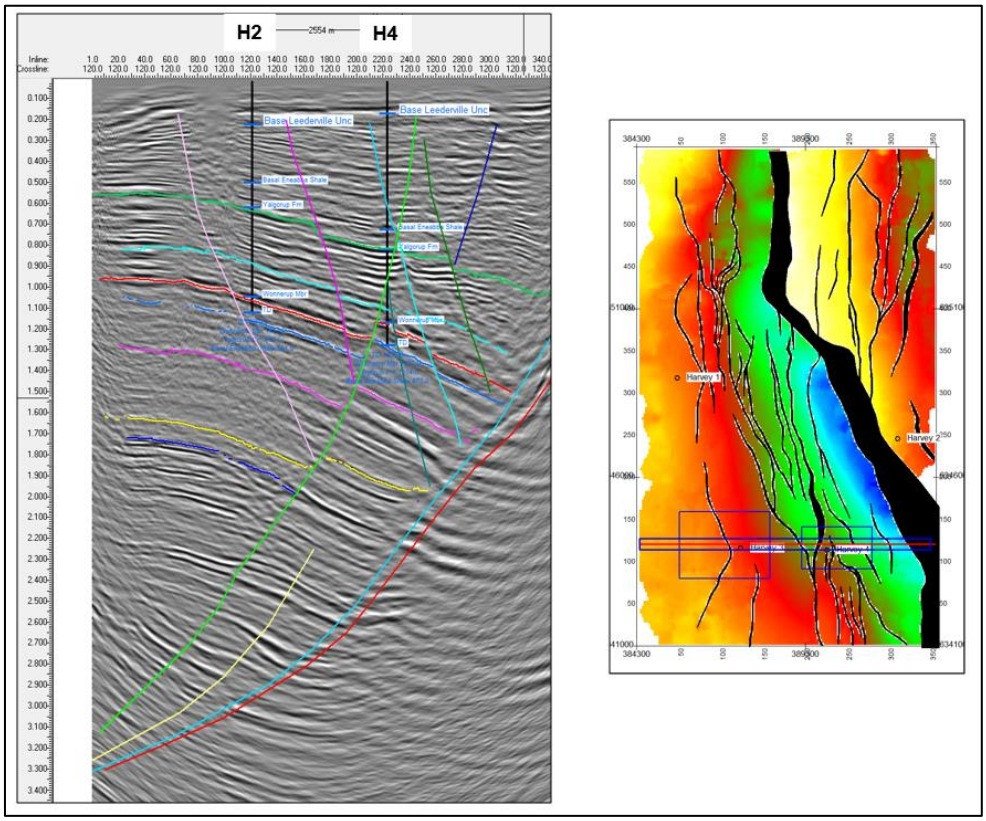

Figure 4.12 Seismic Interpretation Example: XL 120

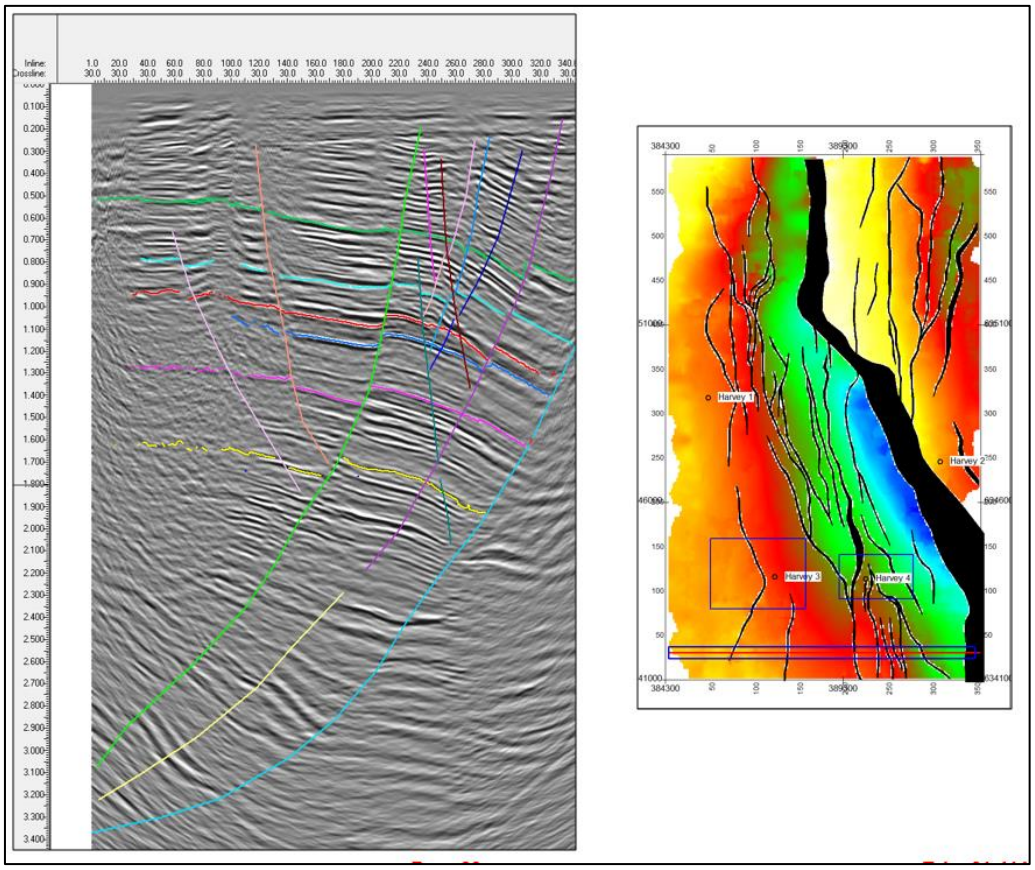

Figure 4.13 Seismic Interpretation Example: XL 030

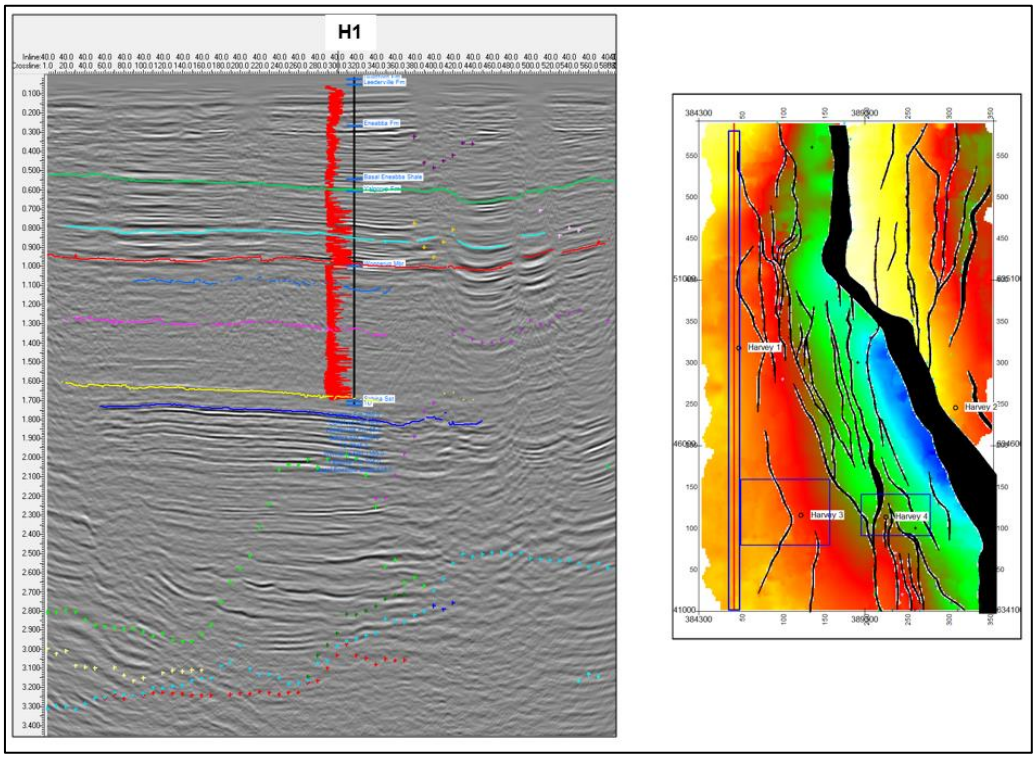

Figure 4.14 Seismic Interpretation Example: IL 40

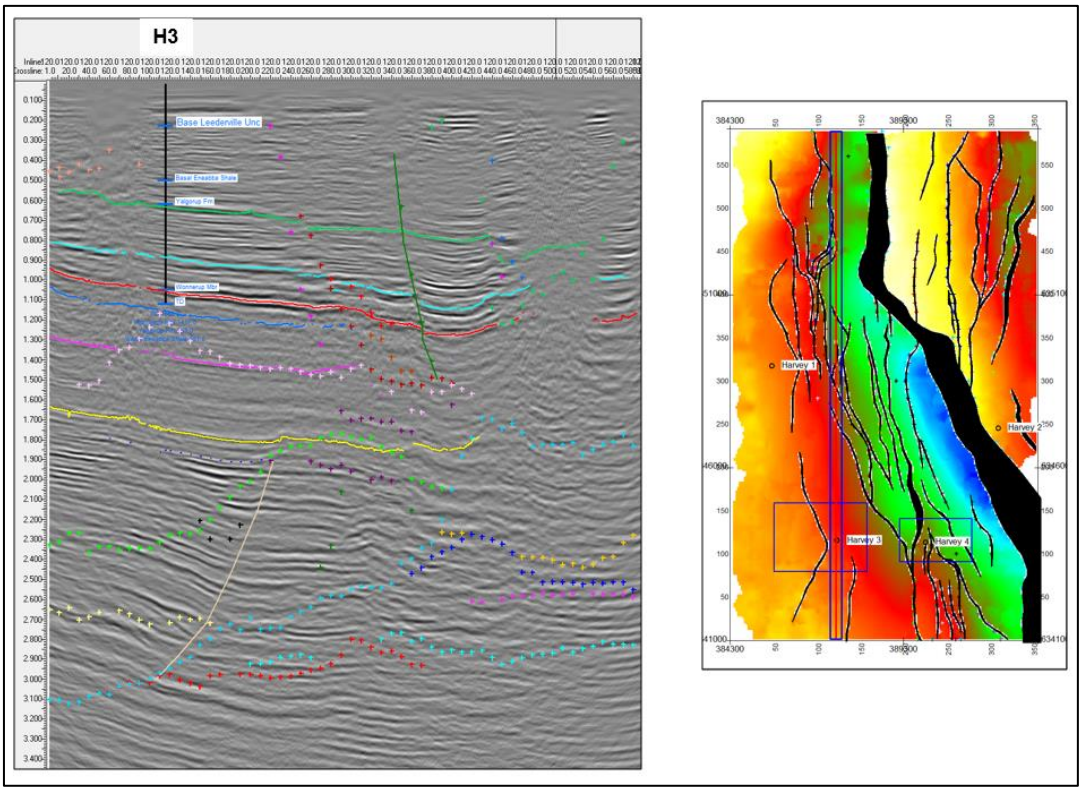

Figure 4.15 Seismic Interpretation Example: IL 120

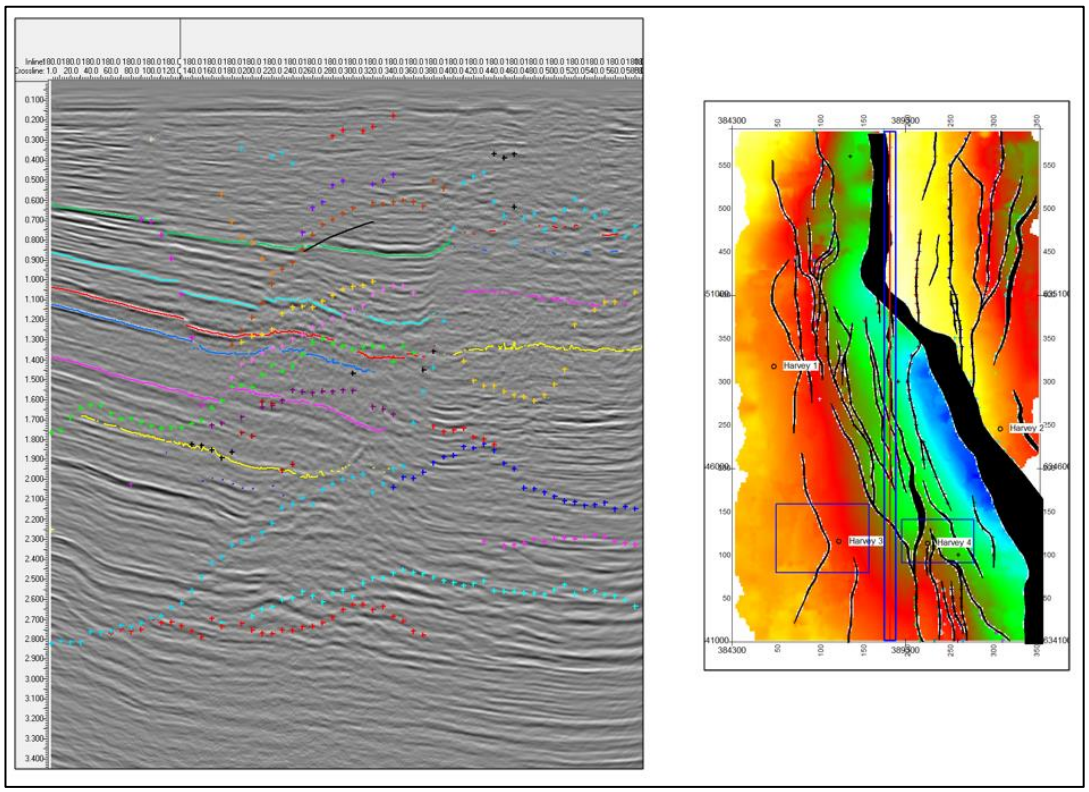

Figure 4.16 Seismic Interpretation Example: IL 180

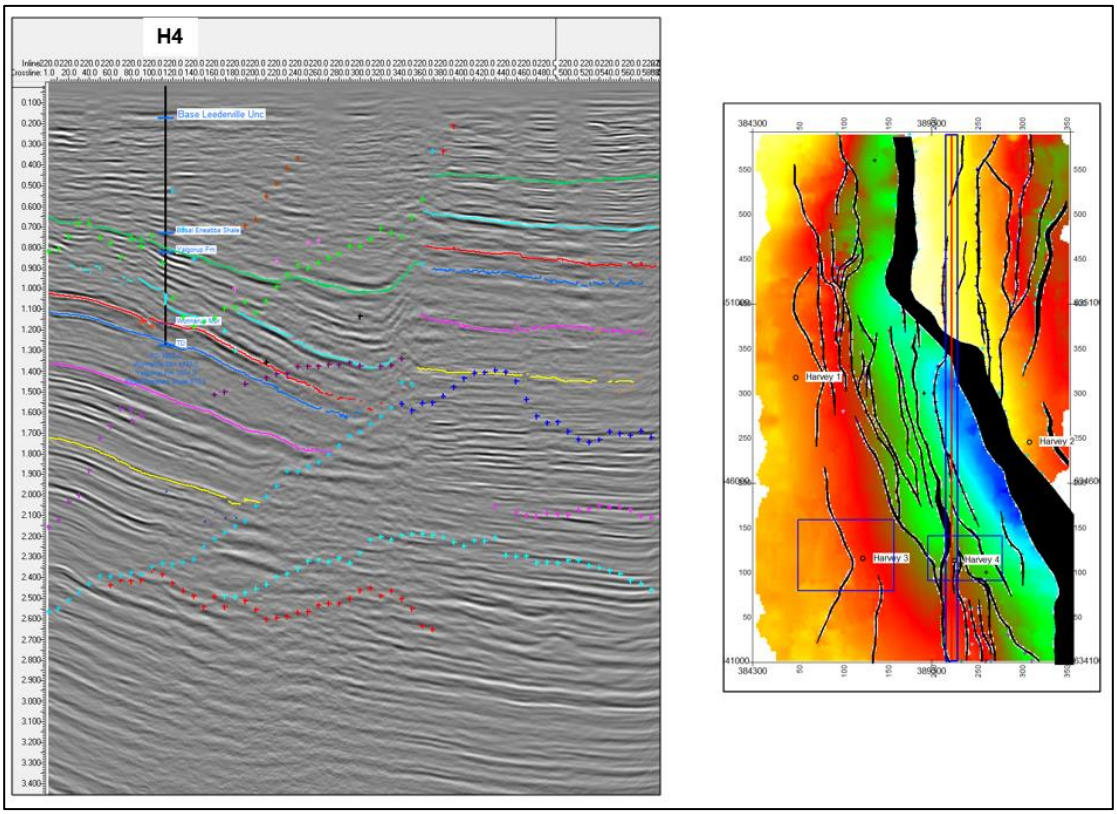

Figure 4.17 Seismic Interpretation Example: IL 220

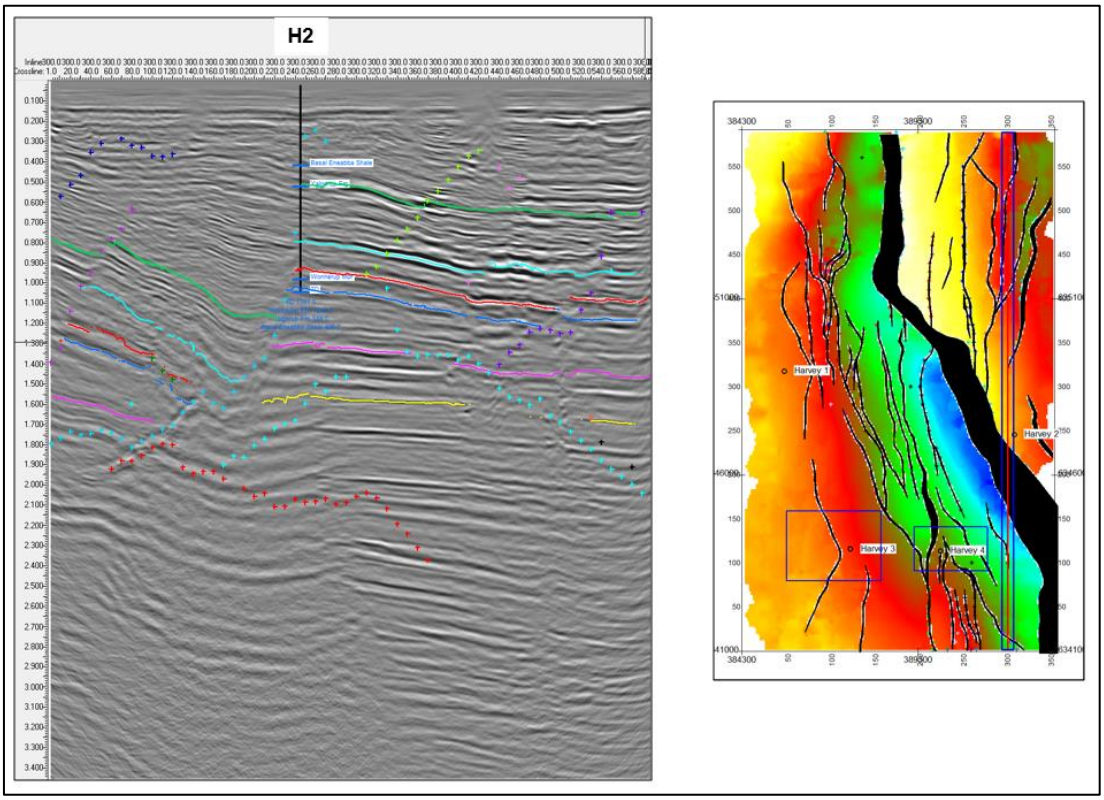

Figure 4.18 Seismic Interpretation Example: IL 300

5. TWO WAY TIME MAPPING

Two way time structure maps were created for each the interpreted horizon.

Fault polygons were manually drawn within the Kingdom software platform for each horizon by correlating the assigned fault cuts on the base map for each surface. The fault polygons, along with the raw (un-gridded) two-way time seismic interpretation for each of the picked surfaces were exported from Kingdom and imported into the Petrosys Mapping software package

Within Petrosys, the data for each surface were gridded and contoured. Various mapping parameters, including grid cell dimensions and smoothing algorithms, were trialled in order to select the optimum parameters for generation of the final two-way time structure maps. In general, a grid cell size of 50m x 50m was employed for the gridding.

The final two-way time structure map for each of the interpreted horizons is presented at (Figure 5.1) to (Figure 5.4) below. In each of these figures, the panel on the left-hand side is a representative section with all interpreted horizons included but with the horizon relevant to the map on the right-hand side emboldened on the section.

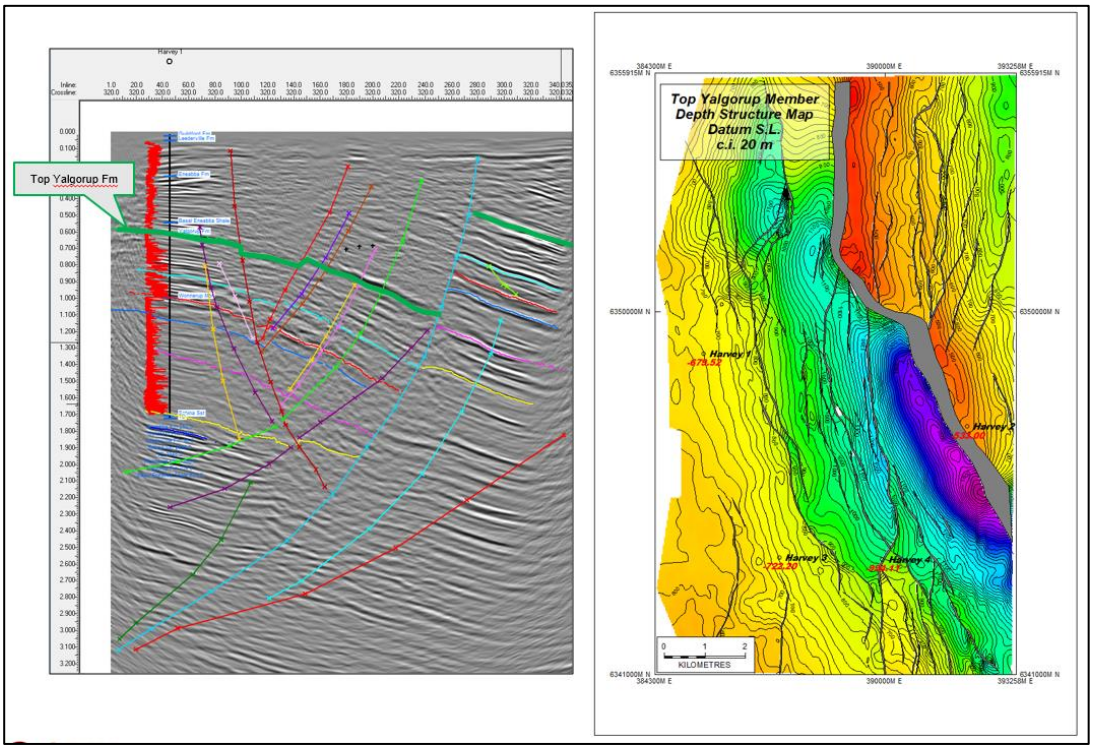

Figure 5.1 Top Yalgorup TWT Structure Map

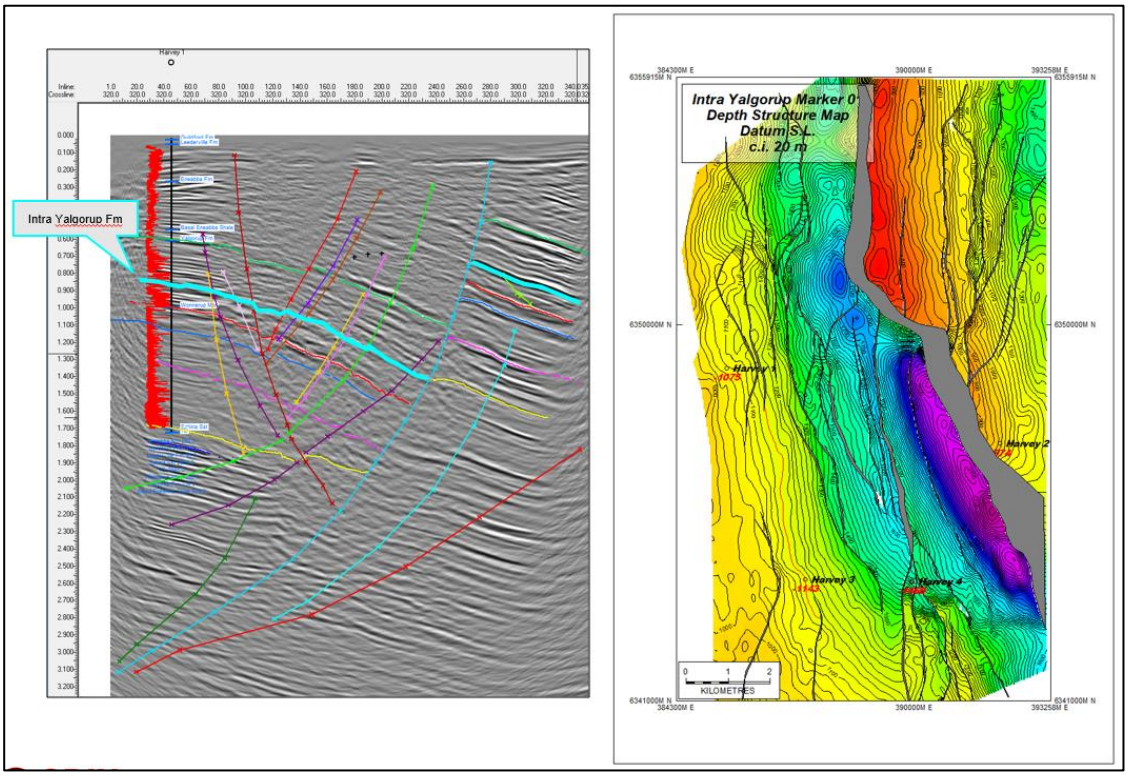

Figure 5.2 Intra Yalgorup TWT Structure Map

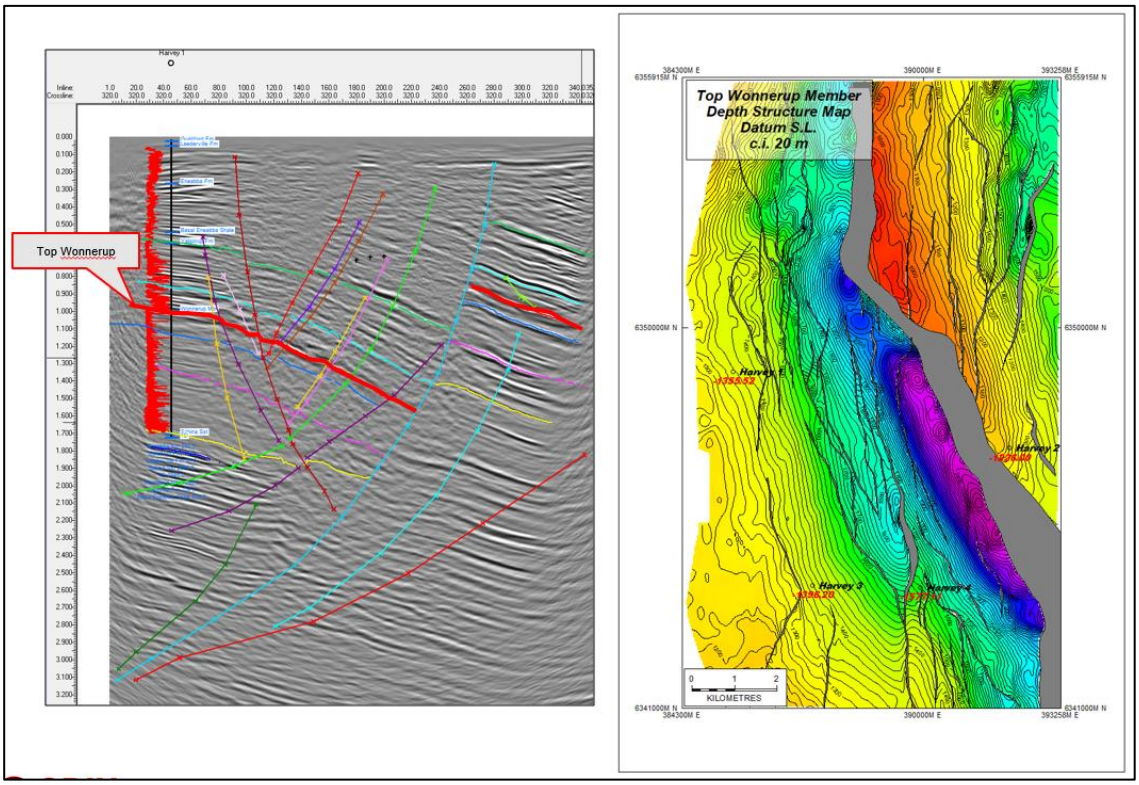

Figure 5.3 Top Wonnerup TWT Structure Map

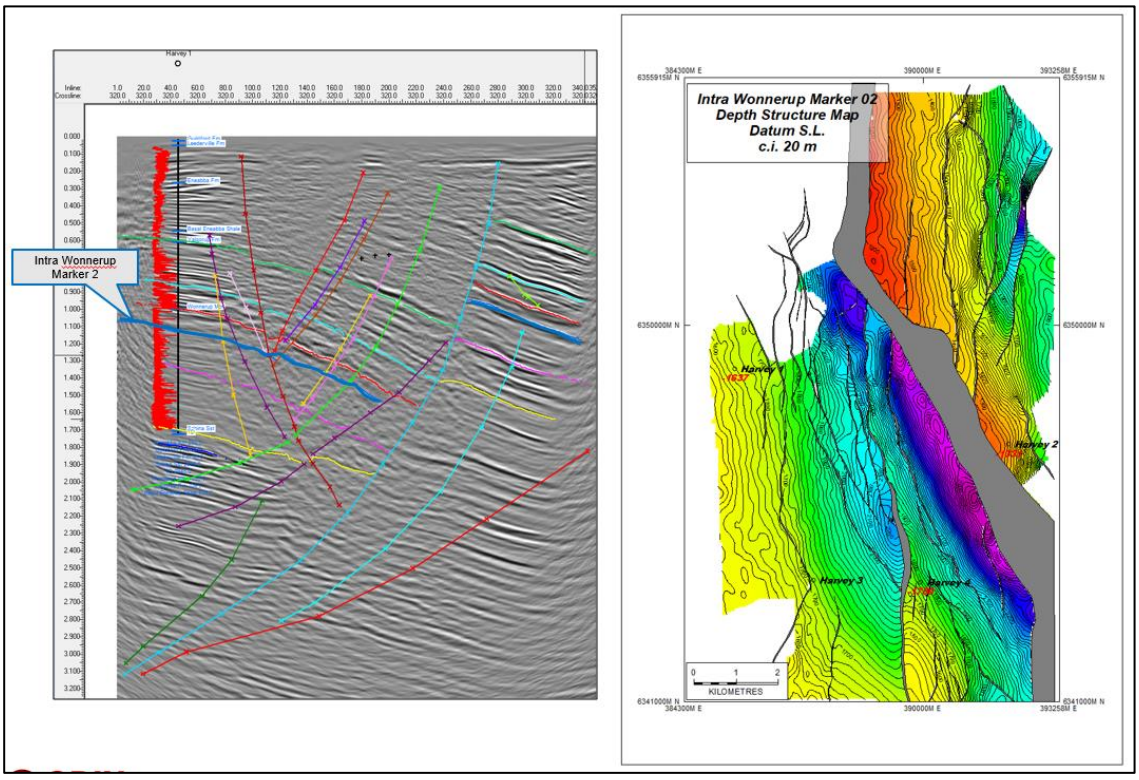

Figure 5.4 Intra Wonnerup Marker 02 TWT Structure Map

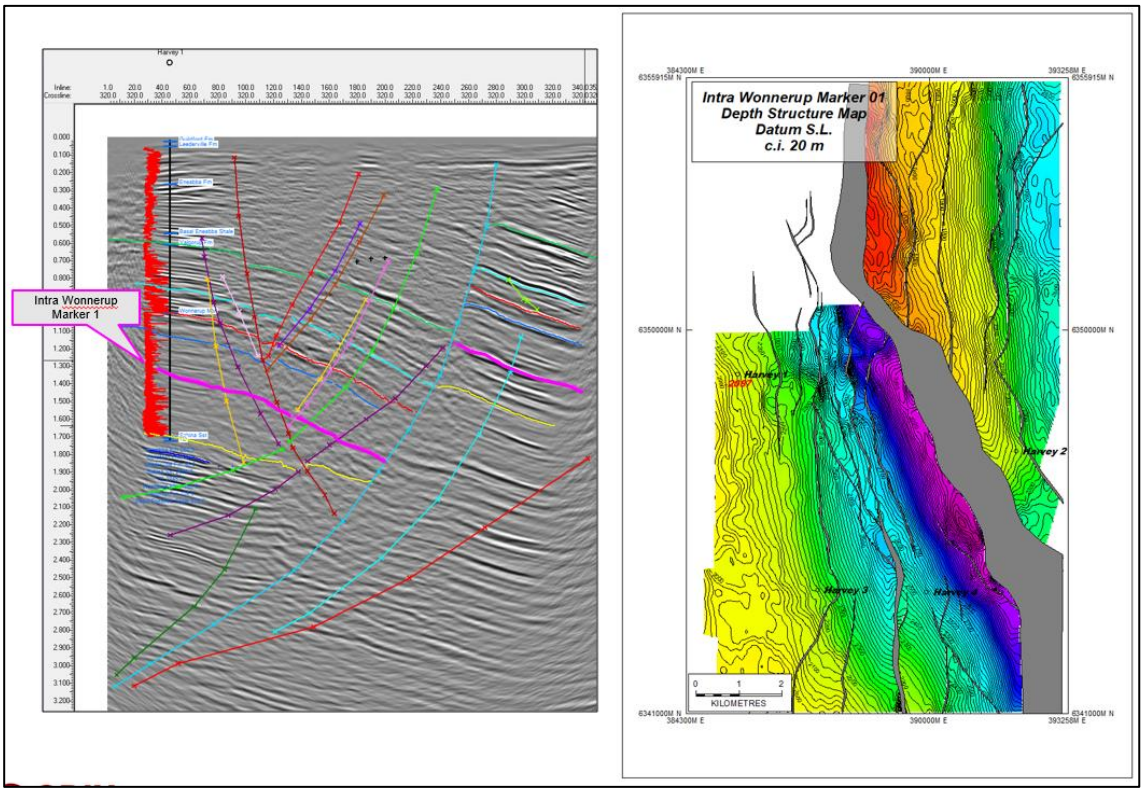

Figure 5.5 Intra Wonnerup Marker 01 TWT Structure Map

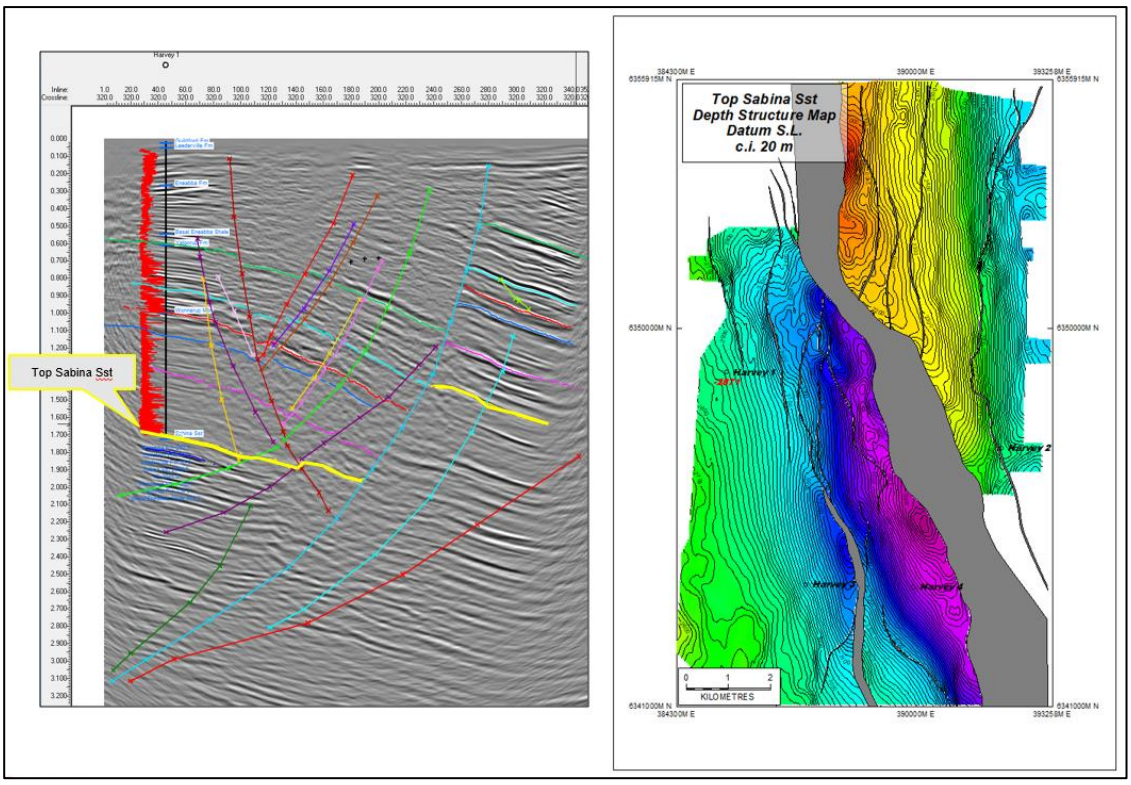

Figure 5.6 Top Sabina Sandstone TWT Structure Map

The structural form of these horizons are very similar to each other. The survey area is dominated by the major, generally north-south fault designated the 'F10' fault. The fault patterns have been described in Section 4.2.1.

The Top Yalgorup Member (Figure 5.1) represents the upper shalier/mudstone upper unit of the Lesueur Formation. This reflector has a strong seismic amplitude character and corresponds to the top of the containment unit overlying the Wonnerup Member. The Yalgorup Member interval is comprised of a sequence of interbedded sands and shales, deposited within a channelized environment. The sands are typically higher energy point bar sands. The channelized nature of the Yalgorup section makes it difficult to map individual units to any great extent. However, the Intra Yalgorup Marker (Figure 5.2) was identified as a relatively strong, continuous marker across the majority of the survey area. This reflector was picked in order to provide an additional control surface between the Top Yalgorup and Top Wonnerup surfaces as required for the reservoir modelling study. An intra Yalgorup surface had not been previously interpreted.

The Top Wonnerup Member (Figure 5.3) represents the top of the Lower Lesueur Formation. In contrast to the Yalgorup Member, the Wonnerup Member is seismically more homogeneous. A complete section was intersected at GSWA Harvey 1 which is interpreted to be largely comprised of stacked, amalgamated braided stream deposits with only minor shaley streaks – these are more common in the lower part of the Wonnerup unit. The seismic section shown at (Figure 5.7) which passes through the GSWA Harvey 1 well, illustrates the contrasting seismic character between the more reflective Yalgorup Member section and the relatively blander Wonnerup Member section

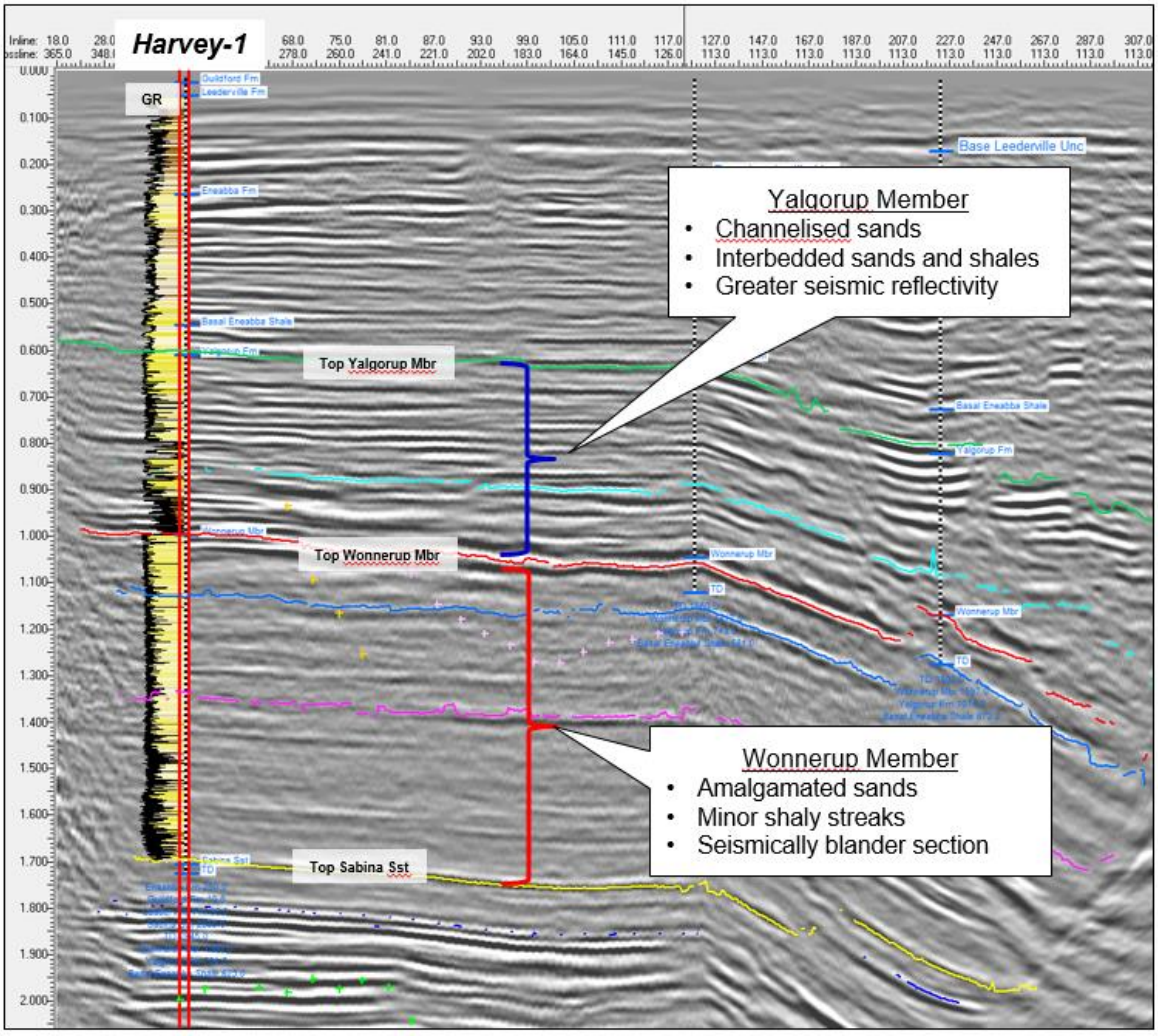

Figure 5.7 Seismic section through GSWA Harvey 1 illustrating contrasting seismic reflectivities

The maps at (Figure 5.4) and (Figure 5.5) are two additional seismic markers that have been identified within the Wonnerup section. These too have not been previously interpreted and have been included within this study to provide additional control for subsequent reservoir modelling studies.

The deepest horizon that has been mapped is the Top Sabina Sandstone which was intersected at the base of the GSWA Harvey 1 well. This event also represents the base of the Wonnerup succession.

Data quality deterioration has impacted the deeper surfaces below the Top Wonnerup – particularly in the northwest and southwest sectors of the survey area.

6. DEPTH CONVERSION

6.1 Velocity Mapping

As part of the data processing products, an ASCII format file of the Harvey 3D smoothed, average velocity profiles was provided by the Curtin University Data Processing Department. These were derived from the stacking velocities.

These ASCII profiles of TWT vs average velocity were loaded into Petrosys mapping software at their specified locations and QC'd.

Once loaded, a horizon slice of the average velocity values coinciding with the TWT of the horizon (calculated at the grid position for each of velocity profiles), was able to be extracted from the velocity profiles.

As a further quality control, the average velocity profile nearest each of the wells within the area of the Harvey 3D, was compared the average velocity profile for each of the wells. The comparisons are provided at (Figure 6.1). In general, there is reasonable agreement between the curves considering that these are not precisely co-located and that the processing based average velocities have been derived from stacking velocities – these can be very much affected by data quality. The latter is especially relevant in the Harvey 3D data set given the data acquisition limitations and the impact this has had on the data processing.

The average velocity profiles for each of the wells were also compared against each other – this comparison is shown at (Figure 6.2). At a time of say 900msec (within the section of interest), represented by the black dashed line on the plot and seismic section (note the time scales are matched to each other), the GSWA Harvey 1 (H1) profile (orange) and the DMP Harvey 3 (H3) profile (yellow) are approximately coincident. This is not surprising given the similarity in the stratigraphic intersection in each of these wells at the 900msec time line on the section on the right-hand panel (i.e. the 900msec line occurs just below the light blue marker on the section for those two wells). This would suggest there is negligible lateral velocity variability between these two wells but also not surprising given the similar position of these wells relative to the strike of the structure.

The DMP Harvey 4 average velocity at the 900msec reference level is slower than those for GSWA Harvey 1 and DMP Harvey 3. This too is not surprising given the younger stratigraphic section that is intersected in DMP Harvey 4 at that time as indicated by the interpretation on seismic section on the right-hand panel.

DMP Harvey 2 has the slowest of the well velocities even though the section at 900msec is similar to that in GSWA Harvey 1 and DMP Harvey 3 however, given that this well is located on the footwall of the dominant F10 fault and also in close proximity to the fault, and there may be a number of reasons for the relatively slower velocity.

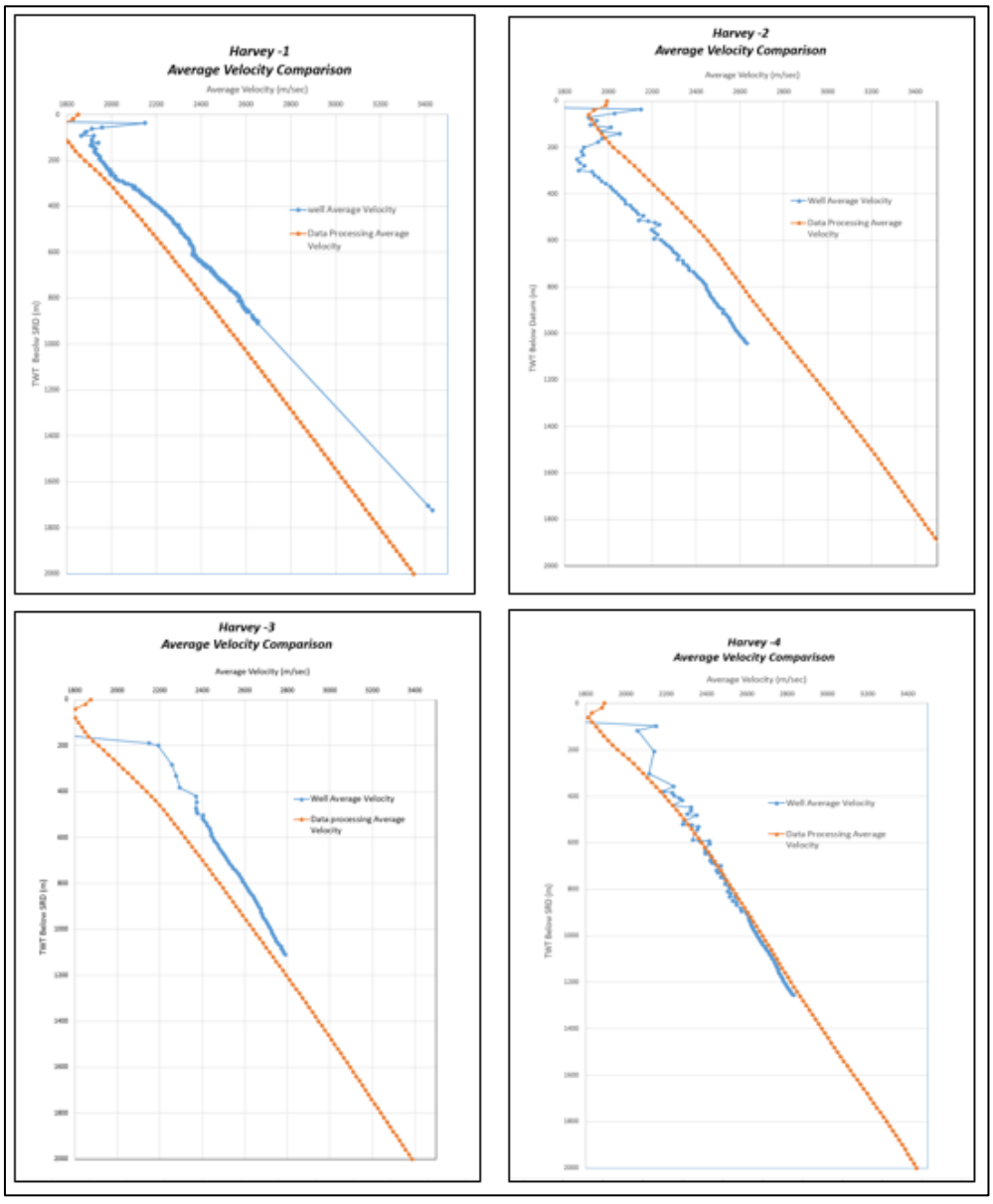

Figure 6.1 Average Velocity comparison

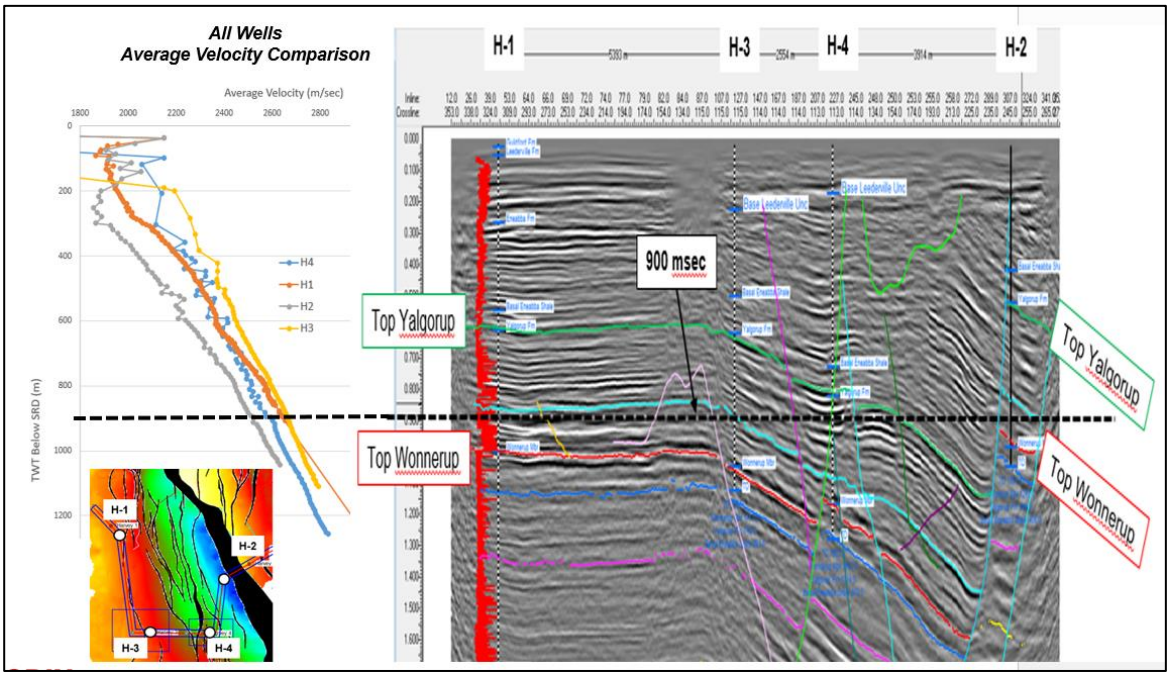

Figure 6.2 Average Velocity Comparison – All Wells

The horizon-consistent average velocity points were then gridded and contoured. The initial grids are reviewed and edited as required to remove noisy data (e.g. “bullseyes”). Following this, various grid cell sizes and smoothing algorithms were trialled to select the optimum parameters.

The resultant average velocity maps are scrutinized and compared at all levels for geological plausibility. As the input data had already been smoothed in the data processing department, little further smoothing was required.

The final Average Velocity Maps for each of the mapped horizon are shown at (Figure 6.3 to Figure 6.5). As expected, these maps show a smoothly varying average velocity field that reflects the depth of burial trend i.e. the faster average velocities (as indicated by the darker blue and magenta colours) lie within the deeper sections of the surface. As such, the average velocity maps tend to mimic the structure maps for each surface.

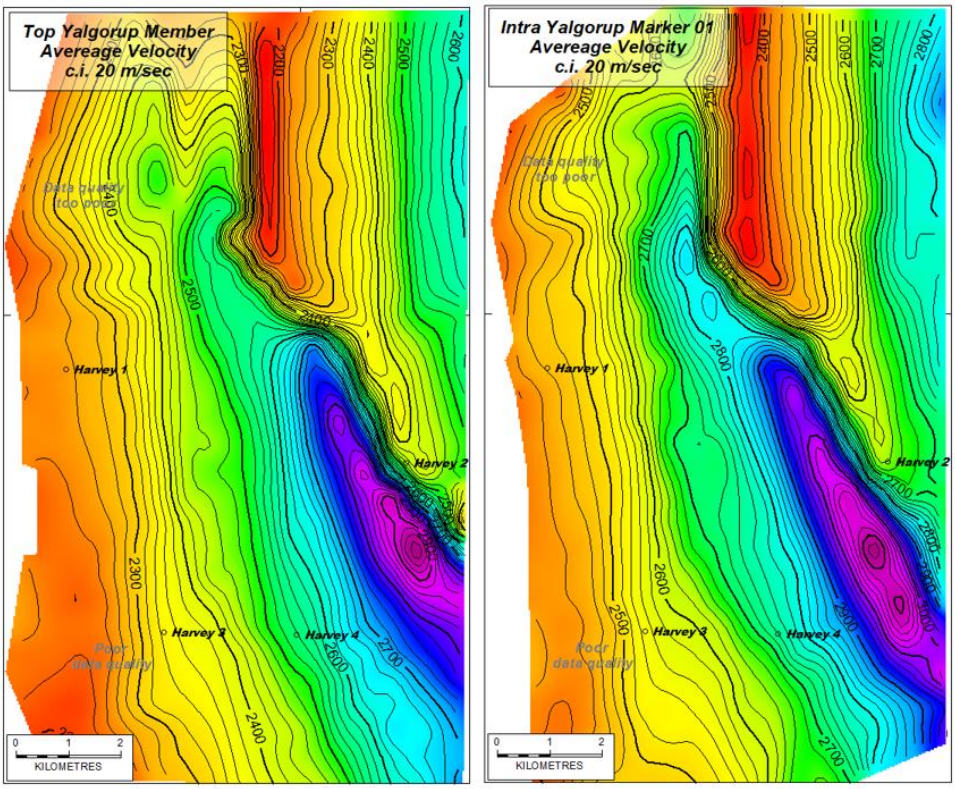

Figure 6.3 Average Velocity Map for Top Yalgorup Member and Intra Yalgorup Marker

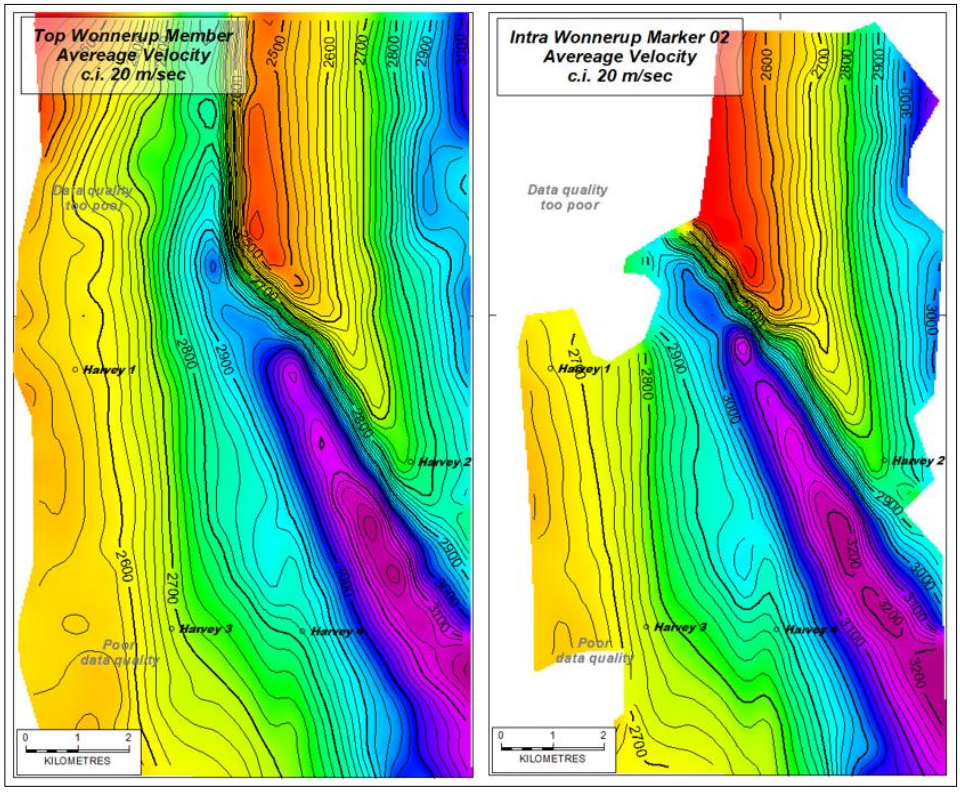

Figure 6.4 Average Velocity Map for Top Wonnerup Member and Intra Wonnerup Marker 02

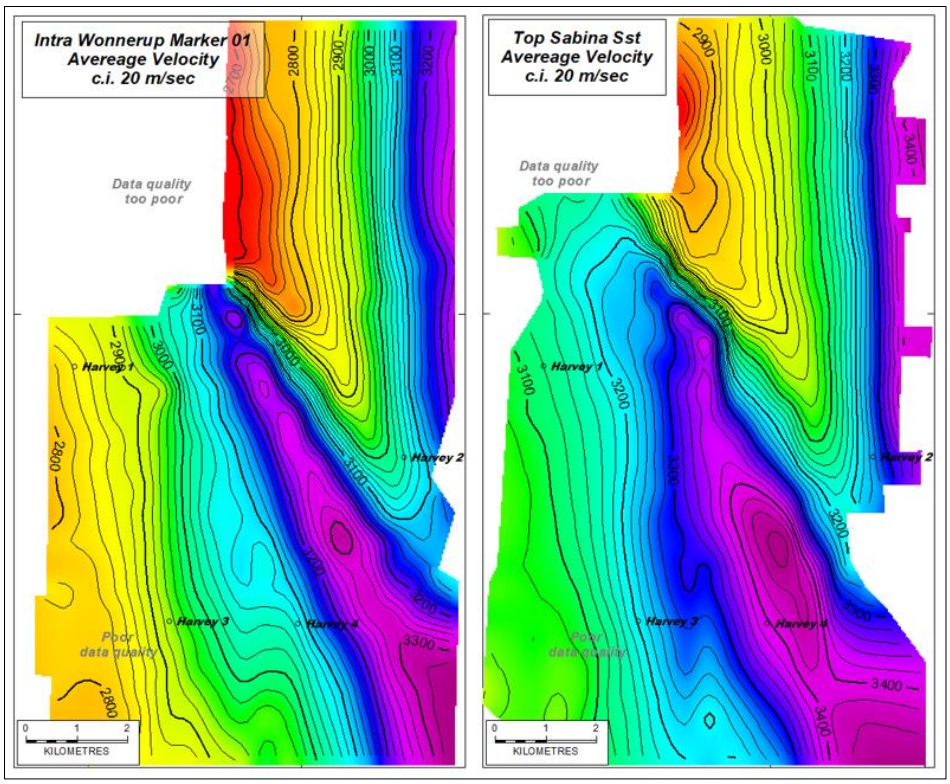

Figure 6.5 Average Velocity Map for Intra Wonnerup Marker 02 and Top Sabina Sandstone

6.2 Depth Mapping

Given the straight forward nature of the velocities across the study region, conversion of the two way time surfaces to depth was simply achieved by multiplying the two way time grid (correcting for two way time) by the average velocity grid. Finally, to correct for any residual errors (which is usual), the resultant depth grid was re-gridded to tie the well tops for each surface yielding the final, well-tied depth surfaces for each of the mapped surfaces. The final depth maps are provided at (Figure 6.6 to Figure 6.11).

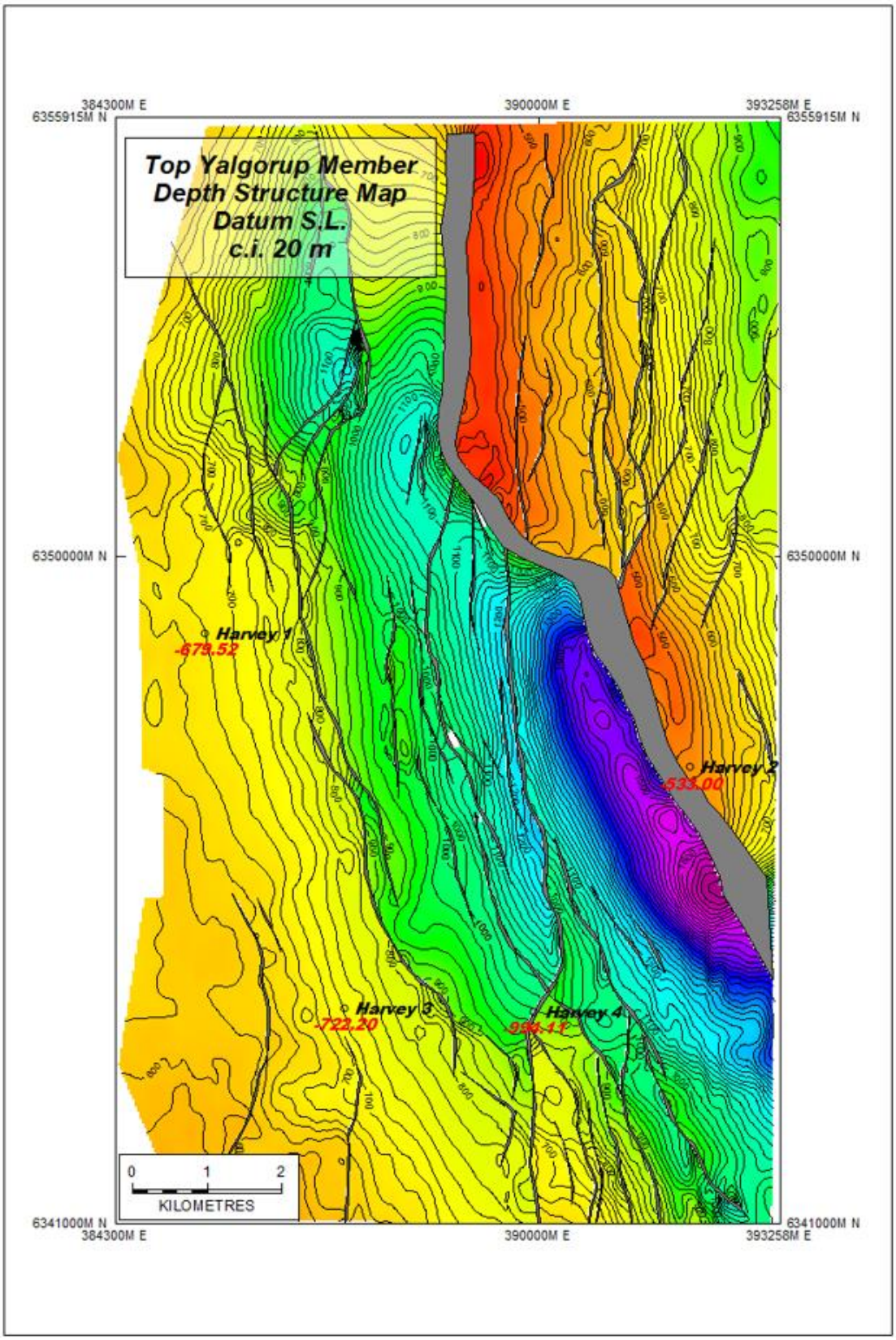

Figure 6.6 Top Yalgorup Member Depth Map

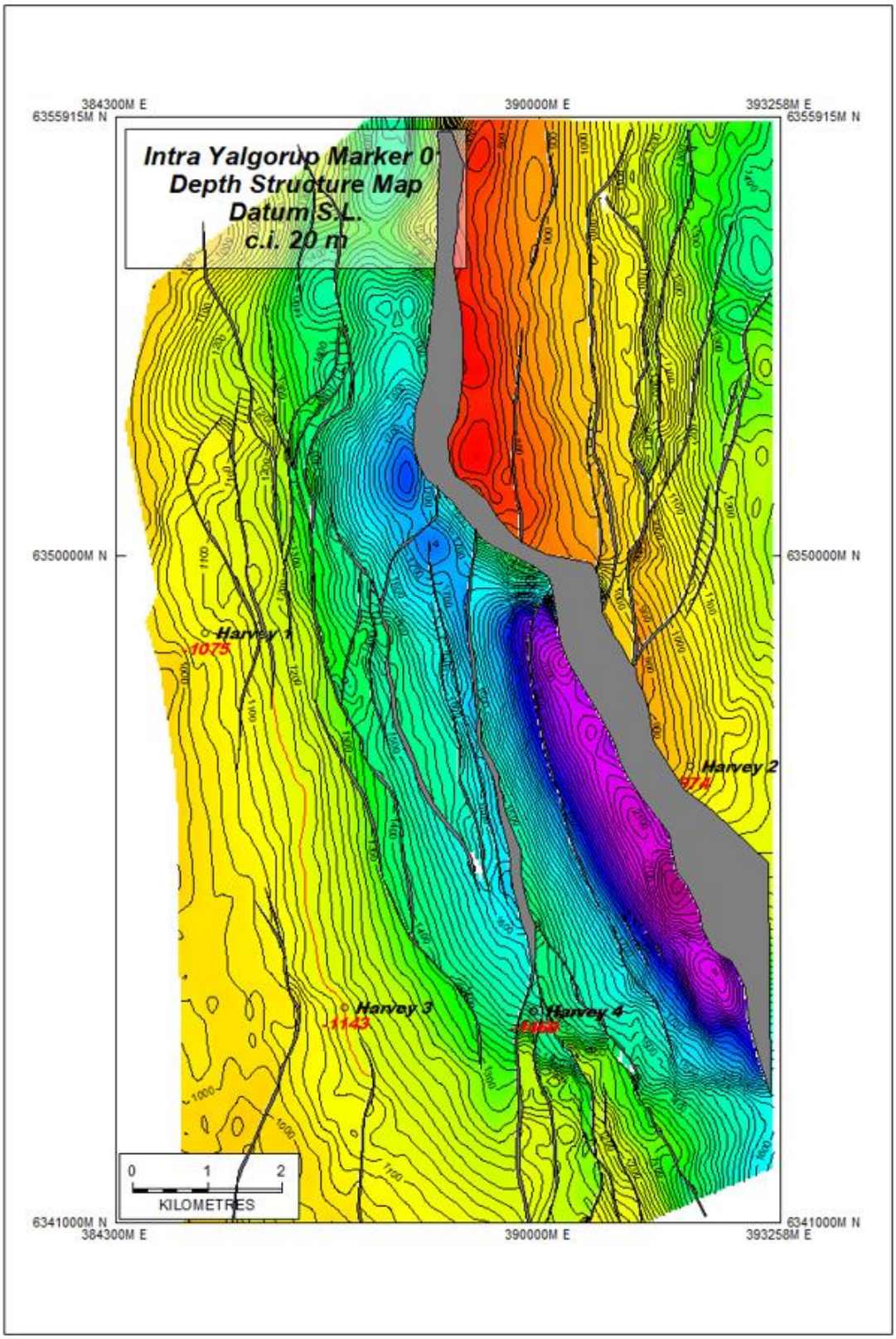

Figure 6.7 Intra Yalgorup Marker 01 Depth Map

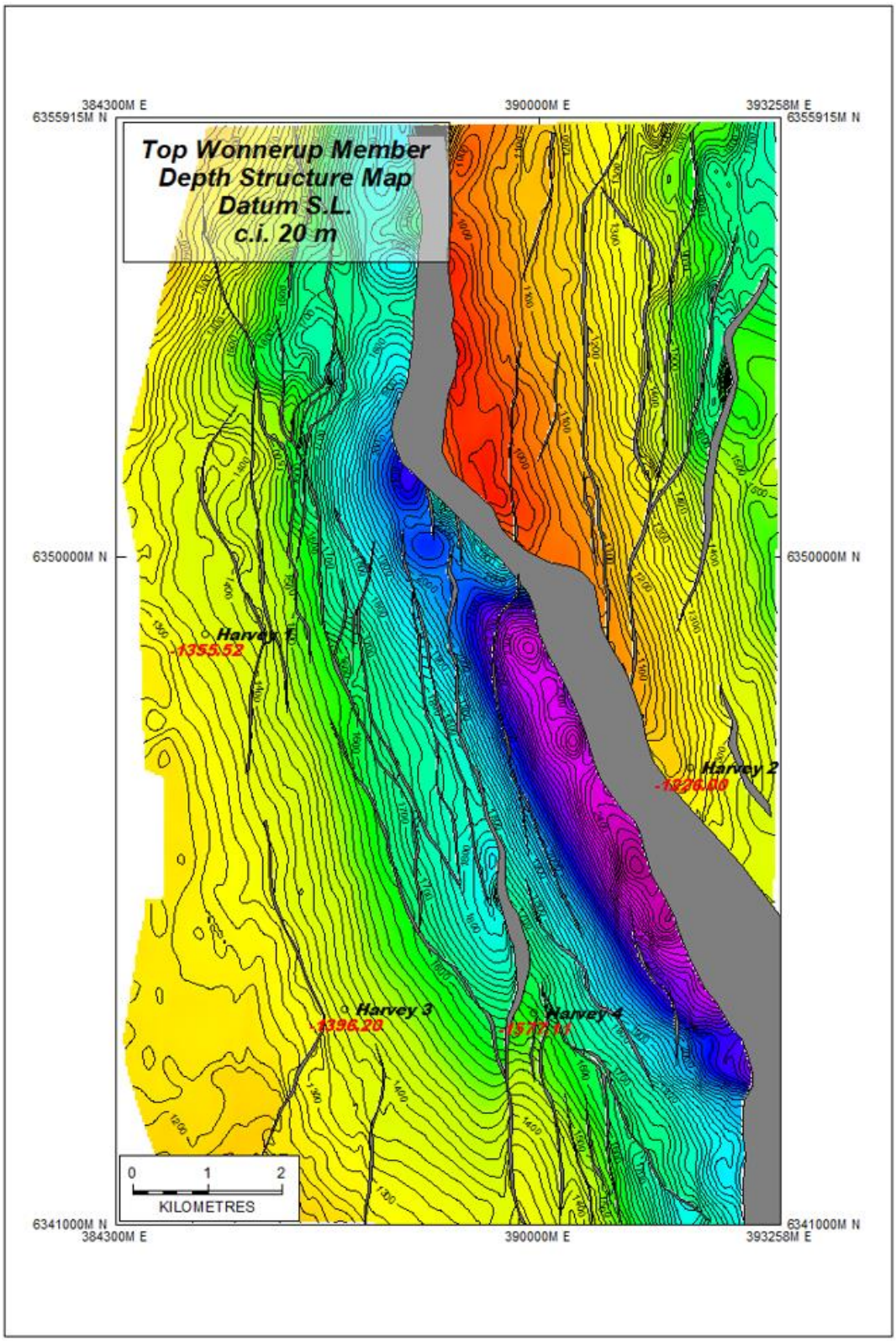

Figure 6.8 Top Wonnerup Member Depth Map

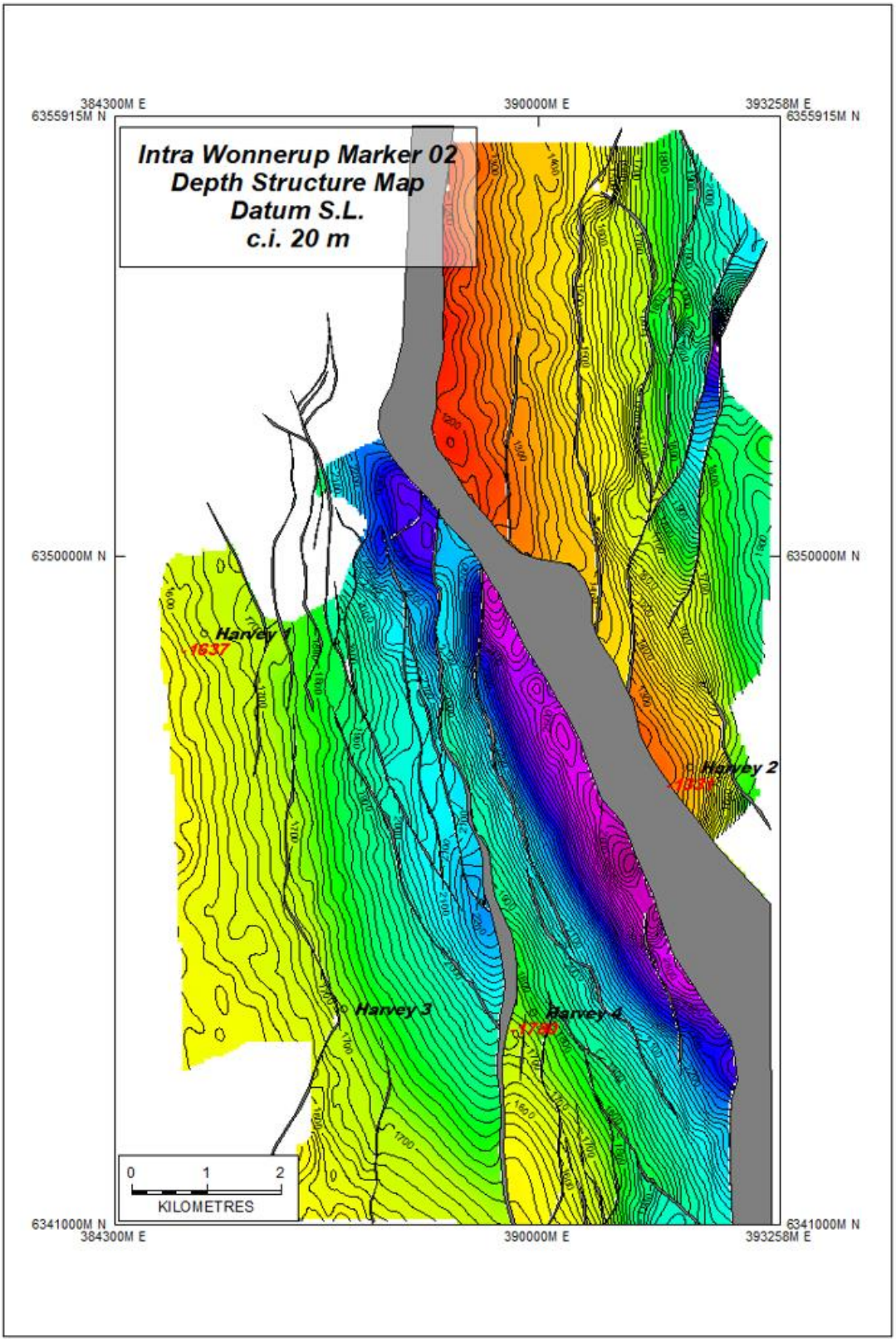

Figure 6.9 Intra Wonnerup Marker 02 Depth Map

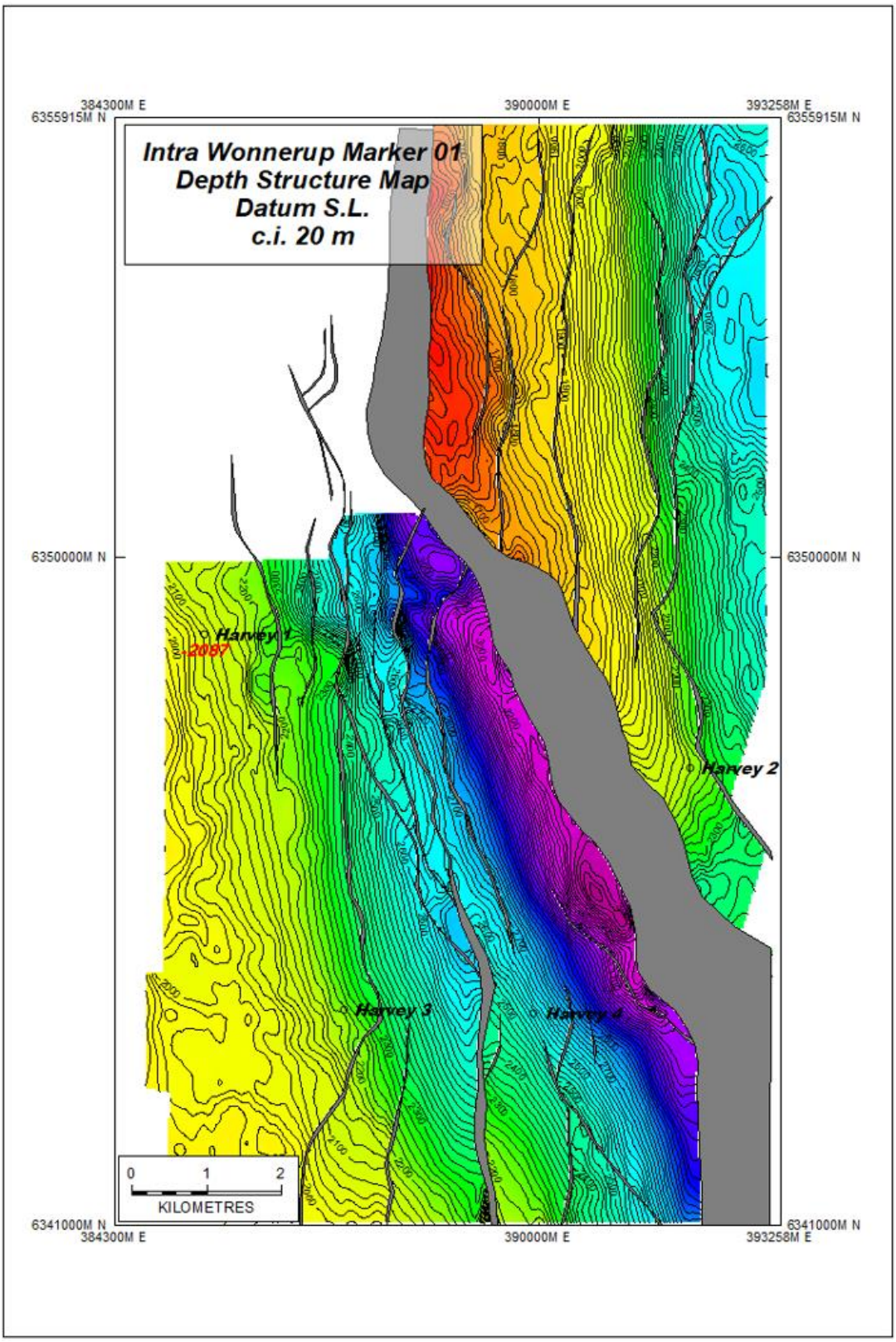

Figure 6.10 Intra Wonnerup Marker 01 Depth Map

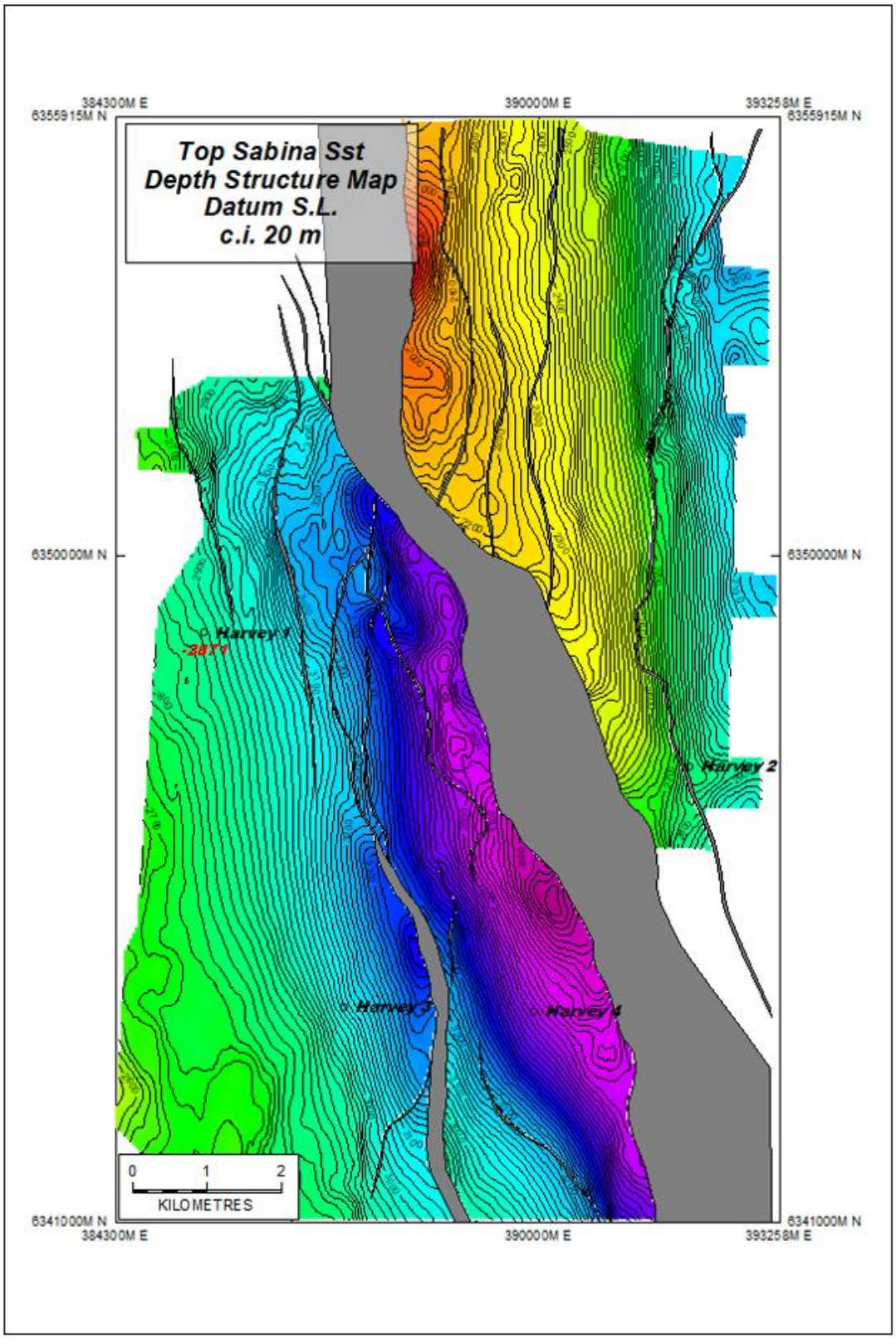

Figure 6.11 Top Sabina Sandstone Depth Map

6.3 Structural Model

The change in the orientation of dominant F10 that is present at all levels throughout the Yalgorup and Wonnerup section may provide an insight to the faulting pattern for the immediate region. The Top Wonnerup surface is used for this investigation. A 3D view of the Top Wonnerup surface is shown alongside the depth structure map (for reference) in (Figure 6.12), the dominant F10 fault is annotated on both displays.

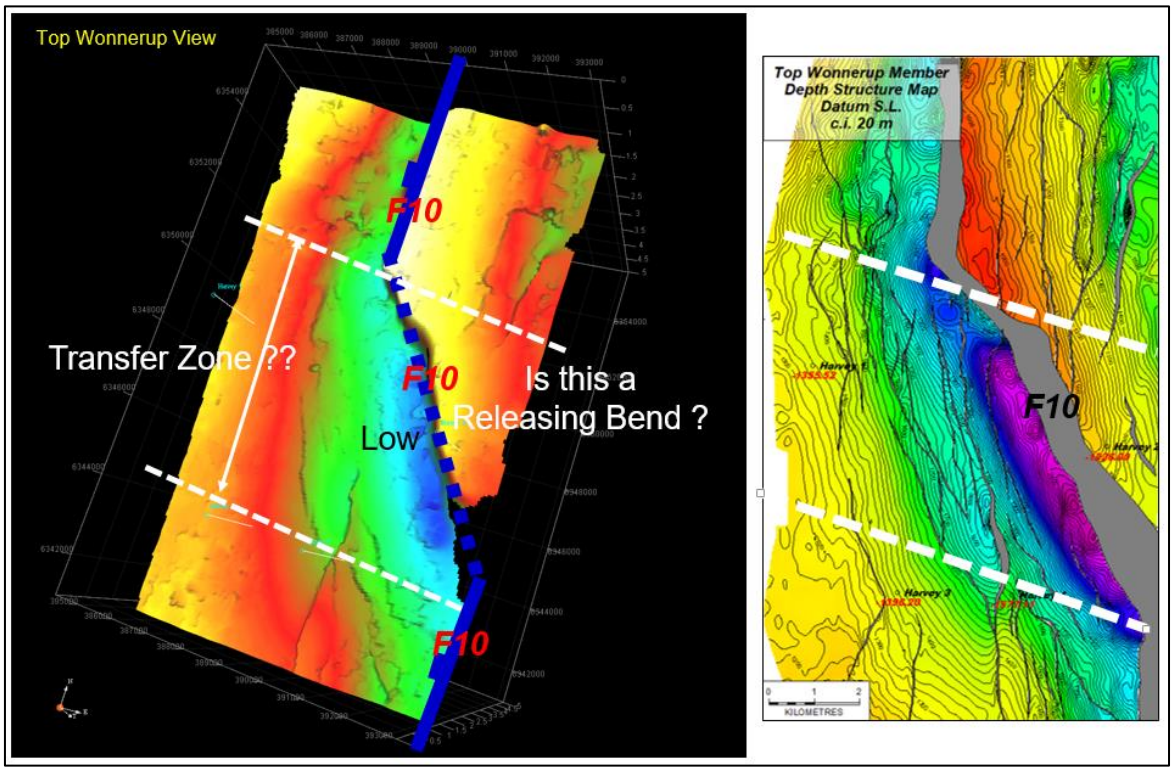

Figure 6.12 Structural Model

On the 3D view at the left-hand panel (Figure 6.12), the F10 fault can be divided into 3 distinct segments; the upper and lower segments are aligned north-south but offset laterally by approximately 4.5km. The middle segment is orientated north-northwest and connects the upper and lower segments. The Top Wonnerup Map on the right-hand panel appears to show that the majority of the subsidiary faults west of the F10 fault, are concentrated in the middle region opposite the middle segment.

A possible structural model to describe this pattern may be either a Transfer Zone or perhaps a releasing bend. In this case, the Transfer Zone model is preferred, particularly as Transfer Zones have been described more regionally in the Perth Basin. The Harvey Transfer highlighted on the Tectonic Elements Map at (Figure 2) appears to be located in an

approximately similar position to the potential Transfer Zone suggested in (Figure 6.12). A Transfer Zone (also called “Accommodation Zone”) would typically comprise a series of relay faults to accommodate the movement and offset of the dominant trend fault(s) – in this case, the F10 fault. The concentrated faults opposite the middle segment in (Figure 6.12) above may indeed represent a series of relay ramp and compensating faults across a Transfer Zone.

This interpretation may have significance as it may assist in the construction of reservoir model in determining where the greater concentration faults may be (i.e. faults that have not been resolved or properly imaged by the seismic data), their likely attitude and style.

7. SEISMIC ATTRIBUTES

7.1 Amplitude Extractions

A key component of the 2017 Harvey 3D Reprocessing and Re-Interpretation Study was to undertake qualitative and quantitative facies prediction using 3D seismic data. This would greatly assist the preparation of the 3-dimensional reservoir model.

In circumstances where the seismic data quality permits, extracted seismic attributes are often able to provide some spectacular results. Unfortunately, this has not been the case within the Harvey 3D data volume.

As has been described in preceding sections, the data quality of the Harvey 3D is severely compromised - this is largely attributable to the access restrictions during the acquisition of the Harvey 3D which have resulted in significant surface coverage gaps. This in turn has impacted the data processing resulting in data gaps extending deep into the section, variable fold coverage, compromised migration (migration smiles) of the data and dispersed amplitudes. Figure 7.1 and Figure 7.2 below provide an illustration of how the data has been affected.

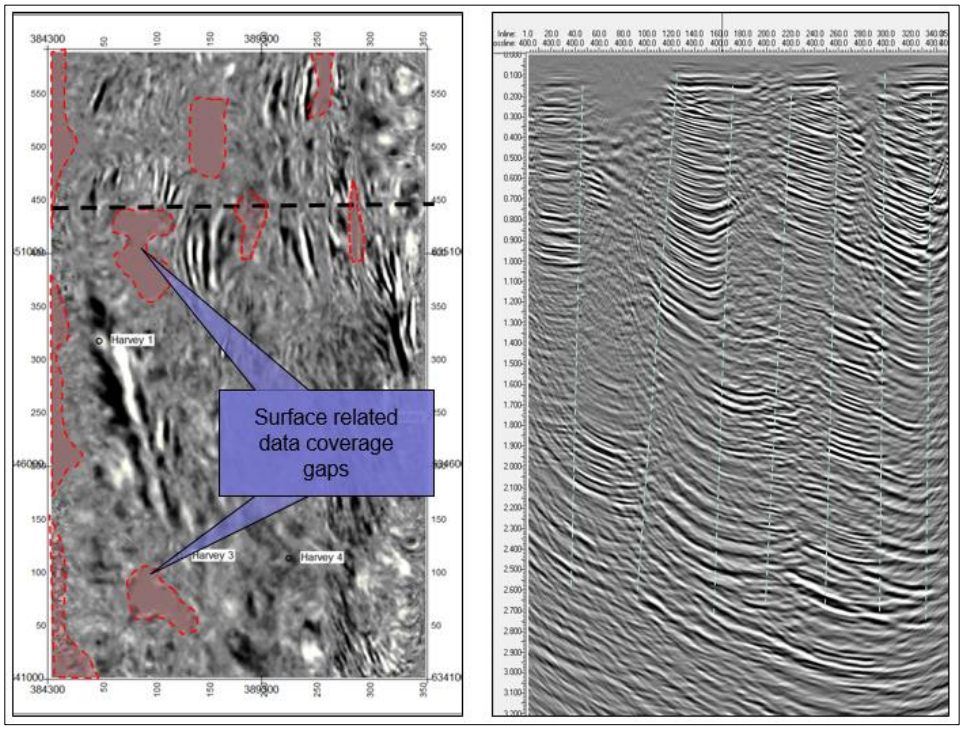

Figure 7.1 Example 1- seismic section illustrating amplitude extraction issues

In Figure 7.1, surface related gaps (seen on the left-hand panel) have resulted in vertical “chimneys” of alternating data and no-data zones – these are clearly observed within the dashed lines on the east–west section at the right-hand panel. Migration smiles at the edge of the no-data zones are common throughout. Clearly, this vertical amplitude “banding” prohibits meaningful amplitude extraction.

An example of a north-south orientated line is provided at Figure 7.2. The positon of the section is indicated on the right-hand panel. The coloured arrows correspond on section and time slice. The data gaps on the section are obvious and very broad. These extend down and beyond the Sabina Sandstone reflector (yellow horizon) with no useful data recorded across the zones of interest in those regions.

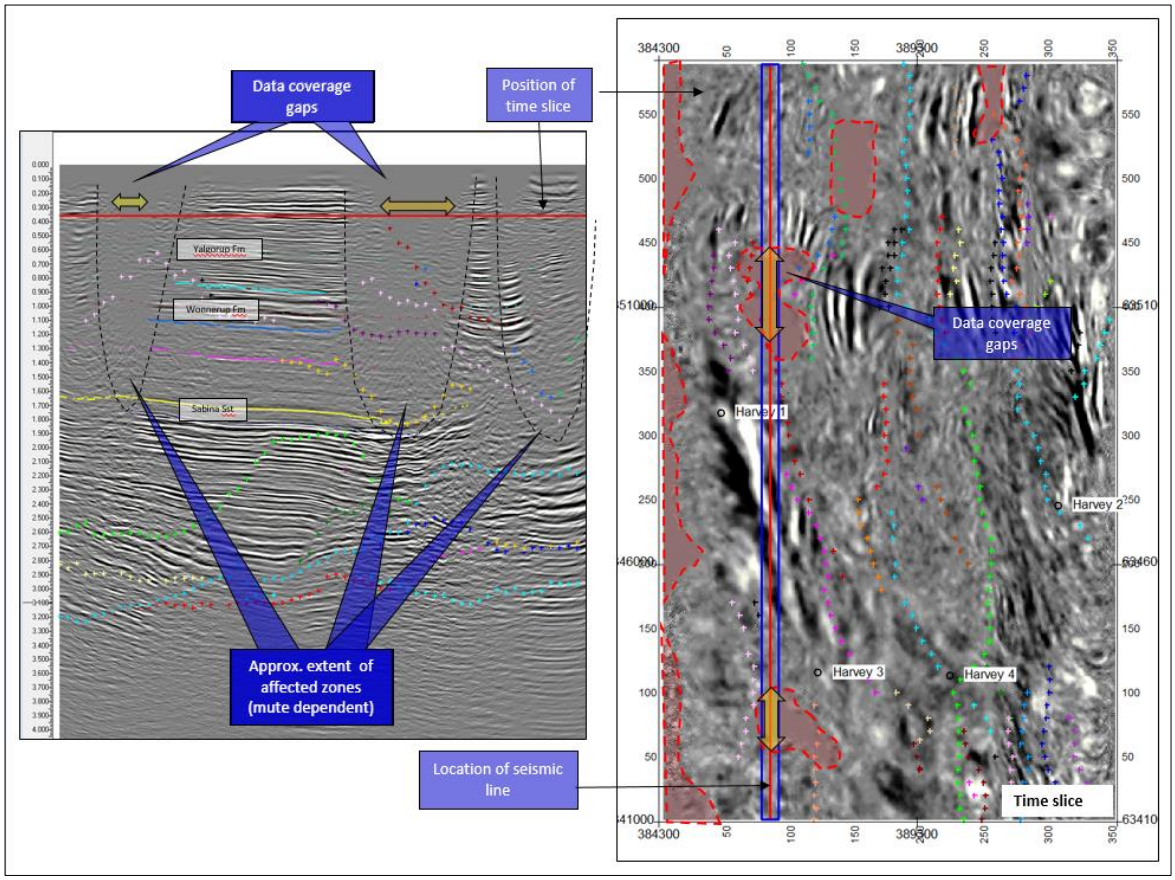

Figure 7.2 Example 2- seismic section illustrating amplitude extraction issues

Despite, the known data limitations, a number of amplitude extractions were performed of which several of these are included in the figures below. Whilst these are flawed, they do however provide a useful illustration of how such displays could be misinterpreted unless one has an understanding of the data from which these displays were derived. All extractions

were performed on the amplitude preserved stacks (PSTM_PRA Stack) that were provided by Curtin University.

Figure 7.3 shows the RMS Amplitudes extraction taken from a window which extended from 15msec above to 15msec below the Top Wonnerup Horizon. The left-hand panel provides a reference for the Top Wonnerup Horizon, as indicated by the yellow arrows on either side of the section. The resultant amplitude on the right-hand side provides an impression that there exists discrete fairways of anomalous amplitudes on either side of the main F10 fault.

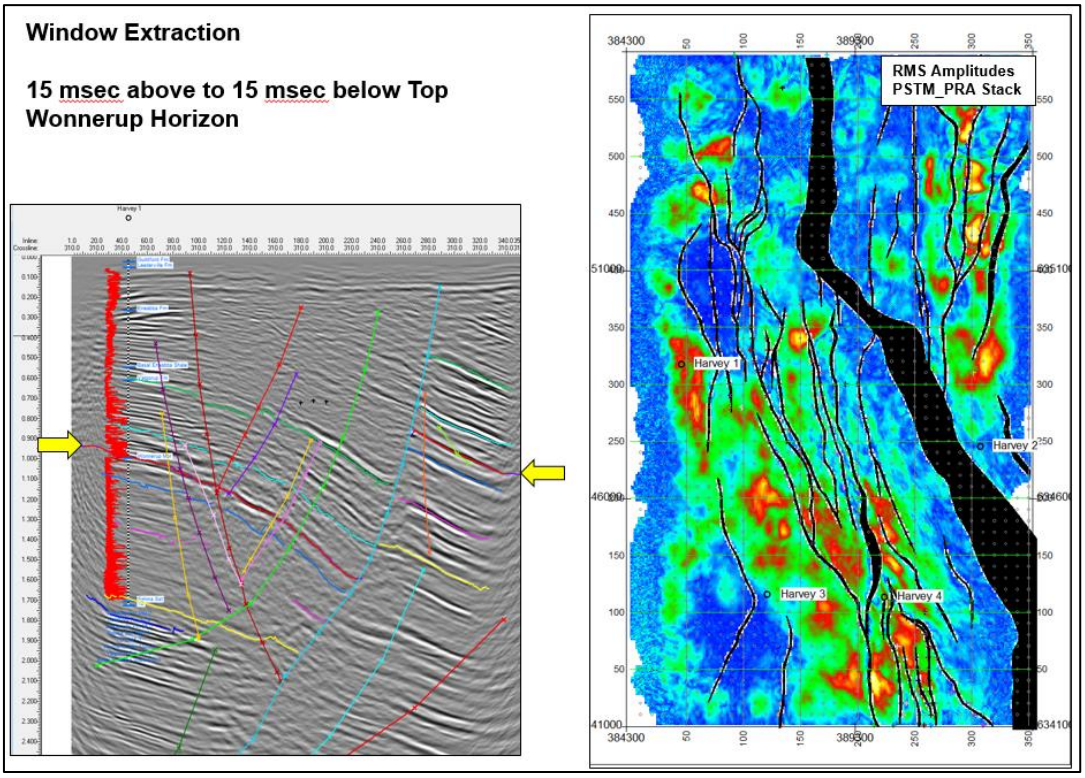

Figure 7.3 Amplitude Extraction – Example 1 Top Wonnerup

However, upon closer inspection of the seismic data, pitfalls are evident - an example is given at (Figure 7.4). The position of the section is highlighted on the map. The dark blue patch (low RMS amplitudes) on the map may suggest an area of relatively lower amplitudes surrounded by a higher amplitudes (green) from which various facies interpretations could be made. But as shown on the seismic section which runs through the “blue” patch, the lower amplitudes are derived from a zone of “no data” related to an acquisition limitation. Without this knowledge, erroneous interpretations could be made.

On the other hand, the anomalous amplitudes (red and orange colours) in the southern region of the study area (Figure 7.5) in the vicinity of DMP Harvey 4 appear to have greater validity, especially as the section above the amplitudes within the yellow ellipse is unaffected by surface related issues. The seismic panels on the side are the same except that one has all interpretation removed so not to obscure the prominence of the amplitudes. Despite interference of the data affected zones, the anomalous amplitudes do not appear to suggest a particular depositional geometry.

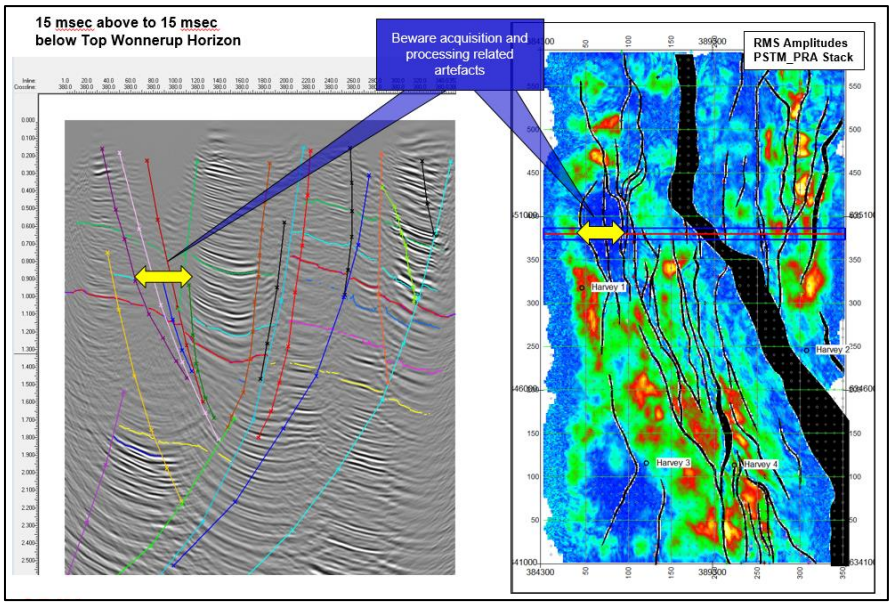

Figure 7.4 Amplitude Extraction – Example 1 Top Wonnerup – Explanation 1

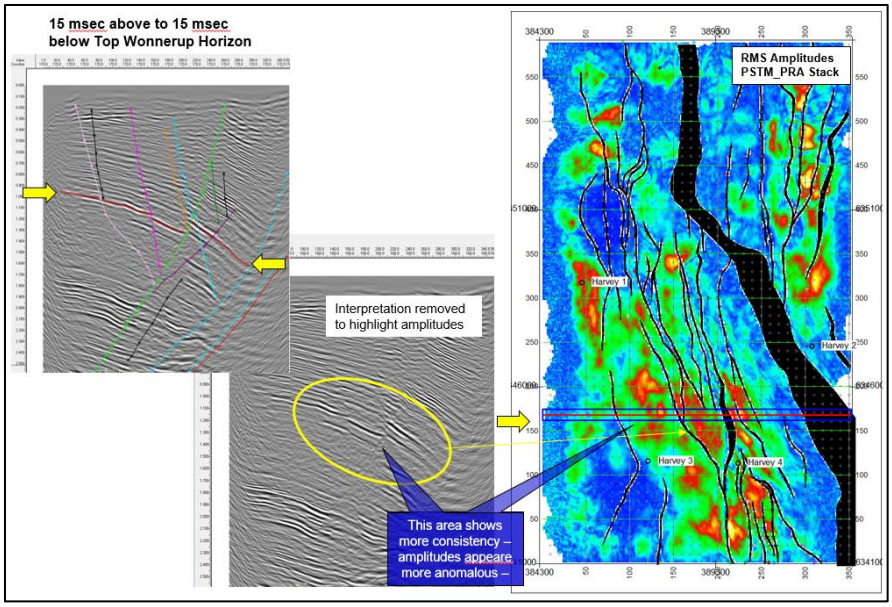

Figure 7.5 Amplitude Extraction – Example 1 Top Wonnerup – Explanation 2

Figure 7.6 provides an example of a second amplitude map – this was extracted from a 150ms window extending from 50 to 150msec below the Top Wonnerup Horizon. The extraction window and the targeted amplitudes are shown on the left-hand panel.

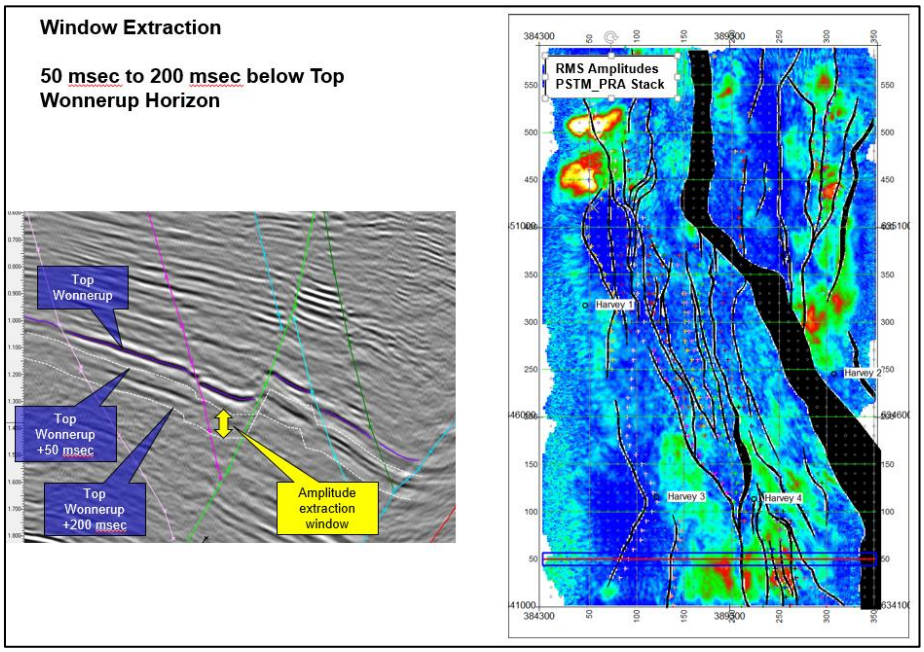

Figure 7.6 Amplitude Extraction – Example 2

Again, this extraction has a similar pitfall as per the previous example. These are described in (Figure 7.7 and Figure 7.8).

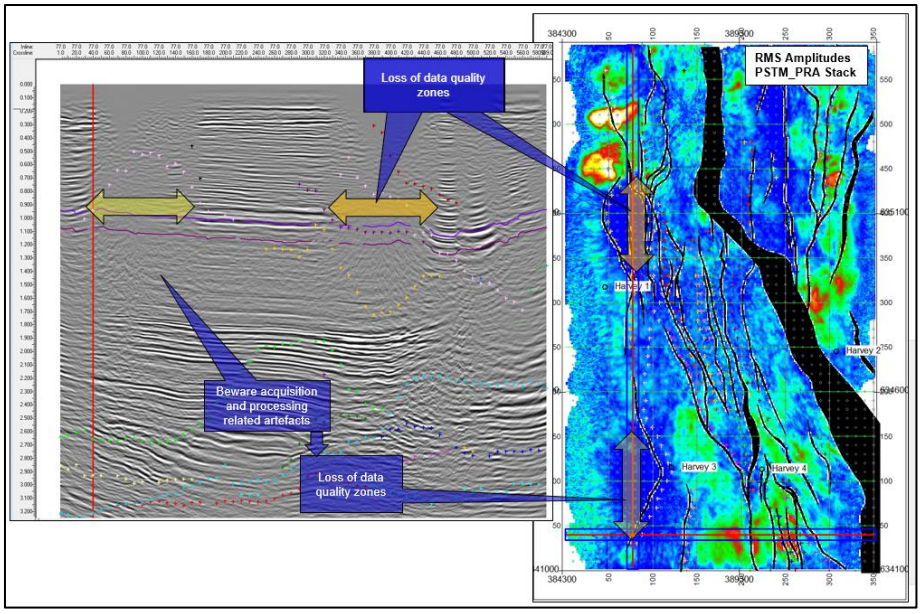

Figure 7.7 Amplitude Extraction – Example 2 Inta Wonnerup – Explanation 1

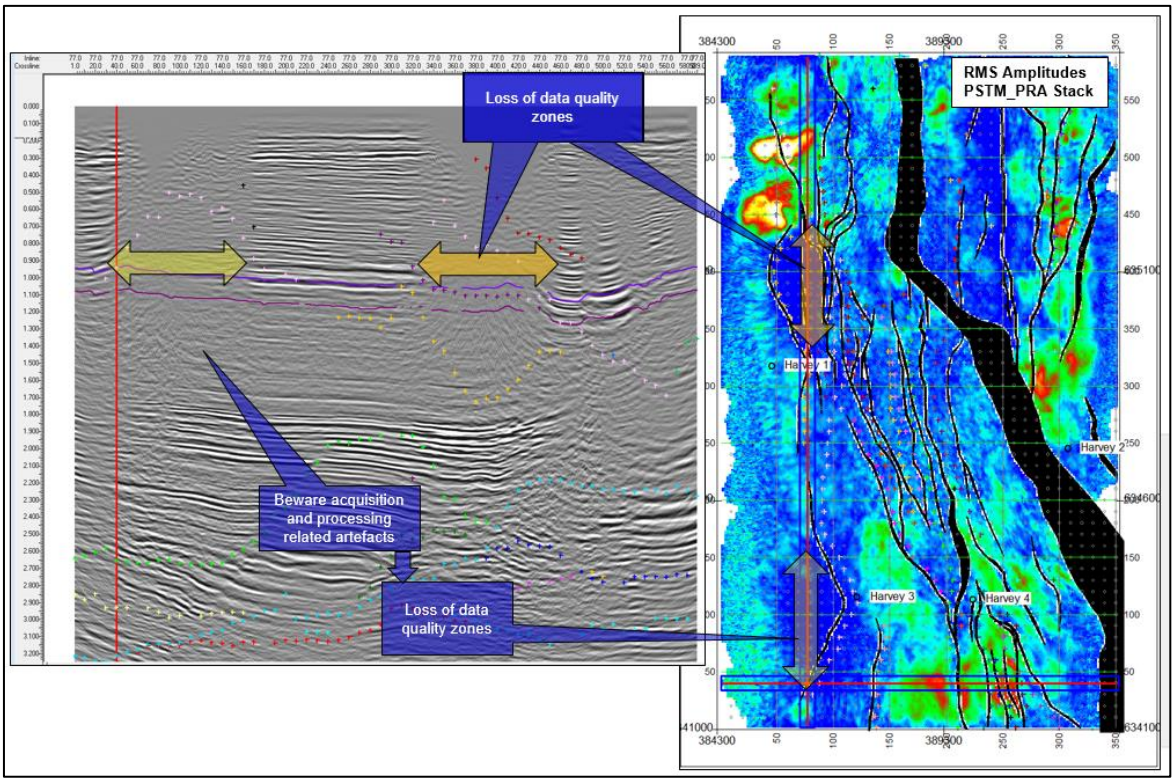

Figure 7.8 Amplitude Extraction – Example 2 Intra Wonnerup – Explanation 2

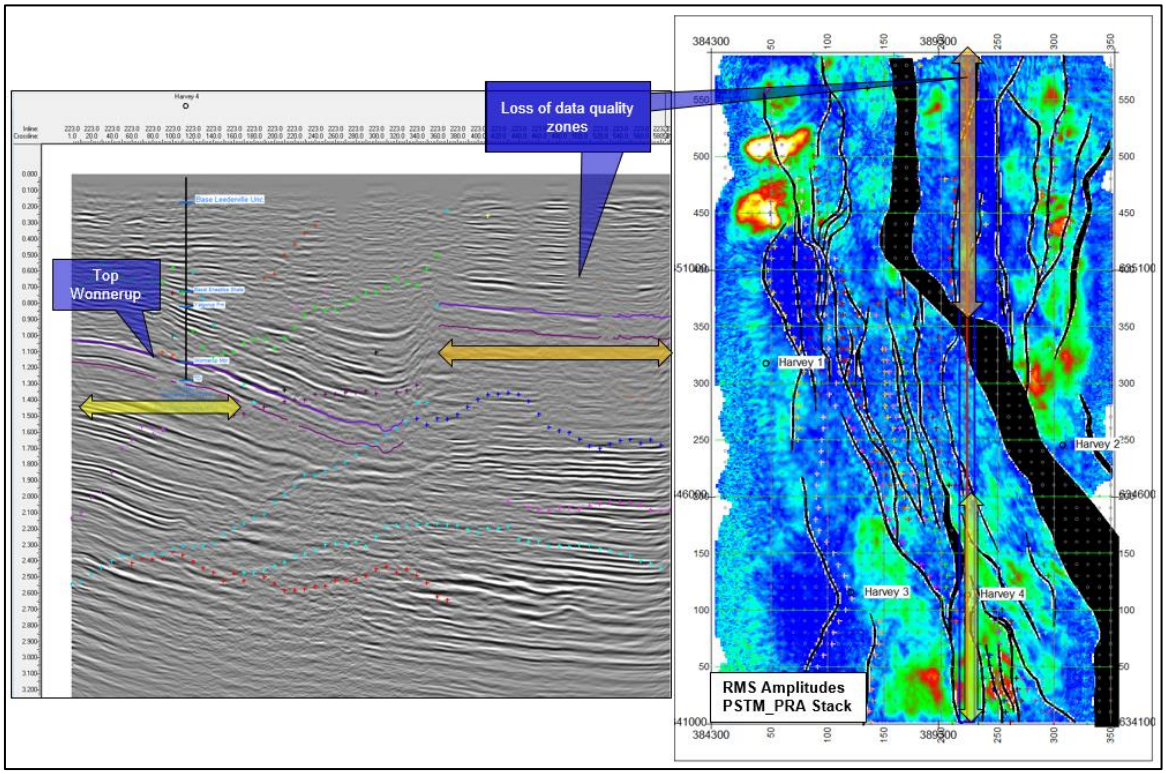

Figure 7.9 Amplitude Extraction – Example 2 Intra Wonnerup – Explanation 3

Figure 7.10 is a third example of an amplitude extraction- in this case RMS amplitudes were extracted from window ranging from 0 to 80msec above the Top Yalgorup horizon. The right-hand panel is mostly featureless except for a curious arcuate feature that is outlined by the white dashed polygon that has the appearance of a meandering channel. Again, as per previous examples, closer analysis as described in (Figure 7.11) shows how this feature is an artefact of “no data” zone and amplitude banding.

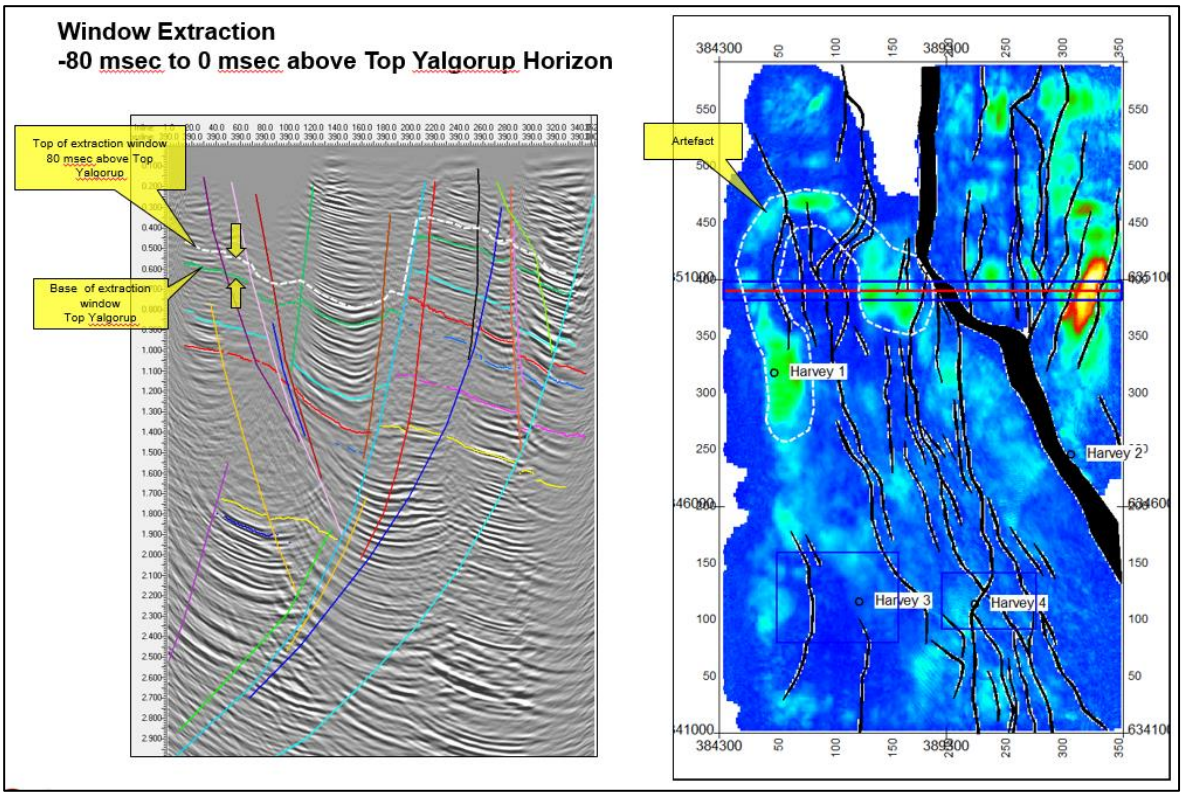

Figure 7.10 Amplitude Extraction –Top Yalgorup - Example 3

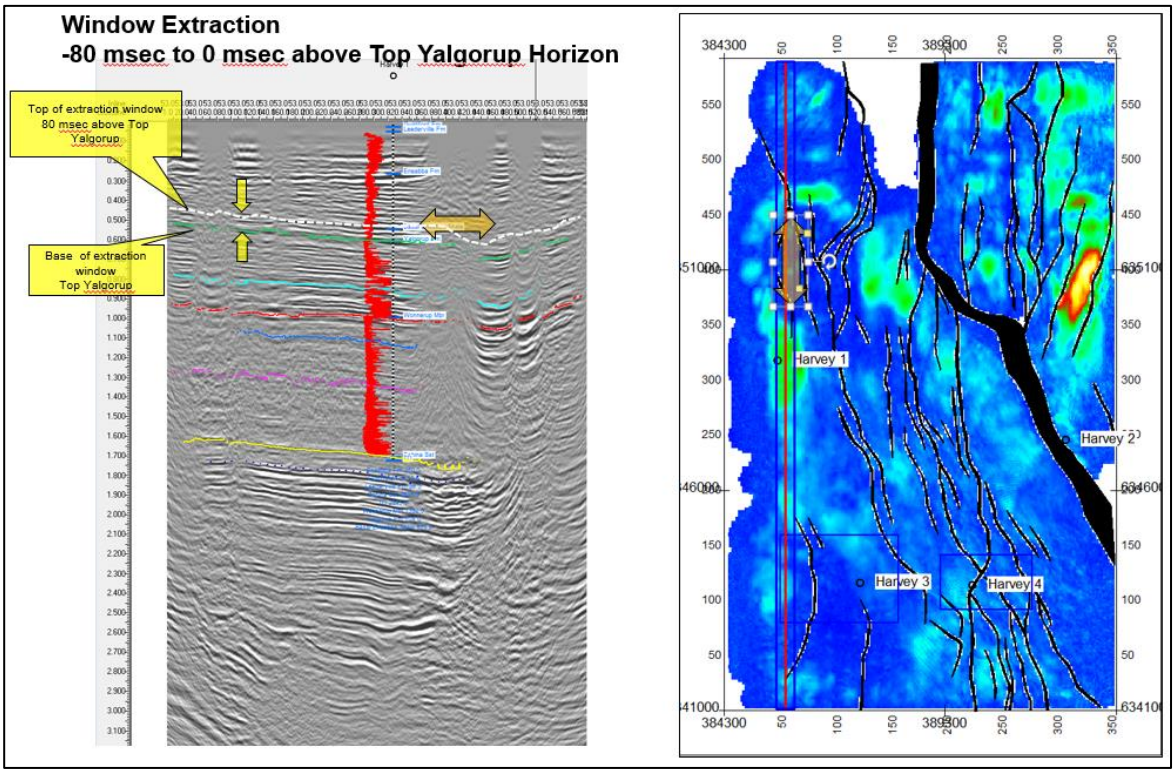

Figure 7.11 Amplitude Extraction – Example 3 Top Yalgorup – Explanation 1

A final example at (Figure 7.12) is taken from a 40msec window, which straddles the Intra Yalgorup horizon. Similar comments apply to this example – the orange and green arrows highlight data gaps that isolate vertical bands of data giving the impression of isolated features on the map grid of extracted amplitudes.

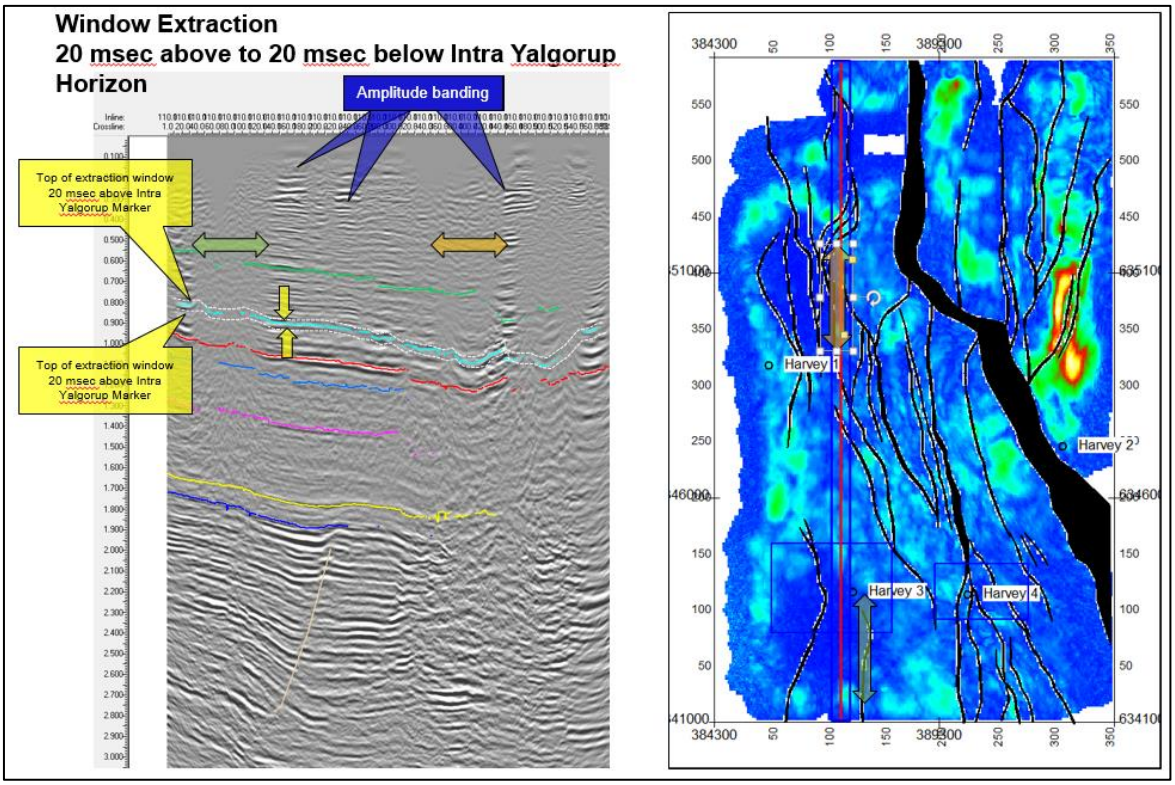

Figure 7.12 Amplitude Extraction – Example 4 Intra Yalgorup

7.2 Horizon Attributes

Horizon attributes including Frequency, Envelope, Hilbert Transform and Phase were attempted at the Top Yalgorup. Intra Yalgorup and Top Wonnerup. These are shown at (Figure 7.13 to Figure 7.15). With the exception of a lineament highlight on the Top Yalgorup panels (Figure 7.14), none of these yielded any meaningful information. The lineament is most likely noise-related.

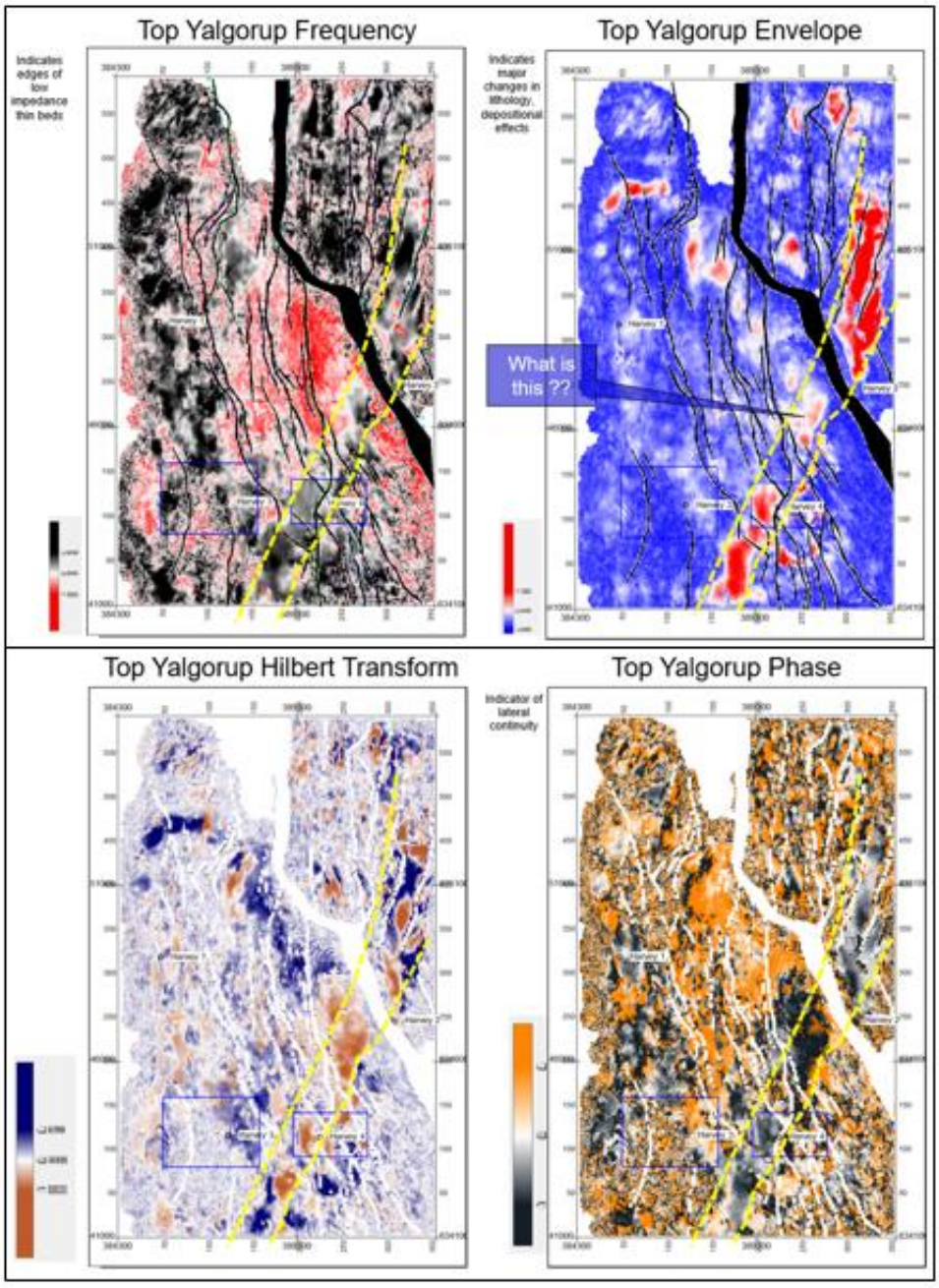

Figure 7.13 Horizon Attributes – Top Yalgorup

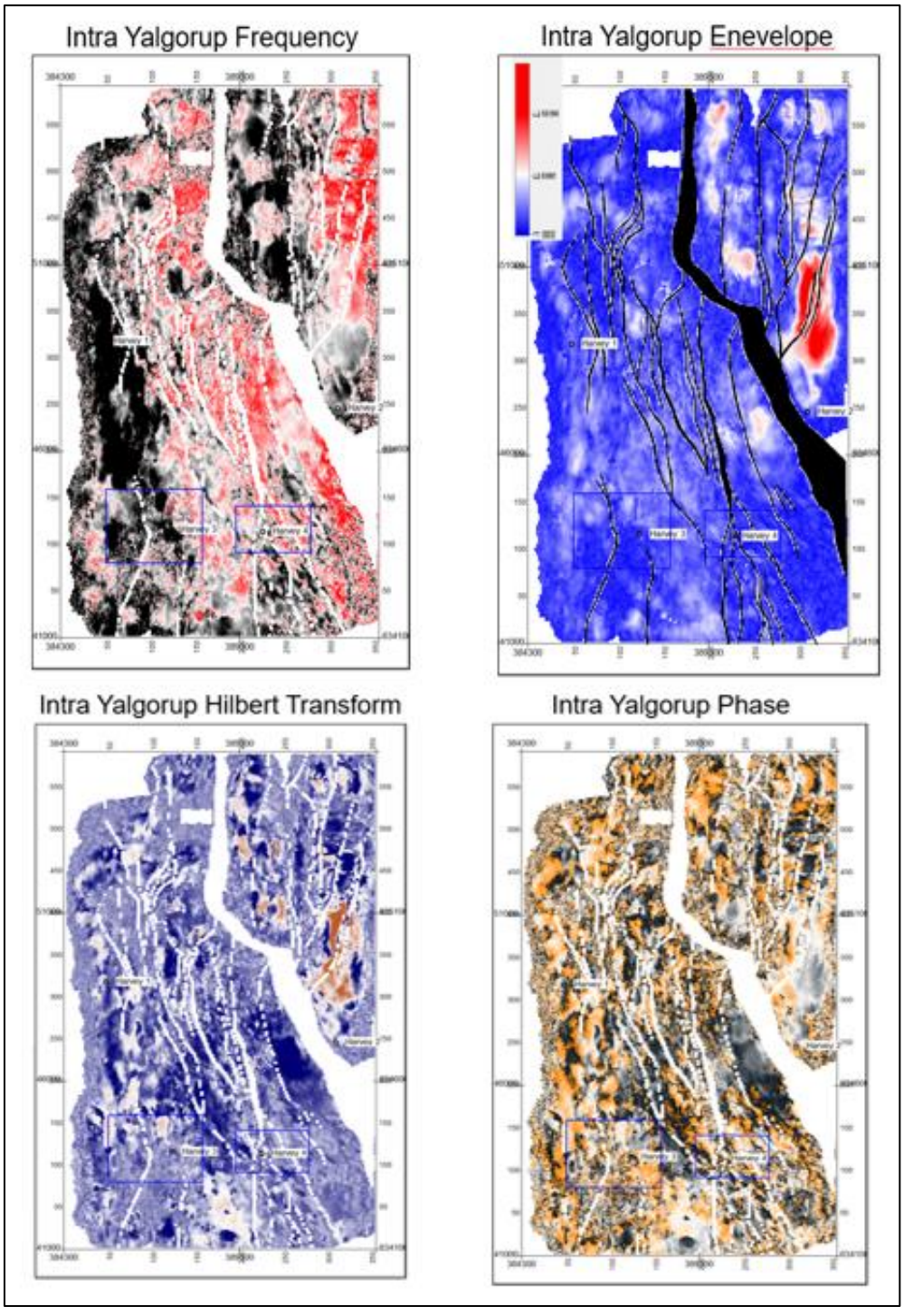

Figure 7.14 Horizon Attributes – Intra Yalgorup

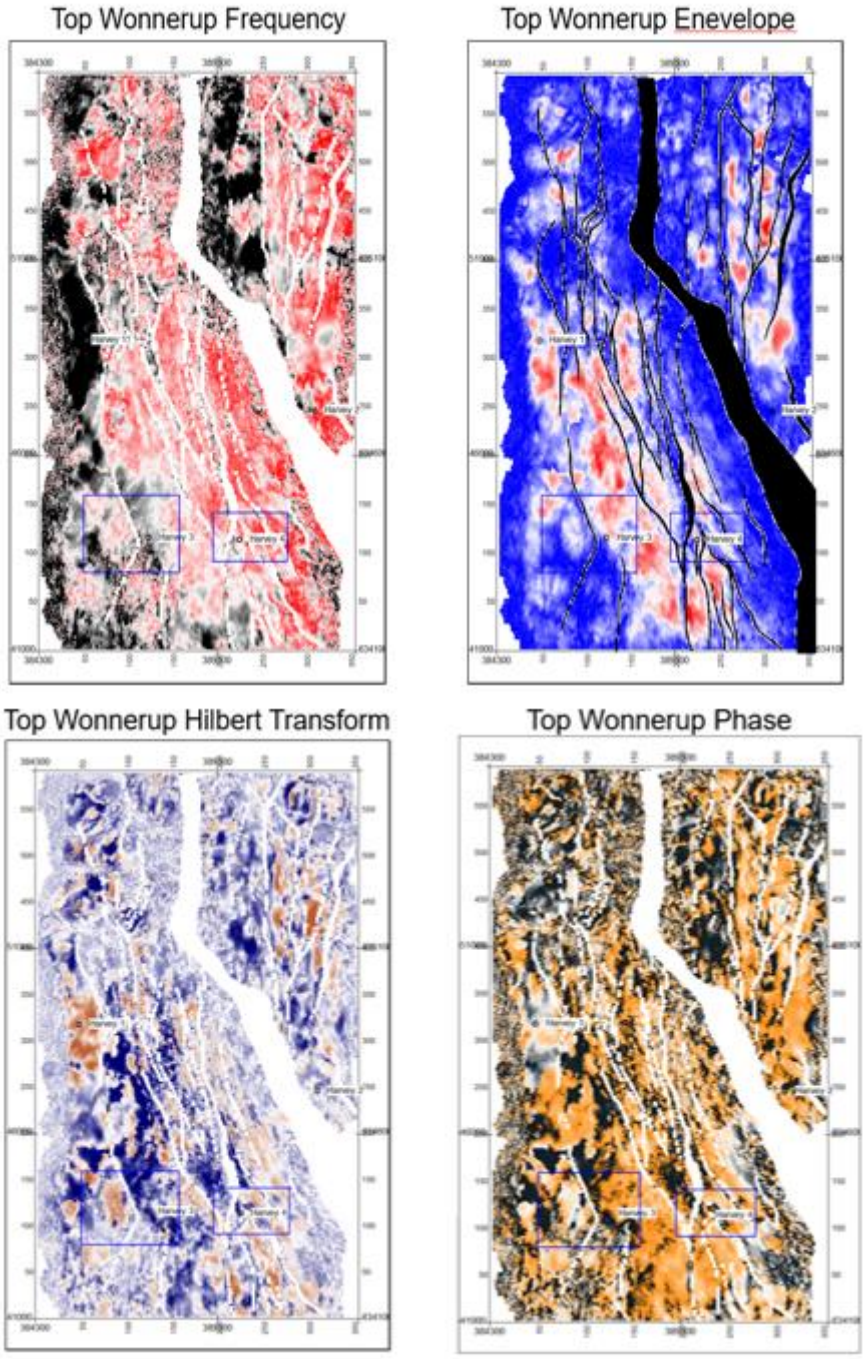

Figure 7.15 Horizon Attributes – Top Wonnerup

7.3 Coherency Attribute

To further investigate whether and internal depositional geometries can be detected from which facies may be inferred, Curtin University produced a seismic coherency attribute volume. A typical time slice view through the volume is shown at, (Figure 7.16).

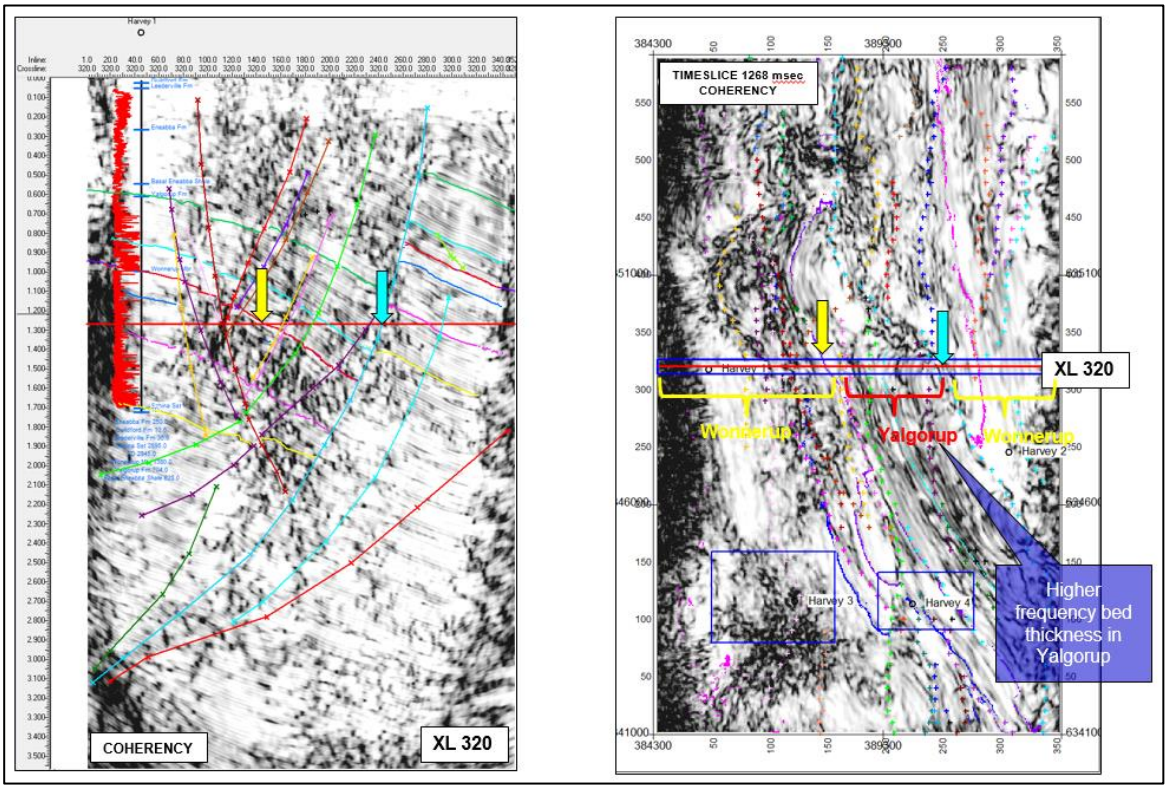

Figure 7.16 Typical Coherency Section and Timeslice view

The position of the timeslice is indicated by the red line on the section view on the left panel. The blue and yellow arrows show corresponding positions of the section and timeslice views. The more reflective interbedded section of the Yalgorup interval is clearly evident on both views.

In order to detect potential depositional geometries, the section must be flattened at the level of investigation i.e. horizon datumming.

Figure 7.17 is a view of the flattened coherency display taken 4msec above the To Wonnerup. From this view there are no clear depositional patterns observable at this level. The faults which were interpreted are appear as the black lineations on the timeslice view – these appear black (no value) since horizon does not extend across the throw of the faulty (heave)

so when the horizon is flattened there are no values there (since there is no horizon). This display is also useful to highlight other faults which may not have been interpreted. In this case there are only a few short, minor potential lineations that could possibly be interpreted as faults.

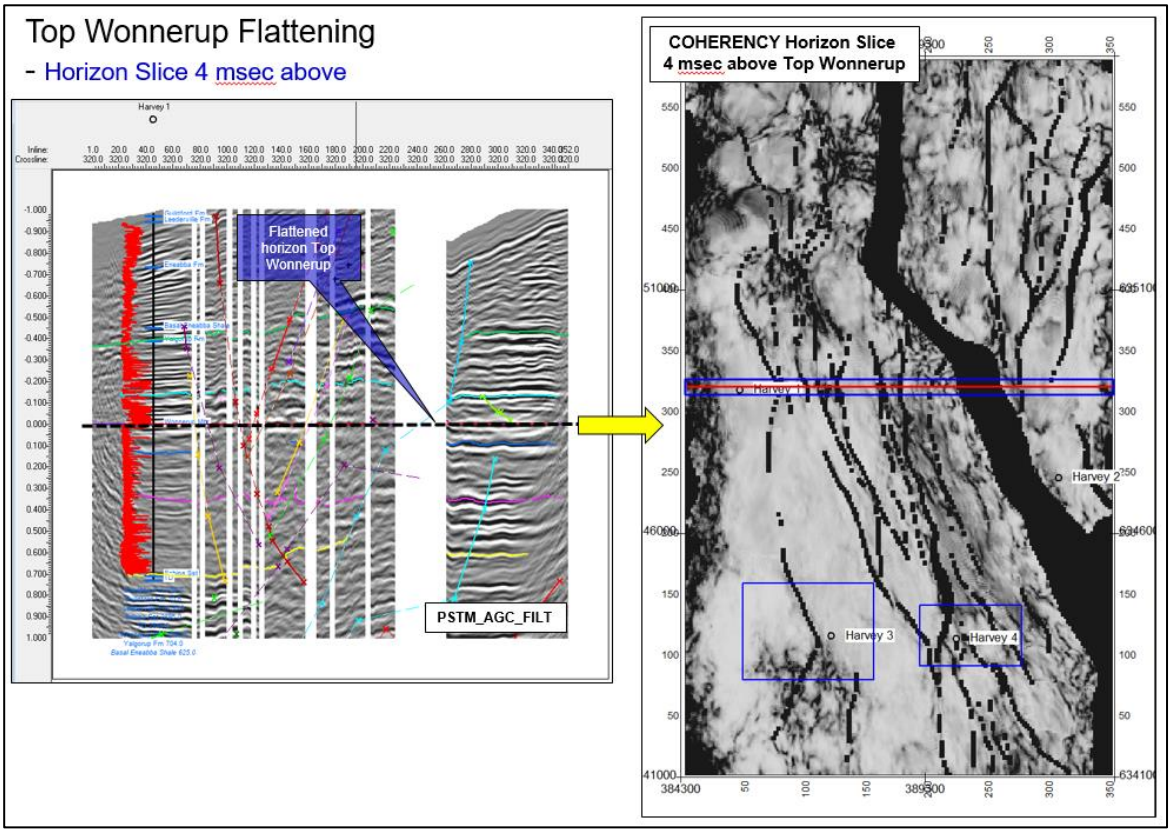

Figure 7.17 Flattened Coherency Display – Top Wonnerup

This investigation was continued throughout the Wonnerup and Yalgorup section however the result were very similar in each case hence no further examples are required here.

8. HI-RESOLUTION 3D SURVEYS – DATA COMPARISONS

As shown in Figure 3.3, two high resolution surveys were acquired – one of these is centred on the DMP Harvey 3 well location and the other is centred on the DMP Harvey 4 well location. The purpose of the surveys was to determine if more structural detail can be recorded tin order to provide a better understanding of the nature and orientation of higher resolution (sub-seismic) faults and fractures. Figure 8.1 is a seismic view taken from a Curtin processed seismic data cube in which the Hi-resolution (Hi-Res) processed data have been merged into the Harvey 3D PSTM data cube. A line that runs through the DMP Harvey 3 and DMP Harvey 4 well is provided. The yellow arrows indicate the extent of each of the Hi-Res data.

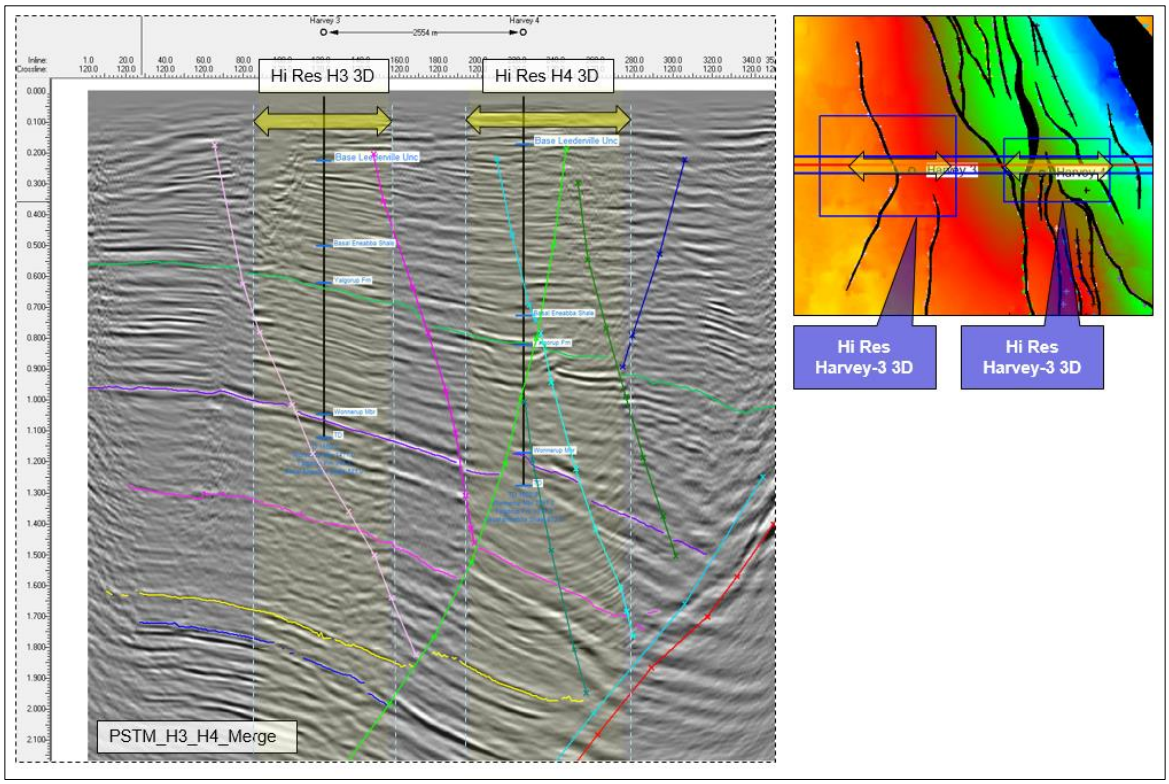

Figure 8.1 Hi Resolution 3D Comparison – Harvey 3D line through DMP Harvey 3 and DMP Harvey 4

To make the comparison clearer, firstly, (Figure 8.2) is a zoomed in view of the same section as in (Figure 8.1) but in this case, the un-merged data on the Harvey 3D PSTM is shown. This section can then be directly compared to (Figure 8.3) in which the Hi-Res 3D surveys have been merged – thus a direct comparison can be made.

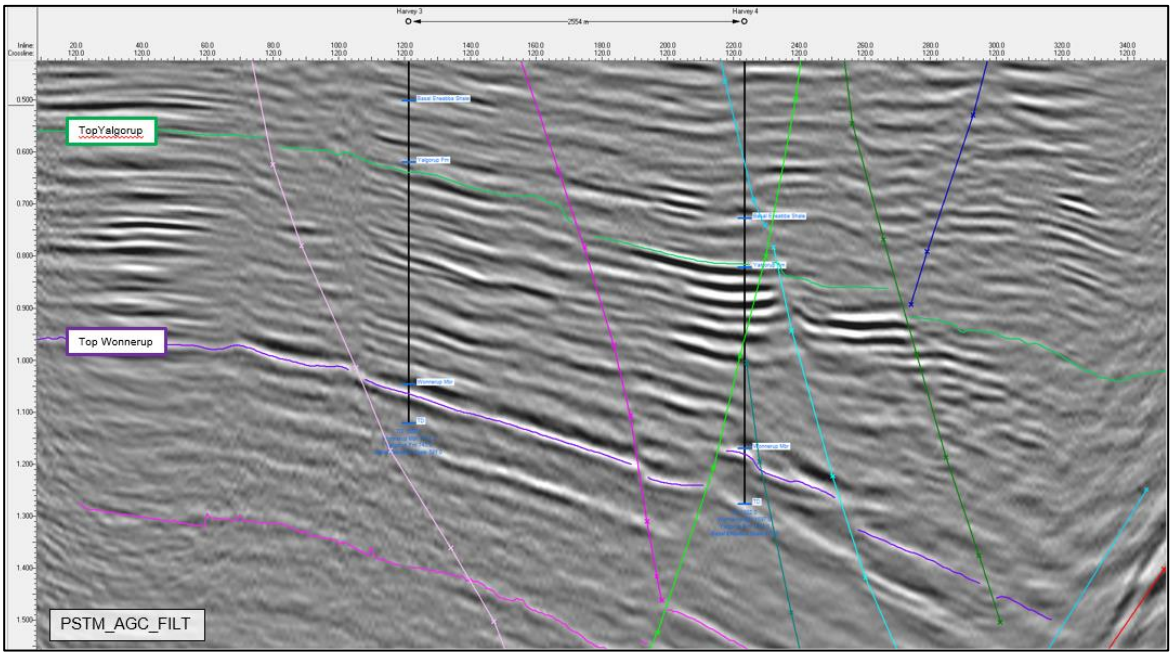

Figure 8.2 Hi Res 3D Comparison Zoomed – No Merge

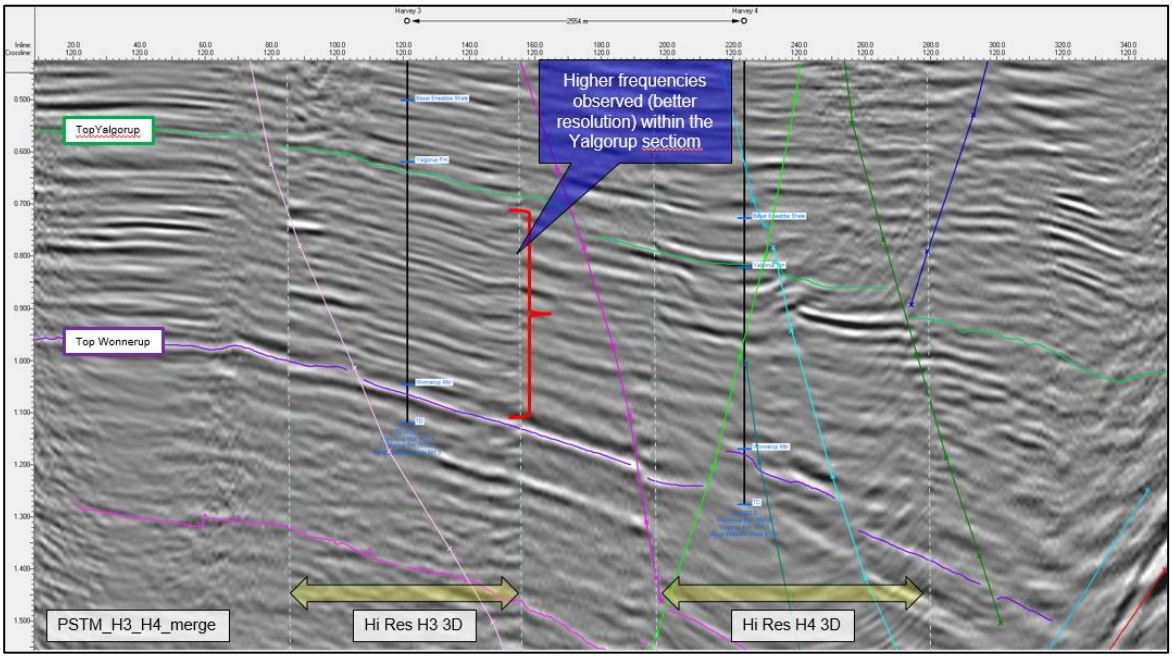

Figure 8.3 Hi Res 3D Comparison Zoomed – Merged

The tie and character at the key markers, specifically the Top Wonnerup, is very good and unequivocal. Higher frequencies are certainly noted, with the DMP Harvey 3 Hi-Res Yalgorup section compared to the Harvey 3D data however, this is not as clear on the DMP Harvey 4 Hi-Res data. A further comparison is made utilizing the coherency attribute for each of the survey data.

Figure 8.4 shows the coherency attribute data for an Inline passing through the DMP Harvey 3 well within the H3 Hi-Res survey volume (left panel) and similarly the right-hand panel shows an Inline passing through the DMP Harvey 4 well within the H4 Hi-Res survey volume.

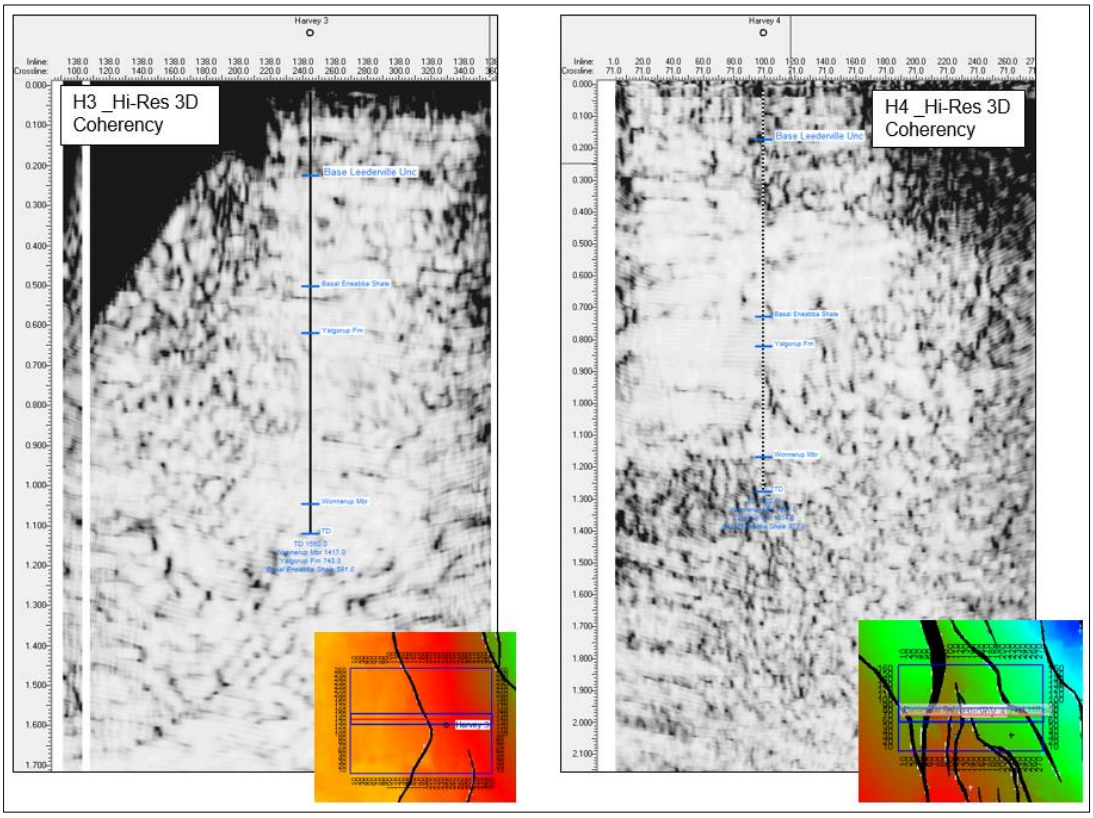

Figure 8.4 Hi Res Coherency Comparison – Hi Res Inline views

For comparison, in (Figure 8.5) the coherency data from the Harvey 3D survey is displayed in panels that match exactly those for the Hi-Res survey Inlines in the previous figure. Figure 8.6 is the same except with the horizon and fault interpretation overlain.

It is evident in (Figure 8.6) that there is a broad correspondence of the coherency signal that matches the fault interpretation – more so on the H4 Hi Res display. However, these fault trends are not discernible on the Hi-Res displays at (Figure 8.4). This is demonstrated further at (Figure 8.7).

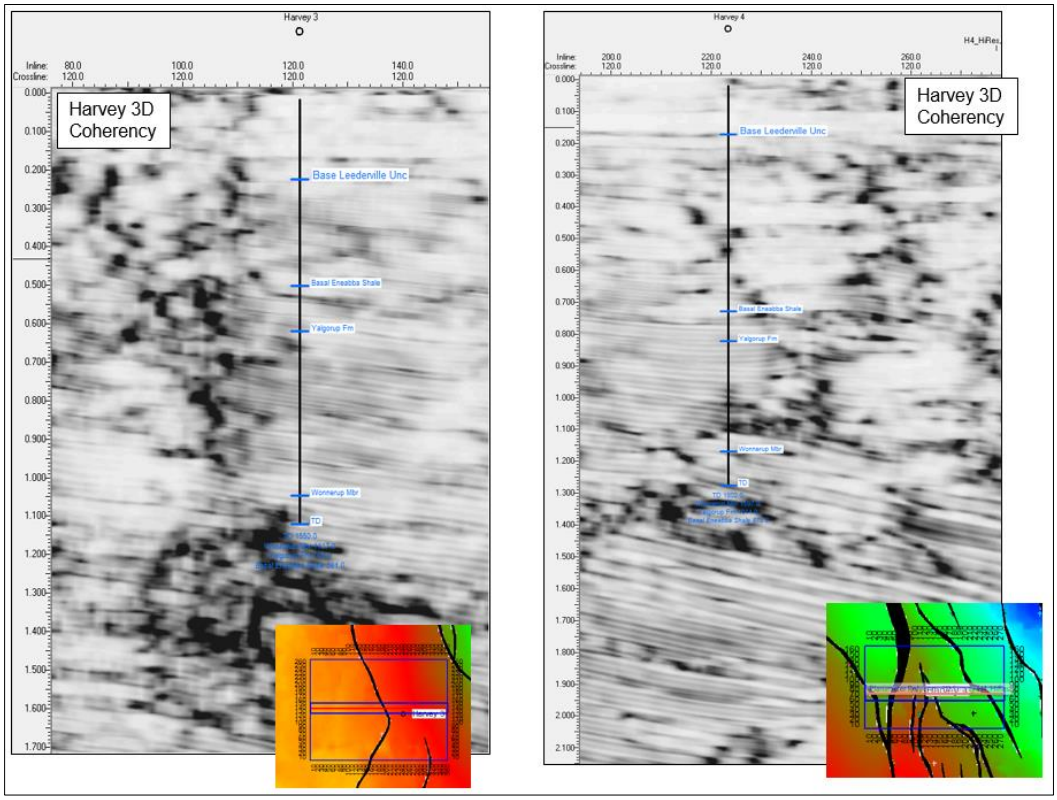

Figure 8.5 Hi Res Coherency Comparison – Harvey 3D coherency data displayed in same panels as Hi-Res Surveys

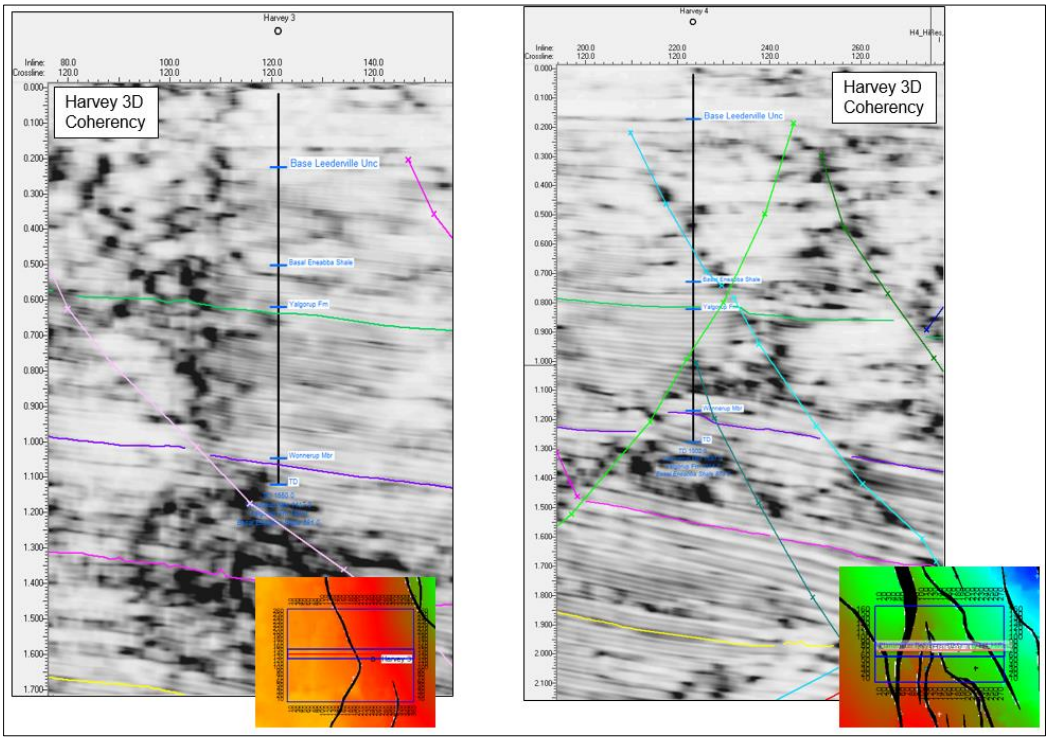

Figure 8.6 Hi Res Coherency Comparison – Harvey 3D coherency data displayed in same panels as Hi-Res Surveys – including interpretation

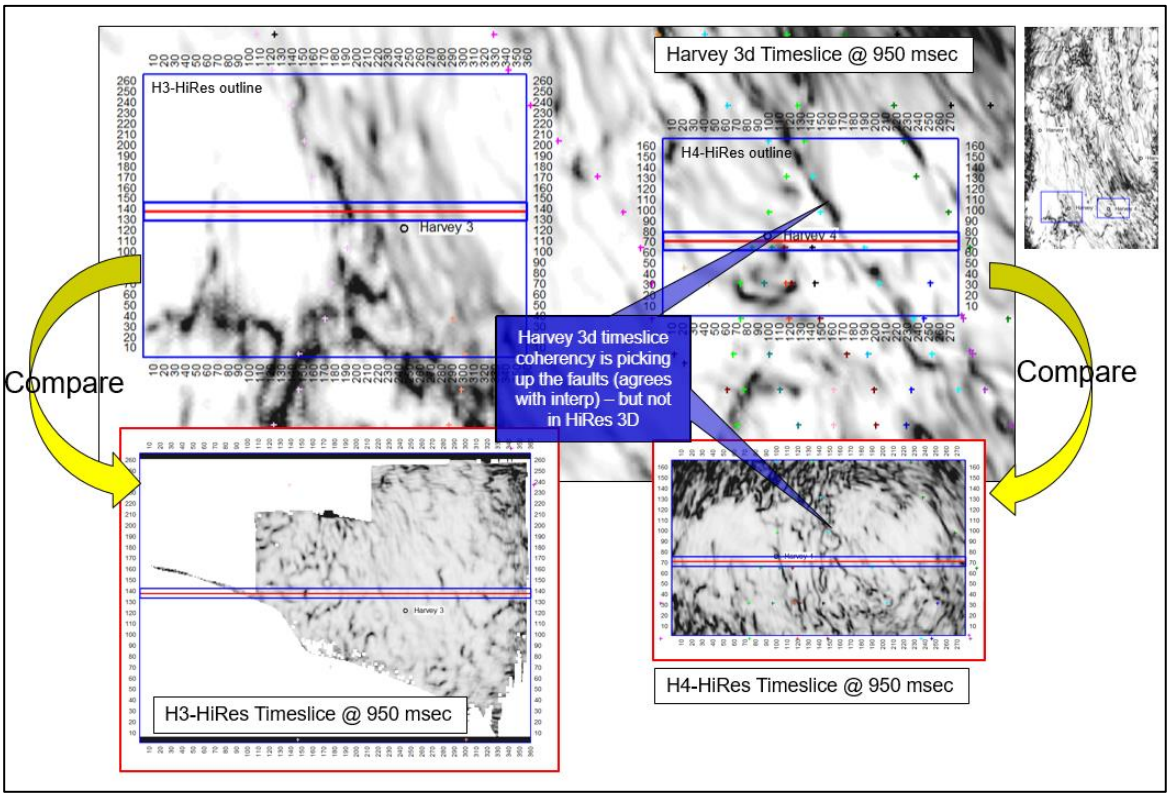

Figure 8.7 Hi Res Coherency Comparison – Time Slice View

The upper panels in (Figure 8.7) are time slice views (taken at 950msec). The outline of the Hi-Res surveys is shown by the blue polygon and the coherency data in the background belongs to the Harvey 3D survey. The red line within the blue box shows the position of the Inline sections from the preceding figures. The small coloured crosses on the time slice views mark the positions of the interpreted fault cuts.

The cyan coloured fault which showed good correspondence to the Harvey 3D coherency in Figure 8.6 continues to show good correlation as the fault cuts are directly aligned with the relatively strong lineament on the Harvey 3D coherency display at the upper right-hand panel.

To compare, the red boxes below show the time slice at the same level (950msec) but with the coherency data for the H3 Hi-Res Survey (bottom left) and the H4 Hi-Res Survey (bottom right). Each of these is directly comparable to the box directly above.

It is clear that the Hi-Res coherency data struggle to provide the same level of information as the broader Harvey 3D survey. However, despite this comparison, it should be considered that perhaps the area of the Hi-Res survey is insufficient to allow appropriate imaging at the

depths in interest for this study. It can be seen from the arcuate patterns around the fringe of the H4 Hi-Res display (bottom right) that much of the area is affected by migration smiles. A larger area Hi-Res survey may indeed yield a very different result.

9. CONCLUSIONS

A detailed interpretation of horizons and faults has been completed. Additional horizons within the Yalgorup Member and the Wonnerup Member have been included compared to the previous study. The fault interpretation comprises greater detail as the reprocessing has allowed.

Time and depth maps for all horizons interpreted have been completed for this study. A structural model has been proposed that appropriately fits the detailed Harvey 3D interpretation into a regional context.

A comprehensive effort has been applied to investigate the validity of qualitative and quantitative facies prediction using a variety of attributes. These included amplitude extraction grids across many surfaces and intervals, horizon attributes at all key surfaces and coherency attribute analysis at many levels.

Unfortunately, the limitations in the data acquisition and the subsequent impact this has had on the data processing has precluded the derivation of meaningful attributes that can be reliably used for facies prediction. In particular;

- Data quality and coverage is highly variable across the extent of the Harvey 3D area
- As such, horizon based amplitude extraction is unable to provide meaningful results
- Whilst there appear to be patches of reasonable data quality and amplitude “patterns”, the true extent of these is not known.
- These may only appear anomalous as their limit is controlled by the encroachment of “bad data” zones
- Qualitative and quantitative facies prediction using the Harvey 3D seismic data is unable to provide a reliable interpretation.

Lastly, the two high-resolution surveys that were acquired across the Harvey 3 and the Harvey 4 well locations have not been able to provide any additional information to assist with the interpretation of potentially sub-resolution faults in the existing and more extensive Harvey 3D. Rather than a failure of method, it is considered that the reason for this result is more likely a function of the limited area of the high-resolution surveys. The high-resolution surveys were designed to be effective above -1000mSS but the objectives of this study (Yalgorup & Wonnerup Members) are deeper than this within the survey areas.

10. REFERENCES

IASKY, R.P., 1993—A Structural Study of the Southern Perth basin: Western Australia Geological Survey, Report 31,

CROSTELLA.A. AND BACKHOUSE, J., 2000—Geology and Petroleum Exploration of the Central and Southern Perth Basin, Western Australia. Western Australia Geological Survey, Report 57,

Iasky, R. P. and Lockwood, A. M., 2004, Gravity and Magnetic Interpretation of the Southern Perth Basin, Geological Survey of Western Australia

YOUNG, R. J. B., and JOHANSON, J. N., 1973, Lake Preston 1 Well Completion Report: Western Australia Geological Survey, S-Series, S811 (unpublished)

Y Zhan, 2014, 2D Seismic Interpretation of the Harvey Area, Southern Perth Basin, Western Australia, Record 2014/7: Geological Survey of Western Australia;